EJBCS

Eurasian Journal of Biological and Chemical Sciences (Eurasian J. Bio. Chem. Sci.)

Cilt: 6 Volume: 2 Year: 2023

e-ISSN 2651-5237

EJBCS
Eurasian Journal of Biological and Chemical Sciences

Cilt: 6 Volume: 2 Year: 2023

Published Biannually

Corresponding Address
Gaziantep University, Faculty of Arts and Sciences, Department of Biology, Gaziantep, Turkey
E-mail: mtdogan1@gmail.com
Web: https://www.dergipark.org.tr/ejbcs

Owner / Publisher
Muhammet DOĞAN
This journal is peer-reviewed and published twice (June, December) a year.

e-ISSN 2651-5237

EJBCS
Eurasian Journal of Biological and Chemical Sciences

Cilt: 6 Volume: 2 Year: 2023

Contents / İçindekiler

RESEARCH ARTICLE
Eurasian J Bio Chem Sci, 6(2):52-62, 2023
https://doi.org/10.46239/ejbcs.1281018

EJBCS

Eurasian Journal of Biological and Chemical Sciences

Journal homepage: www.dergipark.org.tr/ejbcs

Possible inhibitory effects of hoslundal, hoslundin and hoslunddiol on human lactate dehydrogenases: a bioinformatics proof

Yağmur Bilgin, Yasir Yalnızoğlu, Levent Çavaş*
Dokuz Eylül University, Faculty of Science, Department of Chemistry, İzmir, Türkiye

*Corresponding author : levent.cavas@deu.edu.tr
Orcid No: https://orcid.org/0000-0003-2136-6928

Received : 11/04/2023
Accepted : 09/09/2023

Abstract: The development of anti-malarial drugs is of great importance due to the detrimental effects of this disease all around the world. In recent years, bioinformatics tools provide considerable contributions to develop new small molecules which have important bioactivities against many bio-targets. However, missing points in the methodologies or aims of the studies in which in silico tools are used may reveal problematic cases. Hoslundal, hoslundin, and hoslunddiol were proposed by Shadrack et al. (2016) to inhibit *Plasmodium falciparum* lactate dehydrogenase (*Pf*-LDH) to fight malaria. But these molecules may have potential to inhibit mammalian LDHs. To investigate whether these molecules have inhibitions on mammalian LDHs or not, we studied a comprehensive and comparative molecular docking studies as described in the present paper. According to the results, the vina scores of hoslundal without NADH for *Pf*-LDH, Human Muscle-LDH (HM-LDH), Human Heart-LDH (HH-LDH) were found as -7.5, -7.6 and -8.2 kJ/mol, respectively. Moreover, multiple sequence alignment analysis reveals high similarities among sequences. In the light of molecular studies, hoslundal was found to be connected to *Pf*-LDH, HM-LDH, HH-LDH (31, 26, 34), (2, -7, 154), (11, 41, 54), respectively. In conclusion, novel small molecules which are developed via in silico tools could show excellent activities against bio-targets of the pathogenic microorganisms. However, it should not be forgotten that active site of the enzymes may have been conserved, therefore, after a possible proposal of small molecule, its molecular docking and also Swiss-ADME studies for human should be necessarily carried out.

Keywords: anti-malarial drugs, docking, human lactate dehydrogenase, *Plasmodium falciparum*, malaria.

1. Introduction

In anaerobic conditions, the energy as ATP is obtained through the glycolysis pathway in which glucose is converted into pyruvate via ten steps reaction series and this process produces net two moles of ATP. Lactate dehydrogenase (LDH) is a tetrameric enzyme that plays a special role for the continuation of the glycolysis process (Iacovino et al., 2022). It produces nicotinamide adenine dinucleotide (NAD^+) to continue glycolysis, and LDH is classified as the eleventh reaction of glycolysis. LDH produces lactate from pyruvate to provide energy in anaerobic conditions. The result of this process, NAD^+ is produced for use in the sixth reaction of glycolysis in which glyceraldehyde-3-phosphate is transformed into 1,3-bisphosphoglycerate. For mammalians, there are two different types of LDH which can be defined as M and H types. Known isoenzymes of LDH based on their subunits are reported as M_4, M_3H, M_2H_2, MH_3 and H_4 tetrameric structures. H- and M-types are heart and muscle subunits, respectively. M-type is also found in liver (Voet and Voet, 1995). Shadrack et al. (2016) highlighted the danger of the pathogenic microorganism *Plasmodium falciparum* which is the main vector for malaria. It is still a big problem in many countries. According to WHO, estimated cases in 2020 are given 241 million with 627,000 deaths. Most of the cases are reported from Africa (WHO, 2022). Shadrack et al. (2016) proposed hoslundal, hoslundin, and hoslunddiol, the compounds known as secondary metabolites of the plant *Hoslundia opposita*, to inhibit LDH in *P. falciparum* (*Pf*-LDH) for eradication of the disease. Hoslundal, hoslundin, and hoslunddiol (Figure 1) are docked with *Pf*-LDH as a receptor. Since LDH is a haloenzyme, the docking was realized with and without NADH by Shadrack et al. (2016) to estimate the best binding energies, H-bond forming residues and bond lengths. However, there is no information in the paper of Shadrack et al. (2016) related to environmental application of these molecules. One of the application methods of these molecules could be spraying via compressors. If this method is applied, these molecules will be widely spread and they may contaminate water resources. Therefore, there is a very big risk that all animals in the region may negatively be affected by these molecules due to LDH inhibition.

In this investigation, the following research questions will be answered:

1) What are the similarities among *Pf*-LDH, HM-LDH and HH-LDH?
2) What are the docking scores of these compounds against these human LDH forms?
3) If these molecules contaminate water resources, how the animals (mammalians) could be affected?

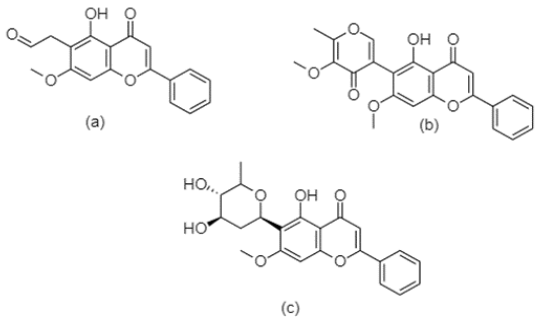

Figure 1. Chemical structures of (a) hoslundal, (b) hoslundin and (c) hoslunddiol

2. Materials and Method

The FASTA sequences of enzymes of *Plasmodium falciparum* lactate dehydrogenase (*Pf*-LDH), Human Muscle L-Lactate Dehydrogenase M Chain (HM-LDH) and Human Heart L-Lactate Dehydrogenase H Chain (HH-LDH) were retrieved via uniprot.org and the active site information was also accessed (Uniprot, 2021). Each of their FASTA formats was selected for multiple sequence analysis. The aim of this comparison is to determine similarities and conserved regions of the enzymes studied. Multiple sequence alignments of the FASTA sequences were carried out by Clustal Omega (Sievers et al., 2018). The default settings were used in the analysis. This database is widely used in many bioinformatics studies, such as determining genetic or evolutionary relationships, detecting structural similarities, and performing evolutionary analyses. Ligands structures of the compounds were retrieved from PubChem and their sdf formats were downloaded (Kim et al., 2021). Swiss-Similarity is the in silico tool that is used for determination of similarity between small molecules according to their chemical structures (Bragina et al., 2022). Cannonical structure of hoslundal, hoslundin and hoslunddiol were obtained from PubChem (Kim et al., 2021). Molecular docking analysis was used to estimate the vina scores to compare the affinity and also determination of the contact residues of the enzymes by using CB-Dock (Liu et al., 2020). Vina scores were compared with and without NADH. CB-Dock and CB-Dock2 are molecular docking tools used in the field of structural bioinformatics. CB-Dock uses a number of computational algorithms to identify chemical bonds and perform energy minimization (Liu et al., 2020). YASARA was used to model the visualization of each enzyme and ligand. YASARA provides an advanced set of tools for analyzing the structure and interactions of proteins, nucleic acids, and other biomolecules. This tool is widely used in many research fields such as molecular modeling, protein design, drug discovery, molecular dynamics simulations, and molecular interaction analysis (Land and Humble, 2018). Protparam is a bioinformatics tool used for protein sequence analysis. This program is used to predict the basic physical and chemical properties of a protein. It calculates a number of important parameters such as the amino acid composition of the protein, its isoelectric point, molecular weight, theoretical pI value, hydrophobicity and hydrophilia scores, alpha helix and beta sheet formation potential (Gasteiger, 2005). Physicochemical properties such as molar reactivity, rotatable bonds, and the pharmacokinetics of the molecules were estimated. Factors such as cytochromes P450 (CYP), Log Kp (skin permeation), GI absorption, and BBB permeation were evaluated. The BOILED EGG model was utilized to represent blood-brain barrier permeation (BBB permeation), and gastrointestinal absorption (GI absorption) was determined using the Swiss-ADME approach (Daina et al., 2017). Flowchart of the methodology was shown in Figure 2.

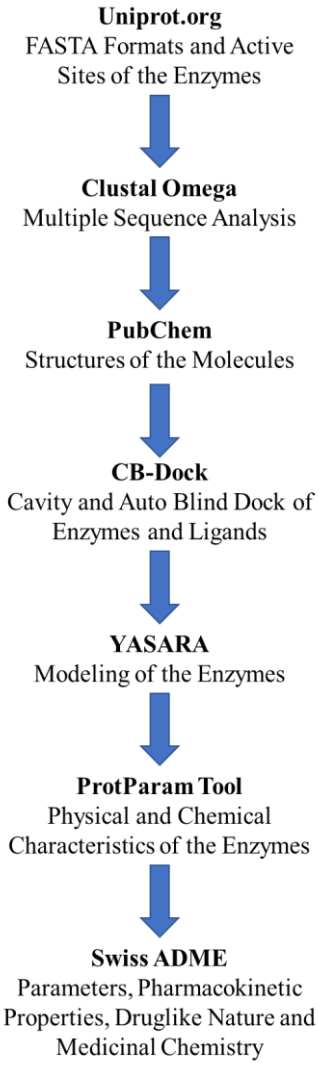

Figure 2. Flowchart of the methodology

3. Results

In this paper, HM-LDH, HM-LDH and *Pf*-LDH were compared by using bioinformatics tools. Clustal Omega was used to determine the similarities between *Pf*-LDH, HM-LDH and HH-LDH (Sievers and Higgins, 2018). According to Figure 3, amino acid lengths of *Pf*-LDH (Uniprot code: A0A024W2N3), HM-LDH (UniProt ID: P00338) and HH-LDH (UniProt ID: P07195) were found as 316, 332 and 334, respectively. As it can be seen from Figure 3, there is a high similarity between HM-LDH and HH-LDH. However, the similarity score was low when *Pf*-LDH was compared with human LDHs.

Swiss-Similarity was used to compare the similarity of hoslundal, holsundin, and hoslunddiol with other small molecules (Bragina et al., 2022). According to Table 1, the three most similar molecules for each hoslundal, hoslundin, and hoslinddiol are identified. Hoslundal shows high similarity with hipidulin (DB14008) with a score of 0.950. The similarity score of hoslundin is very low compared to hetrombogap. Finally, the similarity score of hoslunddiol is determined as 0.832 against puerarin.

Figure 3. Multiple sequence analysis of *Plasmodium falciparum* lactate dehydrogenase (UniProt ID: A0A024W2N3), Human Muscle L-Lactate Dehydrogenase M Chain (UniProt ID: P00338), and Human Heart L-Lactate Dehydrogenase H Chain (UniProt ID: P07195).

Table 1. Swiss-Similarity results of hoslundal, hoslundin and hoslunddiol.

Molecule	Score	Similar Molecule	PubChem ID
Hoslundal	0.950	Hispidulin	DB14008
	0.947	Baicalein	DB16101
	0.925	5,7,2’-trihydoxy-6,8-dimethoxyflavone	DB13983
Hoslundin	0.048	Hetrombopag	DB16184
	0.023	Xanthohumol	DB15359
	0.020	Methyl n-[[2’,4’-difluoro-4-hydroxy-5-iodobiphenyl-3-yl)carbonyl]-beta-alaninate	DB07962
Hoslunddiol	0.832	Puerarin	DB12290
	0.672	Hispidulin	DB14008
	0.647	5,7,2’-trihydroxy-6,8-dimethoxyflavone	DB13983

By using CB-Dock, cavity detection was studied for each enzyme by using hoslundal (Compound CID: 15726097) (Liu et al., 2020). In Figure 4, view of the cavities of each enzyme is shown.

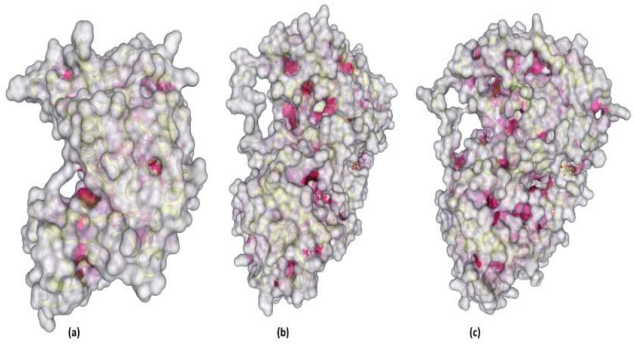

Figure 4. View of the cavities from (a) *Plasmodium falciparum* Lactate Dehydrogenase (UniProt ID: A0A024W2N3), (b) Human Muscle L-Lactate Dehydrogenase M Chain (UniProt ID: P00338), (c) Human Heart L-Lactate Dehydrogenase H Chain (UniProt ID: P07195).

According to Table 2, for each three enzymes, there were five cavities. The highest cavity volume (Å^3) was found for HM-LDH in C1 as 2532 Å^3 and its cavity size coordinates were found as 23, 23, 14. Also, the highest volume values were found at C1 for HH-LDH and *Pf*-LDH as 2003 Å^3 and 809 Å^3, respectively.

The cavities were chosen according to their active sites in Table 3. For this docking, all heteroatoms were removed. Amino acids and their positions were found from uniprot.org (Uniprot, 2021). According to Voet and Voet (1995), Michael Rossman has determined the X-Ray structure of the LDH and NADH complex. As a result of his study, ARG109, ARG171, and HIS195 were determined as active sites of the human LDH. The contact residues were compared and both HM-LDH and HH-LDH had these amino acids at C1. The contact residues of HM-LDH are ARG98, ARG168 and HIS192. HH-LDH contact residues are also found as ARG106, ARG169, and HIS193. When the Table 3 is examined, it is clear that hoslundal is not around the active sites of *Pf*-LDH. HH-LDH has the highest vina score as -8.2 kJ/mol.

The auto blind docking results of *Pf*-LDH, HM-LDH and HH-LDH with coenzyme NADH are shown in Table 4. The ligand was selected as hoslundal. When the contact residues of HH-LDH and HM-LDH are examined, it is clear that the ligand is around the active sites of the enzymes. The contact residues of HM-LDH were found as GLY28, ALA29, VAL30, THR94, ALA95, GLY96, ALA97, ARG98, GLN99, VAL135, SER136, ASN137, LEU164, ARG168, HIS192, ILE241, TYR246, THR247, ILE251. The contact residues in HH-LDH were found to be GLY29, GLN30, VAL31, THR95, GLY97, ARG99, GLN100, ARG106, VAL136, ASN138, SER161, LEU165, ARG169, HIS193, ALA238, ILE242, GLY246, TYR247, THR248, ILE252. *Pf*-LDH contact residues were found as VAL26, GLY27, GLY29, MET30, ILE31, GLY32, PHE52, ASP53, ILE54, VAL55, TYR85, THR97, ALA98, GLY99, THR101, ILE119, ILE123. The highest cavity volume was found as 2532 Å^3 on HM-LDH and the highest vina score was found as -8.2 kJ/mol for HH-LDH.

Table 2. Cavity detection results in the Human Muscle L-Lactate Dehydrogenase M Chain (HM-LDH), Human Heart L-Lactate Dehydrogenase H Chain (HH-LDH) and *Plasmodium falciparum* Lactate Dehydrogenase (*Pf*-LDH) with coenzyme as NADH and ligand as hoslundal by using CB-Dock.

Enzymes	CurPocket ID	Cavity Volume (Å^3)	Center (x, y, z)	Cavity Size (x, y, z)
HM-LDH	C1	2532	2, -7, 154	23, 23, 14
	C2	711	11, -36, 141	16, 10, 17
	C3	393	13, -17, 137	10, 10, 13
	C4	145	17, -2, 151	5, 12, 6
	C5	131	-8, -20, 136	5, 9, 6
HH-LDH	C1	2003	11, 41, 57	22, 18, 11
	C2	861	10, 43, 34	21, 15, 8
	C3	319	24, 14, 51	12, 11, 13
	C4	292	0, 27, 56	9, 10, 12
	C5	259	37, 20, 48	7, 14, 14
Pf-LDH	C1	809	31, 26, 34	15, 13, 22
	C2	738	24, 7, 44	13, 14, 13
	C3	381	8, 17, 43	9, 13, 10
	C4	159	28, 34, 44	7, 9, 6
	C5	154	16, 28, 41	8, 8, 10

Table 3. The molecular docking results of hoslundal for Human Muscle L-Lactate Dehydrogenase M Chain (HM-LDH), Human Heart L-Lactate Dehydrogenase H Chain (HH-LDH) and *Plasmodium falciparum* Lactate Dehydrogenase (*Pf*-LDH) without NADH.

Enzymes	CurPocket ID	Vina score (kJ/mol)	Cavity volume (Å³)	Center (x, y, z)	Docking size (x, y, z)	Contact residues
HM-LDH	C1	-7.6	2532	2, -7, 154	28, 28, 21	**Chain A:** GLY28, ALA29, VAL30, THR94, ALA95, GLY96, ALA97, ARG98, GLN99, VAL135, SER136, ASN137, LEU164, ARG168, HIS192, ILE241, TYR246, THR247, ILE251
HH-LDH	C1	-8.2	2003	11, 41, 54	27, 21, 21	**Chain A:** GLY29, GLN30, VAL31, THR95, GLY97, ARG99, GLN100, ARG106, VAL136, ASN138, SER161, LEU165, ARG169, HIS193, ALA238, ILE242, GLY246, TYR247, THR248, ILE252
***Pf*-LDH**	C1	-7.5	809	31, 26, 34	21, 21, 17	**Chain A:** VAL26, GLY27, GLY29, MET30, ILE31, GLY32, PHE52, ASP53, ILE54, VAL55, TYR85, THR97, ALA98, GLY99, THR101, ILE119, ILE123

Table 4. The molecular docking results of hoslundal for Human Muscle L-Lactate Dehydrogenase M Chain (HM-LDH), Human Heart L-Lactate Dehydrogenase H Chain (HH-LDH) and *Plasmodium falciparum* Lactate Dehydrogenase (*Pf*-LDH) with NADH.

Enzymes	CurPocket ID	Vina score (kJ/mol)	Cavity volume (Å³)	Center (x, y, z)	Docking size (x, y, z)	Contact residues
HM-LDH	C1	-7.6	2532	2, -7, 154	28, 28, 21	**Chain A:** GLY28, ALA29, VAL30, THR94, ALA95, GLY96, ALA97, ARG98, GLN99, VAL135, SER136, ASN137, LEU164, ARG168, HIS192, ILE241, TYR246, THR247, ILE251
HH-LDH	C1	-8.2	2003	11, 41, 57	27, 21, 21	**Chain A:** GLY29, GLN30, VAL31, THR95, GLY97, ARG99, GLN100, ARG106, VAL136, ASN138, SER161, LEU165, ARG169, HIS193, ALA238, ILE242, GLY246, TYR247, THR248, ILE252
***Pf*-LDH**	C1	-7.5	809	31, 26, 34	21, 21, 27	**Chain A:** VAL26, GLY27, GLY29, MET30, ILE31, GLY32, PHE52, ASP53, ILE54, VAL55, TYR85, THR97, ALA98, GLY99, THR101, ILE119, ILE123

In Table 5, hoslundin was selected as the ligand and it was docked with each enzyme (without NADH). All heteroatoms were released for docking. CurPocket ID of each enzyme was selected as C1. HM-LDH contact residues were found as GLY26, VAL27, GLY28, ALA29, VAL30, ASP51, LYS56, THR94, ALA95, GLY96, ALA97, ARG98, GLN99, ARG105, LEU108, ASN112, VAL135, SER136, ASN137, LEU164, ARG168, HIS192, ALA237, ILE241, TYR246, THR247, SER248, ILE251. Active sites were found to be ARG105, ARG168 and HIS192. HH-LDH contact residues such as GLY27, VAL28, GLY29, GLN30, VAL31, ASP52, LEU54, THR95, ALA96, GLY97, VAL98, ARG99, GLN100, ARG106, LEU109, ASN113, VAL136, SER137, ASN138, LEU165, HIS193, ALA238, ILE242, TYR247, THR248, ILE252. Active sites were determined to be ARG106 and HIS193. *Pf*-LDH contact residues found as VAL26, GLY27, SER28, GLY29, MET30, ILE31, GLY32, PHE52, ASP53, ILE54, VAL55, TYR85, THR97, ALA98, GLY99, PHE100, THR101, LYS102, ILE119, ILE123. The highest cavity volume was found as 2532 on HM-LDH and the highest vina score was found as 9.2 kJ/mol on HH-LDH.

In Table 6, hoslundin was docked to HM-LDH, HH-LDH and *Pf*-LDH with coenzyme NADH. Contact residues of HM-LDH were found as GLY26, VAL27, GLY28, ALA29, VAL30, ASP51, LYS56, THR94, ALA95, GLY96, ALA97, ARG98, GLN99, ARG105, LEU108, ASN112, VAL135, SER136, ASN137, LEU164, ARG168, HIS192, ALA237, ILE241, TYR246, THR247, ILE251. Contact residues of HH-LDH were found to be GLY27, VAL28, GLY29, GLN30, VAL31, ASP52, LEU54, THR95, ALA96, GLY97, VAL98, ARG99, GLN100, ARG106, LEU109, ASN113, VAL136, SER137, ASN138, LEU165, HIS193, ALA238, ILE242, TYR247, THR248, ILE252. *Pf*-LDH contact residues were VAL26, GLY27, SER28, GLY29, MET30, ILE31, GLY32, PHE52, ASP53, ILE54, VAL55, TYR85, THR97, ALA98, GLY99, PHE100, THR101, LYS102, ILE119, ILE123. Active sites were found to be same as without NADH.

Table 5. The molecular docking results of hoslundin for Human Muscle L-Lactate Dehydrogenase M Chain (HM-LDH), Human Heart L-Lactate Dehydrogenase H Chain (HH-LDH) and *Plasmodium falciparum* Lactate Dehydrogenase (*Pf*-LDH) without coenzyme NADH.

Enzymes	CurPocket ID	Vina score (kJ/mol)	Cavity volume (Å^3)	Center (x, y, z)	Docking size (x, y, z)	Contact residues
HM-LDH	C1	-9.0	2532	2, -7, 154	24, 24, 24	**Chain A:** GLY26, VAL27, GLY28, ALA29, VAL30, ASP51, LYS56, THR94, ALA95, GLY96, ALA97, ARG98, GLN99, ARG105, LEU108, ASN112, VAL135, SER136, ASN137, LEU164, ARG168, HIS192, ALA237, ILE241, TYR246, THR247, SER248, ILE251
HH-LDH	C1	-9.2	2003	11, 41, 57	24, 24, 24	**Chain A:** GLY27, VAL28, GLY29, GLN30, VAL31, ASP52, LEU54, THR95, ALA96, GLY97, VAL98, ARG99, GLN100, ARG106, LEU109, ASN113, VAL136, SER137, ASN138, LEU165, HIS193, ALA238, ILE242, TYR247, THR248, ILE252
***Pf*-LDH**	C1	-8.8	809	31, 26, 34	24, 24, 24	**Chain A:** VAL26, GLY27, SER28, GLY29, MET30, ILE31, GLY32, PHE52, ASP53, ILE54, VAL55, TYR85, THR97, ALA98, GLY99, PHE100, THR101, LYS102, ILE119, ILE123

Table 6. The molecular docking results of hoslundin for Human Muscle L-Lactate Dehydrogenase M Chain (HM-LDH), Human Heart L-Lactate Dehydrogenase H Chain (HH-LDH) and *Plasmodium falciparum* Lactate Dehydrogenase (*Pf*-LDH) with coenzyme NADH.

Enzymes	CurPocket ID	Vina score (kJ/mol)	Cavity volume (Å^3)	Center (x, y, z)	Docking size (x, y, z)	Contact residues
HM-LDH	C1	-8.9	2532	2, -7, 154	24, 24, 24	**Chain A:** GLY26, VAL27, GLY28, ALA29, VAL30, ASP51, LYS56, THR94, ALA95, GLY96, ALA97, ARG98, GLN99, ARG105, LEU108, ASN112, VAL135, SER136, ASN137, LEU164, ARG168, HIS192, ALA237, ILE241, TYR246, THR247, ILE251
HH-LDH	C1	-9.2	2003	11, 41, 57	24, 24, 24	**Chain A:** GLY27, VAL28, GLY29, GLN30, VAL31, ASP52, LEU54, THR95, ALA96, GLY97, VAL98, ARG99, GLN100, ARG106, LEU109, ASN113, VAL136, SER137, ASN138, LEU165, HIS193, ALA238, ILE242, TYR247, THR248, ILE252
***Pf*-LDH**	C1	-8.8	809	31, 26, 34	24, 24, 24	**Chain A:** VAL26, GLY27, SER28, GLY29, MET30, ILE31, GLY32, PHE52, ASP53, ILE54, VAL55, TYR85, THR97, ALA98, GLY99, PHE100, THR101, LYS102, ILE119, ILE123

Table 7. The docking results of hoslunddiol for Human L-Lactate Dehydrogenase M Chain (HM-LDH), Human Heart L-Lactate Dehydrogenase H Chain (HH-LDH) and *Plasmodium falciparum* Lactate Dehydrogenase (*Pf*-LDH) without NADH.

Enzyme	CurPocket ID	Vina score (kJ/mol)	Cavity volume (Å^3)	Center (x, y, z)	Docking size (x, y, z)	Contact residues
HM-LDH	C1	-8.9	2532	2, -7, 154	23, 23, 23	**Chain A:** GLY26, VAL27, GLY28, ALA29, VAL30, ASP51, VAL52, THR94, ALA95, GLY96, ALA97, ARG98, GLN99, ARG105, LEU108, VAL135, SER136, ASN137, ARG168, HIS192, ALA237, ILE241, TYR246, THR247, ILE251
HH-LDH	C1	-9.0	2003	11, 41, 57	23, 23, 23	**Chain A:** GLY27, VAL28, GLY29, GLN30, VAL31, ASP52, VAL53, LEU54, THR95, ALA96, GLY97, VAL98, ARG99, GLN100, LEU109, VAL136, SER137, ASN138, LEU165, ARG169, HIS193, ALA238, ILE242, TYR247, THR248, ASN249, ILE252
***Pf*-LDH**	C1	-8.2	809	31, 26, 34	23, 23, 23	**Chain A:** VAL26, GLY27, SER28, GLY29, MET30, ILE31, GLY32, PHE52, ASP53, ILE54, VAL55, TYR85, THR97, ALA98, GLY99, THR101, LYS102, ILE119, ILE123

In Table 7, hoslunddiol was selected as ligand and *Pf*-LDH, HM-LDH and HH-LDH were selected as LDHs without heteroatoms and NADH. The contact residues of HM-LDH were found as GLY26, VAL27, GLY28, ALA29, VAL30, ASP51, VAL52, THR94, ALA95, GLY96, ALA97, ARG98, GLN99, ARG105, LEU108, VAL135, SER136, ASN137, ARG168, HIS192, ALA237, ILE241, TYR246, THR247, ILE251. Active sites were found ARG105, ARG168 and HIS192. HH-LDH contact residues were found as GLY27, VAL28, GLY29, GLN30, VAL31, ASP52, VAL53, LEU54, THR95, ALA96, GLY97, VAL98, ARG99, GLN100, LEU109, VAL136, SER137, ASN138, LEU165, ARG169, HIS193, ALA238, ILE242, TYR247, THR248, ASN249, ILE252. Active sites were found as ARG169 and HIS193. *Pf*-LDH contact residues were found as VAL26, GLY27, SER28, GLY29, MET30, ILE31, GLY32, PHE52, ASP53, ILE54, VAL55, TYR85, THR97, ALA98, GLY99, THR101, LYS102, ILE119, ILE123. The highest cavity volume was found to be 2532 on HM-LDH and the highest vina score was found to be -9.0 kJ/mol.

In Table 8, hoslunddiol was selected as ligand and the enzymes were selected with coenzyme NADH. HM-LDH contact residues were found to be GLY26, VAL27, GLY28, ALA29, VAL30, ASP51, VAL52, THR94, ALA95, GLY96, ALA97, ARG98, GLN99, ARG105, LEU108, VAL135, SER136, ASN137, HIS192, ALA237, ILE241, TYR246, THR247, ILE251. Active sites of the enzyme were found as ARG105 and HIS192. HH-LDH contact residues were found as GLY27, VAL28, GLY29, GLN30, VAL31, ASP52, VAL53, LEU54, THR95, ALA96, GLY97, VAL98, ARG99, GLN100, LEU109, VAL136, SER137, ASN138, ARG169, ALA238, ILE242, TYR247, THR248, ASN249, ILE252 and the active site was found to be ARG169. *Pf*-LDH contact residues were found to be VAL26, GLY27, SER28, GLY29, MET30, ILE31, GLY32, PHE52, ASP53, ILE54, VAL55, TYR85, THR97, ALA98, GLY99, THR101, LYS102, ILE119, ILE123. The highest cavity volume was found as 2532.

In Figure 5, active sites of the HM-LDH, HH-LDH and *Pf*-LDH without NADH were modeled by YASARA and active sites of the HM-LDH, HH-LDH and *Pf*-LDH were shown. When hoslundal, hoslundin and hoslunddiol are docked to these enzymes, they interact with the active sites. They have methoxy, carbonyl and hydroxyl groups in their structures and these molecules form hydrogen bonds with enzymes. ARG is one of the positively charged R-group amino acids and it is a non-essential amino acid. Also, HIS is a member of the same amino acid group, and it also has an imidazolium ring on its functional group. When hoslundal, hoslindin, and hoslinddiol dock with the enzyme, they are interact with these amino acids and the binding energy must be high.

According to Table 9, most abundance amino acids were found as valine, leucine, alanine, and isoleucine to be 10.1, 9.8 and 8.5% for *Pf*-LDH. Leucine, valine, and lysine were the most abundance amino acids to be 11.4, 10.2 and 8.4% for the HM-LDH and valine, leucine, lysine, and serine to be 11.4, 10.8, and 7.8% for HH-LDH, respectively. Theoretical pI values were found nearly between HM-LDH and *Pf*-LDH to be 8.44 and 7.12. Net charges were found for HM-LDH, HH-LDH, and *Pf*-LDH to be 3, -6, and 0, respectively. The highest instability index was found as 29.73 for *Pf*-LDH and the other values were close (Table 10). Swiss-ADME properties such as molar reactivity, pharmacokinetics, rotatable bonds of hoslundal, hoslundin and hoslunddiol were investigated (Table 11).

Table 8. The molecular docking results of hoslunddiol Human Muscle L-Lactate Dehydrogenase M Chain (HM-LDH), Human Heart L-Lactate Dehydrogenase H Chain (HH-LDH) and *Plasmodium falciparum* Lactate Dehydrogenase (*Pf*-LDH) with coenzyme as NADH.

Enzyme	CurPocket ID	Vina score (kJ/mol)	Cavity volume (Å³)	Center (x, y, z)	Docking size (x, y, z)	Contact residues
HM-LDH	C1	-8.9	2532	2, -7, 154	23, 23, 23	**Chain A:** GLY26, VAL27, GLY28, ALA29, VAL30, ASP51, VAL52, THR94, ALA95, GLY96, ALA97, ARG98, GLN99, ARG105, LEU108, VAL135, SER136, ASN137, HIS192, ALA237, ILE241, TYR246, THR247, ILE251
HH-LDH	C1	-9.0	2003	11, 41, 57	23, 23, 23	**Chain A:** GLY27, VAL28, GLY29, GLN30, VAL31, ASP52, VAL53, LEU54, THR95, ALA96, GLY97, VAL98, ARG99, GLN100, LEU109, VAL136, SER137, ASN138, ARG169, ALA238, ILE242, TYR247, THR248, ASN249, ILE252
***Pf*-LDH**	C1	-8.2	809	31, 26, 34	23, 23, 23	**Chain A:** VAL26, GLY27, SER28, GLY29, MET30, ILE31, GLY32, PHE52, ASP53, ILE54, VAL55, TYR85, THR97, ALA98, GLY99, THR101, LYS102, ILE119, ILE123

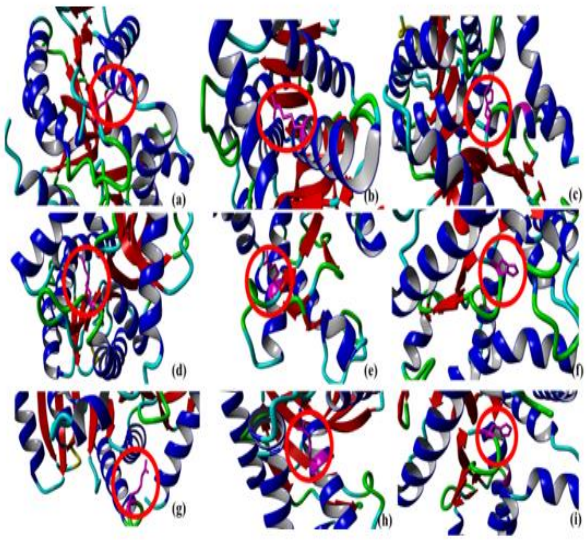

Figure 5. YASARA visualisation of HM-LDH, HH-LDH and *Pf*-LDH without NADH, with active site amino acids (a) ARG98, (b) ARG168, and (c) HIS192, (d) ARG106, (e) ARG171, (f) HIS193, (g) ARG109, (h) ARG171 and (i) HIS195 colored in pink.

Table 9. Number, percentages and abbreviations of the amino acids in *Pf*-LDH, HM-LDH, HH-LDH

Amino acids	*Pf*-LDH		HM-LDH		HH-LDH	
	#	%	#	%	#	%
Ala (A)	27	8.5	18	5.4	21	6.3
Arg (R)	6	1.9	11	3.3	8	2.4
Asn (N)	21	6.6	15	4.5	17	5.1
Asp (D)	17	5.4	18	5.4	19	5.7
Cys (C)	4	1.3	5	1.5	5	1.5
Gln (Q)	8	2.5	12	3.6	11	3.3
Glu (E)	15	4.7	18	5.4	21	6.3
Gly (G)	26	8.2	26	7.8	23	6.9
His (H)	9	2.8	7	2.1	7	2.1
Ile (I)	27	8.5	23	6.9	24	7.8
Leu (L)	31	9.8	38	11.4	36	10.8
Lys (K)	26	8.2	28	8.4	26	7.8
Met (M)	10	3.2	9	2.7	10	3.0
Phe (F)	7	2.2	7	2.1	5	1.5
Pro (P)	12	3.8	11	3.3	11	3.3
Ser (S)	15	4.7	24	7.2	26	7.8
Thr (T)	14	4.4	14	4.2	13	3.9
Trp (W)	1	0.3	6	1.8	6	1.8
Tyr (Y)	8	2.5	8	2.4	7	2.1
Val (V)	32	10.1	34	10.2	38	11.4

Table 10. Protein parameters of HM-LDH, HH-LDH and *Pf*-LDH (aa: amino acids, Mw: molecular weight, pI: isoelectric point).

Enzymes	#aa	Mw	Theoretical pI	Negatively Charged Residues (Asp+Glu)	Positively Charged Residues (Arg+Lys)	Net Charge	Instability Index
HM-LDH	332	36688.72	8.44	36	39	3	24.79
HH-LDH	334	36638.49	5.71	40	34	-6	26.87
***Pf*-LDH**	316	34107.75	7.12	32	32	0	29.73

Also, the pharmacokinetics of the molecules such as cytochromes P450 (CYP), Log Kp (skin permeation), GI absorption, BBB permeant were estimated and the results were given in Table 11. BOILED EGG model represents the blood-brain barrier permeant (BBB permeant) and gastrointestinal absorption (GI absorption). If the molecule is in the yellow part of the BOILED EGG model, BBB permeant and at the white part, GI absorption is observed. The blue dot also indicates that the molecule has a high affinity for P glycoprotein and could be easily released into the system. The red dot shows the affinity of the molecule is low, and it stays in the system for a long time (Daina and Zoete, 2016; Shaaban et al., 2022). In Table 11, Hoslundal is at the intersection of the white and yellow parts, which have both GI absorption and BBB permeant and it has a red dot, which means the molecule stays in the system for a long time. Hoslundin is at the white part with the red dot; it has GI absorption. Hoslunddiol is at the white part with the blue dot.

4. Discussion

About 409,000 people have been dying each year because of malaria. *P. falciparum* has a resistance to anti-malarial drugs and this resistance mechanism has so far been unresolved. Up to date, no validated vaccine has been reported in the scientific literature (Kayamba et al., 2021). Shadrack et al. (2016) selected three molecules that have inhibitory properties on the *Pf*-LDH and they used in silico methods to understand these interactions between enzymes and ligands. However, they did not mention the application method of these three compounds in the real enviromental conditions. This paper was aimed at understanding the inhibitory effects of these molecules on human-LDHs by using in silico methodology as well.

Table 11. Swiss-ADME results of hoslundal, hoslundin and hoslunddiol.

<table>
<tr>
<td>

a. Hoslundal

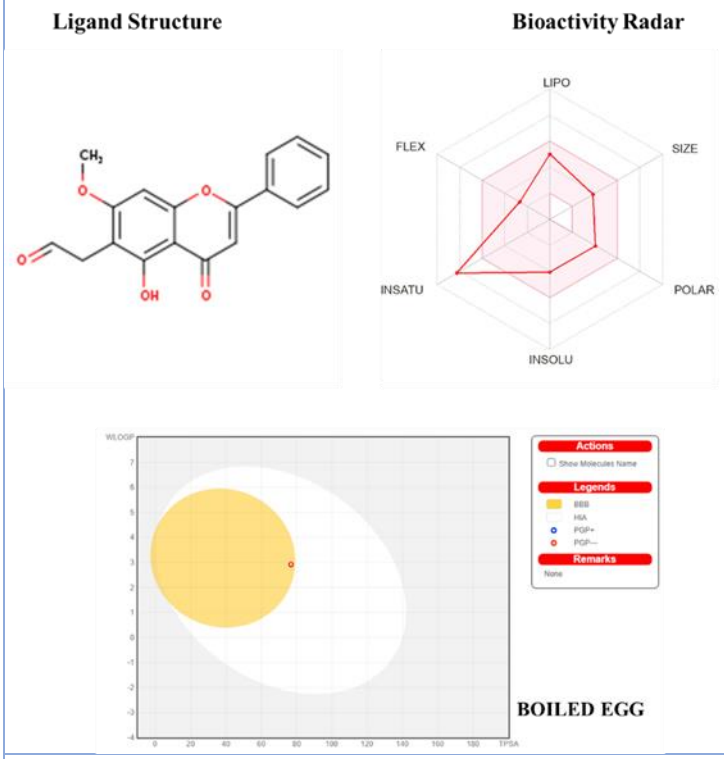

</td>
<td>

Pharmacokinetics and drug-likeness

- Lipophilicity: XLOGP3= 3.25
- Molar Refractivity= 86.41
- Polarity: TPSA= 76.74 Å^2
- Saturation: Fraction Csp3= 0.11
- Num. of rotatable bonds= 4
- BBB permeant= Yes
- Log K_P (skin permeation) = -5.89 cm/s
- P-gp substrate= No
- Consensus Log $P_{o/w}$= 2.77
- Bioavailability Score: 0.55
- CYP1A2 inhibitor= Yes
- CYP2C19 inhibitor= Yes
- CYP2C9 inhibitor= Yes
- CYP2D6 inhibitor= No
- CYP3A4 inhibitor= Yes
- GI absorption= High
- Lead likeness= Yes

</td>
</tr>
<tr>
<td>

b. Hoslundin

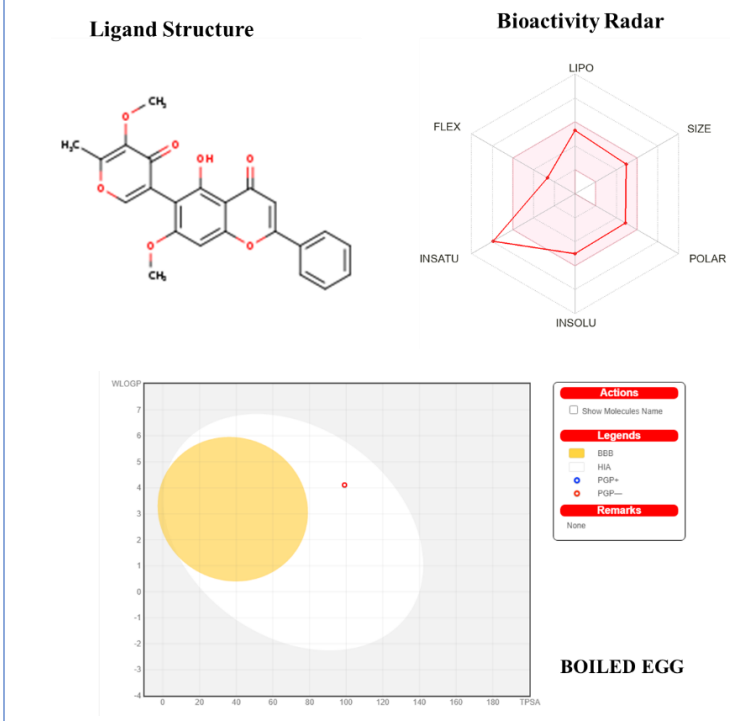

</td>
<td>

Pharmacokinetics and drug-likeness

- Lipophilicity: XLOGP3= 3.74
- Molar Refractivity= 111.86
- Polarity: TPSA= 99.11 Å^2
- Saturation: Fraction Csp3= 0.13
- Num. of rotatable bonds= 4
- BBB permeant= No
- Log K_P (skin permeation) = -6.12 cm/s
- P-gp substrate= No
- Consensus Log $P_{o/w}$= 3.42
- Bioavailability Score: 0.55
- CYP1A2 inhibitor= No
- CYP2C19 inhibitor= No
- CYP2C9 inhibitor= Yes
- CYP2D6 inhibitor= No
- CYP3A4 inhibitor= Yes
- GI absorption= High
- Lead likeness= No; 2 violations: MW>350, XLOGP3>3.5

</td>
</tr>
</table>

c. Hoslunddiol

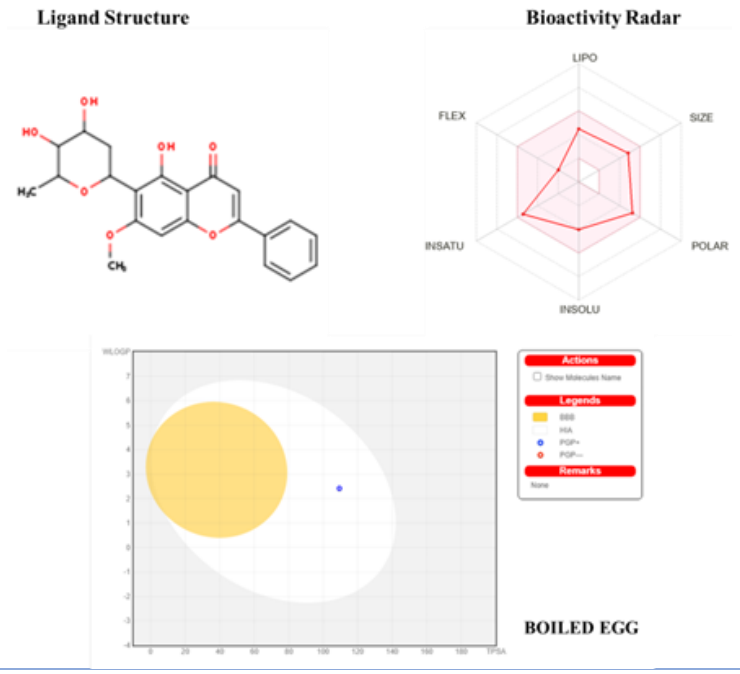

Pharmacokinetics and drug-likeness

- Lipophilicity: XLOGP3= 2.36
- Molar Refractivity= 106.73
- Polarity: TPSA= 109.36 Å^2
- Saturation: Fraction Csp3= 0.32
- Num. of rotatable bonds= 3
- BBB permeant= No
- Log K_P (skin permeation) = -7.05 cm/s
- P-gp substrate= Yes
- Consensus Log $P_{o/w}$= 2.24
- Bioavailability Score: 0.55
- CYP1A2 inhibitor= No
- CYP2C19 inhibitor= No
- CYP2C9 inhibitor= No
- CYP2D6 inhibitor= No
- CYP3A4 inhibitor= Yes
- GI absorption= High
- Lead likeness= No; 1 violation: MW>350

A comprehensive review on the LDH inhibitors can be found from Granchi et al (2010). More and very recent information on not only for human LDH inhibitors but also other species can be accessed via brenda-enzymes.org. CB-Dock was used and the results were estimated with and without NADH. The main idea was to elucidate whether these molecules interact with active sites of the enzymes. When the vina scores were compared, the results showed that they bonded with active site amino acids (ARG109, ARG171 and HIS195). As a result of the study, it was understood that these three molecules may also have inhibitory effects on the human-LDH. Ren et al. (2022) studied Methicillin-resistant *Staphylococcus aureus* USA300, which causes pneumonia. They utilized hispidulin as an inhibitor against *S. aureus* LDH. They tested the compound on the mice lungs. According to Swiss-Similarity results, hoslundal and hispidulin are highly similar, suggesting that hoslundal can also be employed for inhibiting *S. aureus* LDH. Singh et al. (2019) mentioned on *Pf*-LDH that there is a high similarity between *Pf*-LDH and human-LDH. Due to this similarity, usage of anti-pLDH drugs could be risky for all aerobic and anaerobic organisms where these anti-pLDH drugs are applied. The researchers have so far investigated the 3D structures of human-LDH and *Pf*-LDHs. Any anti-malarial inhibition focused on LDHs may be effective on human LDH. Some of the previous studies suggested new compounds as anti-pLDH drugs to inhibit pLDH. Vivas et al. (2005) mentioned that 4-hydroxy-1,2,5-oxidiazole-3-carboxylic acid (OXD1) as an inhibitor of *Pf*-LDH. Heterocyclic azole-based inhibitors bind with OXD1 as an inhibitor of *Pf*-LDH. Heterocyclic azole-based inhibitors bind to *Pf*-LDH, but they do not bind the active site of human LDH. In the Vivas et al. (2005) paper, it was shown that OXD1 has anti-malarial activity *in vitro* and *in vivo*. According to this study, Vivas et al. (2005) suggested and proved that while discovering new anti-malarial drugs, azole derivative compounds have more optimization. According to Shadrack et al. (2016), when the compounds were examined, it was clear that there was no azole-based compound. Thus, three of these molecules are alternatives to anti-malarial drugs. According to the findings, these compounds have *Pf*-LDH inhibition properties. The docking results also prove their inhibitory properties. Kayamba et al. (2021) study is about to emphasize the significance of parasitic LDH and MDH as therapeutic treatment targets for a few specific obligate apicoplast parasites. In the light of this study, their potential as therapeutic targets for both aerobic and anaerobic glycolytic pathways are highlighted. Azole derivatives have been extensively studied in the literature for their ability to inhibit *Pf*-LDH and MDH. As a result of this study, inhibition of MDH and LDH is the best strategy for the anti-malaria drugs. In the present study, three molecules were docked to HH-LDH and HM-LDH that are responsible for the continuation of glycolysis. Vina scores of HH-LDH and HM-LDH are higher than *Pf*-LDH when hoslundal, hoslundin and hoslunddiol were docked. According to these data sets, if these molecules are used, they may also inhibit HH-LDH and HM-LDH. Penna-Coutinho et al. (2011) studied NADH analogs to combat with malaria. They investigated 50 different NADH compounds. Itraconazole, atorvastatin and posaconazole were selected to be the best compound to inhibit pLDHs by using Molegro Virtual Docker software. In contrary to Penna-Coutinho et al. (2011), NADH was removed from the LDHs studied in this study and molecular docking was realized. Therefore, the result may exhibit different binding energies. In silico technologies provide a big contribution to the development of anti-pLDH drugs. However, a common and a validated methodology should be developed before obtaining docking scores with respect to candidate drugs. The main idea is to calculate vina scores while the molecules bind to the active sites. Penna-Coutinho et al. (2011) docked the NADH analogs without coenzyme but lactate dehydrogenase is a

haloenzyme that needs a coenzyme in order to show activity (Berg et al., 2007). We propose that itraconazole, atorvastatin and posaconazole should be docked with NADH and the MolDock score should be evaluated. Also, Penna-Coutinho et al (2011) mentioned that their selected compounds strongly bind to active site at and they called this interaction as "competitive inhibition". However, competitive inhibitors are listed under "reversible" inhibition types and strong interaction are not expected in molecular docking studies such hydrogen bonds, hydrophobic interactions electrostatic interactions, etc. According to Singh et al. (2019), chloroquine (CQ) is used in anti-malarial drugs. As a result of this usage, it caused resistance in *P. falciparum* and *P. vivax*. Both of these parasites are responsible for malaria. Long-term treatment led to retinal toxicity and a decrease in vision deficiency, diplopia, and associated vision loss. In the light of this information, new anti-malarial drugs should be developed.

5. Conclusion

The number of deaths due to malaria has been increasing especially in the Africa. In that case, it is very important to produce new anti-*Pf*-LDH drugs to prevent malaria. The development of bioinformatics tools helps produce new drugs. Also, they prevent time and cost losses. As it is known that anti-malarial drugs have inhibitory effects on *P. falciparum*, it should be noted that both mammalians and parasites have lactate dehydrogenases. As a result of this information, new molecules could inhibit mammalian LDH. According to the present paper, it is clear that three molecules exhibit higher binding energies for both HM-LDH and HH-LDH than those of *Pf*-LDH. Application methods play a crucial role in potantial use of these three small molecules in various inhibition studies. For the further studies, effects of specific application methods on the inhibition process of enzymes should be taken into consideration. Wet-lab studies are strongly recommended for specific inhibition.

Authors' contributions: YB: Collected and analyzed the data, wrote first draft and final version of the manuscript. YY: Collected and analyzed the data, draw the figures, wrote the first draft. LC: Designed the project, collected and analyzed the data, revised the first draft and final version of the manuscript.

Conflict of interest disclosure: The authors declare that they have no known competing financial interests or personal relationships that could have appeared to influence the work reported in this paper.

References

Berg JM, Tymoczko JL, Stryer L. 2007. Biochemistry, 6th ed. W. H. Freeman and Company, New York.

Bragina, ME, Daina, A, Perez MAS, Michielin O, Zoete V. 2022. SwissSimilarity 2021 Web Tool: Novel Chemical Libraries and Additional Methods for an Enhanced Ligand-Based Virtual Screening Experience., Int J Mol Sci. 23(2): 811.

Daina A, Michielin O, Zoete, V. 2017. SwissADME: a free web tool to evaluate pharmacokinetics, drug-likeness and medicinal chemistry friendliness of small molecules. Sci Rep. 7(1):42717.

Daina A, Zoete V. 2016. A boiled-egg to predict gastrointestinal absorption and brain penetration of small molecules. ChemMedChem. 11(11): 1117-1121.

Gasteiger E, Hoogland C, Gattiker A, Wilkins MR, Appel RD, Bairoch A. 2005. Protein identification and analysis tools on the ExPASy server. The Proteomics Protoc Handb. 571–607.

Granchi C, Bertini S, Macchia M, Minutolo F. 2010. Inhibitors of Lactate Dehydrogenase Isoforms and their Therapeutic Potentials, Curr Med Chem. 17(7): 672 – 697.

Iacovino LG, Rossi M, Di Stefano G, Rossi V, Binda C, Brigotti M, Tomaselli F, Pasti AP, Dal Piaz F, Cerini S, Hochkoeppler, A. 2022. Allosteric transitions of rabbit skeletal muscle lactate dehydrogenase induced by pH-dependent dissociation of the tetrameric enzyme. Biochimie. 199:23-35.

Kayamba F, Faya M, Jacob O, Kushwaha B, Deshwar N, Obakachi VA, Nyamori VO, Karpoormath R. 2021. Bioorganic & Medicinal Chemistry Lactate dehydrogenase and malate dehydrogenase: Potential antiparasitic targets for drug development studies. Bioorg Med Chem. 50:116458.

Kim S, Chen J, Cheng T, Gindulyte A, He J, He S, Li, Q, Shoemaker BA, Thiessen PA, Yu B, Zaslavsky L, Zhang J, Bolton EE. 2021. PubChem in 2021: New data content and improved web interfaces. Nucleic Acids Res. 49:D1388-D1395.

Land H, Humble MS. 2018. YASARA: a tool to obtain structural guidance in biocatalytic investigations. Protein Engineering: Methods and Protocols. 43-67.

Liu Y, Grimm M, Dai, W. tao, Hou M. chun, Xiao ZX, Cao Y. 2020. CB-Dock: a web server for cavity detection-guided protein–ligand blind docking. Acta Pharmacol Sin. 41:138–144.

Penna-Coutinho J, Cortopassi WA, Oliveira AA, França TCC, Krettli AU. 2011. Antimalarial Activity of Potential Inhibitors of Plasmodium falciparum Lactate Dehydrogenase Enzyme Selected by Docking Studies. PLoS ONE. 6(7):e21237.

Ren X, Guo X, Liu C, Jing S, Wang T, Wang L, Guan J, Song W, Zhao Y, Shi Y. 2022. Natural flavone hispidulin protects mice from Staphylococcus aureus pneumonia by inhibition of α-hemolysin production via targeting AgrAC Microbiol Res. 261:127071.

Shaaban S, Shaker M, Adam S, El-metwaly NM. 2022. Novel organoselenium-based N -mealanilic acid and its zinc (II) chelate: Catalytic, anticancer, antimicrobial, antioxidant, and computational assessments. J Mol Liq. 363:119907.

Shadrack DM, Nyandoro SS, Munissi JJE, Mubofu EB. 2016. In Silico Evaluation of Anti-Malarial Agents from Hoslundia opposita as Inhibitors of Plasmodium falciparum Lactate Dehydrogenase (PfLDH) Enzyme. Comput Mol Biosci. 6:23–32.

Sievers F, Higgins DG. 2018. Clustal Omega for making accurate alignments of many protein sequences. Protein Sci.27:135–145.

Singh R, Vijah B, Purohit R. 2019. Identification of a novel binding mechanism of quinoline based molecules with lactate dehydrogenase of Plasmodium falciparum. Beilstein Arch. 1-16.

Vivas L, Easton A, Kendrick H, Cameron A, Lavandera J, Barros D, Gomez F, Heras D, Brady RL, Croft SL. 2005. Plasmodium falciparum: Stage specific effects of a selective inhibitor of lactate dehydrogenase. Exp Parasitol. 111:105-114.

Voet D, Voet J. 1995. Biochemistry, 2nd Edition, John Wiley & Sons, Inc., New York, 317

UniProt: the universal protein knowledgebase in 2021. Nucleic acids research. 2021. 49.D1: D480-D489.

WHO, 2022. Retrieval date 27.11.2022. https://www.who.int/news-room/fact-sheets/detail/malaria.

RESEARCH ARTICLE
Eurasian J Bio Chem Sci, 6(2):63-72, 2023
https://doi.org/10.46239/ejbcs.1320487

EJBCS

Eurasian Journal of Biological and Chemical Sciences

Journal homepage: www.dergipark.org.tr/ejbcs

Kırıkhan–Reyhanlı bölgesi tarım topraklarının molibden içeriği ve topraktaki bazı ağır metaller ile ilişkilerinin belirlenmesi

Mehmet Yalçın*

*Hatay Mustafa Kemal Üniversitesi, Ziraat Fakültesi, Toprak Bilimi ve Bitki Besleme Bölümü, Hatay, Türkiye

*Corresponding author : myalcin@mku.edu.tr
Orcid No: https://orcid.org/0000-0002-1690-7681

Received : 27/06/2023
Accepted : 08/08/2023

Özet: Bu çalışmada Hatay ili Kırıkhan-Reyhanlı bölgesi tarım topraklarının molibden içeriğinin belirlenmesi ve toprak içerisindeki bazı ağır metaller ile ilişkilerinin saptanması amaçlanmıştır. Bu amaç için Kırıkhan-Reyhanlı bölgesi tarım topraklarını temsil edecek şekilde iki farklı derinlik (0-20 ve 20-40 cm) ve 30 ayrı noktadan olmak üzere toplamda 60 toprak örneği alınmıştır. Alınan toprak örneklerinde; Kadmiyum (Cd), Kobalt (Co), Krom (Cr), Nikel (Ni), Bakır (Cu), Demir (Fe) ve Molibden (Mo) içerikleri belirlenmiştir. Araştırma sonuçlarına göre; toprakların Cd içerikleri 0.009-0.041 µg/kg; Co içeriği 0.011-0.317 µg/kg; Cr 0.008-0.187 µg/kg, Ni içerikleri 0.787-6.211 ppm; Cu içerikleri 1.11-3.77 ppm; Fe içerikleri 2.80-15.09 ve Mo içerikleri 0.006-0.101 µg/kg arasında bulunmuştur. Toprakların Mo ile Co ve Ni içerikleri arasında pozitif önemli ilişkiler belirlenirken Cr içeriği ile negatif önemli ilişkiler belirlenmiştir. Aynı zamanda Cd ile Co ve Ni; Co ile Ni ve Cu ile Fe aralarında ise pozitif önemli ilişkiler belirlenmiştir. Bölge topraklarının ağır metal içerikleri sınır değerler ile karşılaştırıldığında herhangi bir ağır metal kirliliğine rastlanmamıştır.

Anahtar Kelimeler: Molibden içeriği, Kirkhan-Reyhanli, ağır metaller

Determination of molybdenum content of agricultural soils of Kırıkhan-Reyhanlı region and their relationship with some heavy metals in soil

Abstract: In this study, it was aimed to determine the molybdenum content of agricultural soils in the Kırıkhan-Reyhanlı region of Hatay province and to determine its relations with some heavy metals in the soil. For this purpose, a total of 60 soil samples were taken from two different depths (0-20 and 20-40 cm) and 30 different points, representing the agricultural lands of Kırıkhan-Reyhanlı region. For this purpose, a total of 60 soil samples were taken from two different depths (0-20 and 20-40 cm) and 30 different points, representing the agricultural lands of Kırıkhan-Reyhanlı region. In the soil samples taken; Cadmium (Cd), Cobalt (Co), Chromium (Cr), Nickel (Ni), Copper (Cu), Iron (Fe) and Molybdenum (Mo) contents were determined. According to the research results; Cd contents of soils are 0.009-0.041 µg/kg; Co content 0.011-0.317 µg/kg; Cr 0.008-0.187 µg/kg, Ni contents 0.787-6.211 ppm; Cu contents are 1.11-3.77 ppm; Fe contents were found between 2.80-15.09 and Mo contents between 0.006-0.101 µg/kg. While positive significant relationships were determined between Mo and Co and Ni contents of soils, negative significant relationships were determined with Cr content. Co and Ni with Cd as well; Positive and significant relationships were determined between Co and Ni and Cu and Fe. When the heavy metal contents of the soils of the region were compared with the limit values, no heavy metal pollution was found.

Keywords: Molybdenum content, Kırıkhan-Reyhanlı, heavy metals

1.Giriş

Toprak, tarımsal faaliyetlerini sürdürebilmesi için bitkilerin gereksinim duydukları makro ve mikro besin elementlerinin depolandığı, organizmaların yaşamsal faaliyetlerini sürdürebildiği, canlıların hayatlarını devam ettirebilmeleri için zararlı toksisitelerin olumsuz etkilerini en aza indiren ve doğaya zararlı kirleticileri süzerek dönüşümlerini tamamlayan dinamik bir varlıktır (Acir ve Günal 2020).

Molibden (Mo) doğada nispeten düşük toksisiteye sahip önemli bir elementtir (İpek 2003). Molibden; atomik ağırlığı 95.94, koyu gri siyah renkte yanıcı özellikte olup peryodik cetvelin VI-B serisinde çözünebilen ve çözünemeyen bileşikler şeklinde yer almaktadır (Barceloux 1999). Toprak bünyesinde yetiştirilen bitkilerdeki Mo içeriği; geniş oranda toprağın Mo içeriği ve pH'sı ile

mevsimsel farklılıklara göre değişiklik göstermektedir (McDowell 1992).

Günümüzde artan sanayileşme ve kentleşme ile beraber çeşitli çevre kirlilikleri artmış ve birçok çevresel problem ortaya çıkmıştır. Bu problemlerin başında gelen ağır metaller, hava, toprak ve su kaynaklarında kirliliklere neden olmaktadırlar. Bitki fizyolojisini olumsuz etkileyerek, bitkisel üretimin azalmasına neden olan ağır metaller, besin zinciri yoluyla canlı sağlığını da tehdit altına alırlar (Yerli ve ark. 2020). Ağır metaller, çevredeki konsantrasyonlarının artması ile bir yandan canlı organizmalar için gerekli olan ve diğer yandan yaşamlarında olumsuz bir faktör oluşturan önemli bir çevresel faktördür. Sanayi kuruluşlarının faaliyetleri, araba egzozları ve uygarlığın diğer özellikleri, topraktaki ağır metal içeriğini artırmakta ve sonuç olarak kalitelerini olumsuz yönde etkilemektedir (Breus ve Yevtushenko 2022). Ağır metaller toprak ana materyalinde oluşurken insan aktiviteleri sunucu topraklara katılım ile birlikte miktarları devamlı olarak artmaktadır. Bu katılımlar kimyasal gübreler, endüstriyel atıklar, maden kalıntıları ve otomobil emisyon gazları ile olabilmektedir. Başlıca zararlı ağır metaller; Krom (Cr), Kadmiyum (Cd), Bakır (Cu), Kurşun (Pb), Mangan (Mn), Molibden (Mo), Nikel (Ni) ve Çinko (Zn)'dur (Akyıldız ve Karataş 2018).

Hızlı kentleşme ve nüfus artışı ile birlikte sanayileşmenin yarattığı çevre sorunları tarımsal alanları tehdit eder boyutlara ulaşmakta, bu sorunlar başta bilinçsiz gübre ve ilaç kullanımı gibi tarımın kendi iç dinamikleri ile oluşan sorunlara ilave olarak ve her geçen büyüyerek karşımıza çıkmaktadır (Şimşek ve ark. 2021). Tarım alanlarında kirliliğe neden olan ve gittikçe daha büyük boyutlarda tehlike oluşturan etmenlerin başında potansiyel ağır metal elementler gelmektedir (Şimşek ve ark. 2021). Önemli bir kirletici grubu oluşturdukları bilinen bu elementler, bitkisel üretimde verimliliği olumsuz etkilemesi yanında, besin zincirine de girerek insan ve hayvan sağlığını da tehdit etmektedir (Şimşek ve ark. 2021). Bakır, çinko, mangan, demir ve molibden gibi ağır metaller bitkiler için gerekli besin maddeleri olmalarının yanında doğal olarak topraklarda bulunurlar. Aynı zamanda çeşitli yollarla (asit yağışlar, gübreler, çöpler vb.) toprağa önemli miktarda ağır metallerin girişi mümkün olmaktadır. Bu şekilde toprak içerisine intikal eden civa, kadmiyum ve nikel gibi ağır metaller toprağın kolloid kompleksi tarafından toprakta ve humusta tutulurlar. Bundan dolayı toprak organizmaları üzerindeki toksik etkileri nedeniyle ölümlerine yol açarlar. Dolayısıyla ölü örtü ayrışması engellenmiş olur ve toprak strüktürü bozulmaya uğramış olur (Tolunay 1992).

Tarım topraklarının en önemli kirleticilerinden olan ağır metaller ile ilişkili ülkemizde birçok çalışma yapılmıştır. Aynı bölgede yapılan çalışmada, Yalçın ve Çimrin (2019) Hatay ili Kırıkhan-Reyhanlı arası çayır-mera topraklarının molibden içeriğinin belirlenmesi ve toprak içerisindeki bazı ağır metaller ile ilişkilerinin saptanması amaçlamışlardır. Çalışma sonucuna göre; toprakların kadmiyum içerikleri 0.01-0.32 ppm; kobalt içeriği 0.01-4.97 ppm; nikel içerikleri 0.00-20.00 ppm; kurşun içerikleri 3.00-67.00 ppm; bakır içerikleri 0.26-7.48 ppm; demir içerikleri 4.00-61.00 ve molibden içerikleri 0.001-0.064 ppm arasında bulunmuştur. Toprakların Mo ile Co, Ni, Pb, Cu ve Fe içerikleri arasında pozitif önemli ilişkiler belirlenmiştir. Aynı zamanda Cd ile Co; Co ile Ni, Pb, Fe; Pb ile Cu, Fe ve Cu ile Fe aralarında pozitif önemli ilişkiler belirlenmiştir. Bölge topraklarının ağır metal içerikleri sınır değerler ile karşılaştırıldığında herhangi bir ağır metal kirliliğine rastlanmamıştır. Yakın bir bölgede, Şimşek ve ark. (2021) Osmaniye ilinin tarım topraklarındaki ağır metallerin kirlilik düzeylerinin belirlenmesini amaçlamışlardır. Çalışma sonucuna göre; toplam Mn içeriğinin (% 42), toplam Fe (% 100), toplam Ni (% 58), toplam Cd (% 48) ve toplam Cr (% 28.4) konsantrasyonunun Türkiye'de Toprak Kirliliğinin Kontrolü Yönetmeliğine göre pH'sı 6'nın üzerinde olan topraklarda kabul edilen toplam sınır değerlerin üzerinde olduğunu belirlemişlerdir. Elde edilen sonuçlara göre; bu metallerin yapılacak araştırmalarda bitkilere, hayvanlara ve insanlara gıda zinciriyle geçişinin dikkatlice izlenmesi ve gıda güvenliği açısından önemli olup olmadığının uygun ekstraktörlerle analiz edilip söz konusu ekstraktörün, koreleasyon kalibrasyon çalışmaları ile seçilmesi sonucu elde edilen verilerin, limit değerlerle karşılaştırılıp toksik olup olmayacağının farklı bir araştırma ile netleştirilmesi gerektiğini ortaya koymuşlardır. Başka bir çalışmada, Küçük ve Karaoğlu (2021) Iğdır ili 080 devlet karayolu boyunca tarım topraklarında ağır metal kirliliğinin durumunu araştırmışlardır. Çalışma sonucuna göre; otoyola daha yakın mesafe, daha yüksek element konsantrasyonları ölçülmüştür. Uzaklıktan en çok etkilenen elementler demir ve çinko olmuştur ($p > 0.01$) ve bunları nikel ($p < 0.05$), manganez ve bakır ($p = 0.05$'e yakın) izlemiştir. Otoyoldan 0 ila 10 m uzaklıktaki bölge en kirli bölge olmuştur. Kirlilik indeksleri (PI), toplam konsantrasyonlar için Ni> Cu> Zn> Fe> Mn ve alınabilir değerler için Cu> Zn> Mn> Fe> Ni şeklinde sıralanmıştır. Kirlilik yük endeksleri (PLI) genel olarak nikel (Ni) değerleri dışında toplam mikro besinlerin kirlilik endekslerinden (PI) daha yüksek ve genellikle alınabilir değerlerin kirlilik endekslerinden (PI) daha düşük hesaplanmıştır. Ni ve Cu'nun nispeten daha kısa sürede çevre açısından riskli seviyelere ulaşma ihtimalinin yüksek olduğu sonucuna varılabilir.

Çalışmada Hatay ili Kırıkhan-Reyhanlı bölgesi tarım topraklarının molibden düzeyi ve bunların toprak içerisindeki bazı ağır metaller ile ilişkileri belirlenerek, tarım topraklarının dolayısı ile buradan çiftçilik ile geçinen çiftçilerin elde ettikleri verim ve kaliteye katkı sağlamak amaçlanmıştır.

2.Materyal Ve Yöntem

2.1.Materyal

Çalışmada yöreyi temsil edecek şekilde Hatay ili Kırıkhan-Reyhanlı bölgesindeki tarım toprakları alanlarından 30 noktadan, 0-20 ve 20-40 cm derinliklerinden toplamda 60 toprak örneği usulüne uygun olarak alınmıştır (Tablo 1., Şekil 1.). Aynı gün laboratuvara getirilen toprak örnekleri gölgede hava kurusu olacak biçimde kurutulmuş ve 2 mm' lik elekten geçirilerek analize hazır hale getirilmiştir.

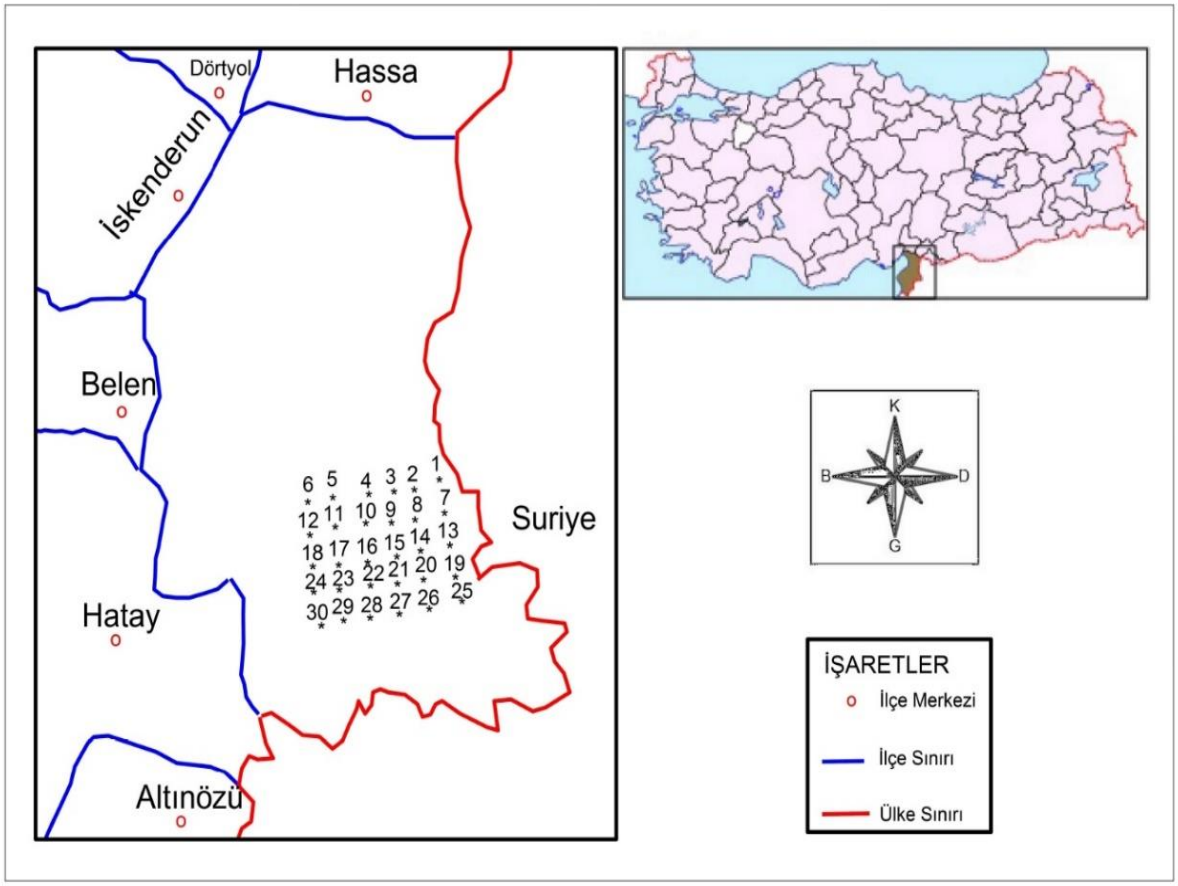

Şekil 1. Alınan Toprak örneklerinin Kırıkhan-Reyhanlı İlçe haritası Üzerindeki Gösterimi

2.2. Yöntem

Toprakların pH değerleri saturasyon çamuru ekstraktında pH metre ile toplam çözünebilir tuz içerikleri ise elektriksel iletkenlik aletinde ölçülerek belirlenmiştir (Horneck ve ark. 1989). Toprakların kireç ($CaCO_3$) içerikleri Scheibler kalsimetresi aleti ile dört tekrarlamalı olarak ölçülmüştür (Nelson 1982). Bünye hidrometre yöntemi ile belirlenmiştir (Bouyoucos 1952). Toprakların organik madde içerikleri, Nelson ve Sommers (1982) tarafından bildirildiği şekilde modifiye edilmiş Walkley-Black yöntemiyle belirlenmiştir. Katyon değişim kapasitesi, sodyum asetat (1N pH: 8.2) ekstraksiyon yöntemi ile (Rhoades 1982). Toprakların yarayışlı kadmiyum (Cd), kobalt (Co), krom (Cr), nikel (Ni), bakır (Cu), demir (Fe) ve molibden (Mo) Lindsay ve Norvell (1978)'e göre 0.005 M DTPA+0.01 M $CaCI_2$+0.1 M TEA (pH 7.3) ekstraktında belirlenmiştir. Toprak özellikleri ile besin elementleri arasındaki korelasyon ve regresyon analizleri SPSS 17 istatistik programında yapılmıştır (Düzgüneş ve ark. 1987).

3.Araştırma Bulguları ve Tartışma

3.1.Toprakların Bazı Fiziksel ve Kimyasal Özellikleri

Araştırmada kullanılan toprak özelliklerinin bazı fiziksel ve kimyasal özelliklerine ait bulgular verilmiştir. Araştırma topraklarının pH içeriği 7.57 ile 8.36 arasında değişerek ortalama olarak 7.96 olup toprak örneklerinin pH'larının tamamının hafif alkalin reaksiyonlu olduğu görülmüştür. Toprakların tuz içeriği % 0.020-0.083 arasında farklılık gösterirken ortalama olarak % 0.041 olup çalışma alanı topraklarının hemen hemen hepsinin tuzsuz sınıfa ait oldukları bulunmuştur. Kırıkhan-Reyhanlı bölgesi tarım topraklarının sırasıyla kil, kum ve silt miktarları ortalama olarak % 49.10, 15.58 ve 35.41 bulunmuştur. Araştırma topraklarının kireç içerikleri % 5.66-51.14 arasında değişirken ortalama % 22.21 olarak genellikle orta kireçli ile çok fazla kireçli topraklar olarak belirlenmiştir. Topraklarının organik madde içeriği % 1.42-4.10 olarak belirlenirken ortalama organik madde % 2.63 bulunmuştur. Topraklarda katyon değişim kapasitesi (KDK) incelendiğinde; toprak örneklerinin 16.89-42.10 me /100 g olarak bulunmuş olup ortalama KDK içeriği ise 31.53 me/100 g olarak bulunmuştur (Yalçın 2023).

Tablo 1. Toprak örneklerinin alındığı yerler

Toprak No	Örnek Yeri	GPS ile N/E Koordinatları	Toprak No	Örnek Yeri	GPS İle N/E Koordinatları
1	Başpınar	(54.2910 - 40.3829)	16	Özkızılkaya-3	(54.4676 - 40.3183)
2	Muratpaşa-1	(54.2162 - 40.3762)	17	Özkızılkaya-4	(54.3927 - 40.3116)
3	Muratpaşa-2	(54.1415 - 40.3696)	18	Akkuyu	(54.3178 - 40.3049)
4	Muratpaşa-3	(54.0667 - 40.3629)	19	Hamam Köyü-1	(54.9522 - 40.2931)
5	Baldıran-1	(53.9920 - 40.3563)	20	Hamam Köyü-2	(54.8536 - 40.2898)
6	Baldıran-2	(53.9172 - 40.3496)	21	Hamam Köyü-3	(54.7549 - 40.2866)
7	Mrtpş-Kızılkaya-1	(54.5006 - 40.3614)	22	Kaletepe-1	(54.6562 - 40.2833)
8	Mrtpş-Kızılkaya-2	(54.4258 - 40.3547)	23	Kaletepe-2	(54.5575 - 40.2800)
9	Mrtpş-Kızılkaya-3	(54.3511 - 40.3481)	24	Muharrem	(54.4588 - 40.2767)
10	Mrtpş-Kızılkaya-4	(54.2763 - 40.3414)	25	Doğu Ayrancı	(54.9716 - 40.2481)
11	Özkızılkaya-1	(54.2016 - 40.3348)	26	Ahmetbeyli-1	(54.8717 - 40.2477)
12	Baldıran-3	(54.1268 - 40.3281)	27	Ahmetbeyli-2	(54.7718 - 40.2473)
13	Akpınar-1	(54.6923 - 40.3383)	28	Paşahöyük-1	(54.6719 - 40.2468)
14	Akpınar-2	(54.6174 - 40.3316)	29	Paşahöyük-2	(54.5720 - 40.2464)
15	Özkızılkaya-2	(54.5425 - 40.3250)	30	Kırcaoğlu	(54.4721 - 40.2460)

3.2. Toprak Örneklerinin Bazı Besin Elementi İçerikleri

Araştırmada kullanılan toprak özelliklerinin bazı besin elementi özelliklerine ait bulgular Çizelge 3'de verilmiştir.

Kadmiyum

Araştırma topraklarının kadmiyum içerikleri örneklerde en düşük 0.009 µg/kg iken, en yüksek kadmiyum içeriği 0.041 µg/kg olarak belirlenmiştir. Toprakların 0-20 cm derinliğindeki örneklerinin ortalama kadmiyum içeriği 0.019 µg/kg iken 20-40 cm derinlikteki örneklerde ise 0.018 µg/kg olup iki derinlikte ortalama olarak 0.019 µg/kg bulunmuştur (Tablo 2.). Farklı bir bölgede yapılan çalışmada, Özkan ve demir (2023) Rize ilinde geleneksel ve organik çay tarımı yapılan alanların topraklarında bazı verimlilik parametreleri ile ağır metal içeriklerinin karşılaştırıldığı çalışma sonucunda toprakların Cd içeriği yönünde çok düşük seviyelerde olduğunu belirleyerek benzer sonuçlar ortaya koymuşlardır. Aynı zamanda, Karaaslan ve ark. (2014) tarafından yapılan bir çalışma, Türkiye'nin farklı bölgelerindeki tarım topraklarında kadmiyum seviyelerini incelemiştir. Bu çalışmada da, toprakların genel olarak düşük kadmiyum içeriğine sahip olduğu bulunmuştur.

Kobalt

Kırıkhan-Reyhanlı alanı tarım topraklarının alınabilir kobalt içerikleri en düşük 0.011 µg/kg iken, en yüksek 0.317 µg/kg olarak belirlenmiştir. Toprakların 0-20 cm derinliğindeki ortalama kobalt içeriği 0.077 µg/kg iken 20-40 cm derinlikteki örneklerde ortalama ise 0.068 µg/kg olup ortalama olarak 0.076 µg/kg bulunmuştur (Tablo 2.). Türkiye'de yer alan tarım topraklarındaki kobalt içeriği üzerine Şahin ve ark. (2016) tarafından yapılan bir çalışmada, Türkiye'nin bazı bölgelerindeki tarım topraklarında kobalt seviyeleri incelenmiştir. Bu çalışmada da, tarım topraklarının genel olarak düşük kobalt içeriğine sahip olduğu belirlenmiş olup benzer sonuçlar ortaya konmuştur.

Krom

Toprakların krom içeriği örneklerde en düşük 0,008 µg/kg iken, en yüksek krom içeriği 0.187 µg/kg olarak belirlenmiştir. Toprakların 0-20 cm derinliğindeki örneklerinin ortalama krom içeriği 0.034 µg/kg iken 20-40 cm derinlikteki örneklerde ise 0,039 µg/kg olup iki derinlikte ortalama olarak 0.038 µg/kg bulunmuştur (Tablo 2.). Farklı bir bölgede yapılan çalışmada, Özkan ve Demir (2023) Rize ilinde geleneksel ve organik çay tarımı yapılan alanların topraklarında bazı verimlilik parametreleri ile ağır metal içeriklerinin karşılaştırıldığı çalışma sonucunda toprakların Cr içeriği yönünde çok düşük seviyelerde olduğunu belirleyerek benzer sonuçlar ortaya koymuşlardır. Şahin ve ark. (2013) tarafından yapılan bir çalışmada, Türkiye'nin bazı bölgelerindeki tarım topraklarında krom seviyelerini incelemiştir. Bu çalışmada da, toprakların genel olarak düşük krom içeriğine sahip olduğu tespit edilmiş olup yakın sonuçlar ortaya konmuştur.

Tablo 2. Hatay ili Kırıkhan-Reyhanlı bölgesi tarım topraklarının Cd, Co, Cr, Ni, Cu, Fe, Mo içerikleri

Toprak No	Derinlik	Cd	Co	Cr	Ni	Cu	Fe	Mo	Bünye
		µg/kg	µg/kg	µg/kg	mg/kg	mg/kg	mg/kg	µg/kg	Sınıfı
1	0-20	0.010	0.056	0.029	1.64	3.26	8.55	0.020	C
	20-40	0.010	0.048	0.123	1.80	3.70	9.09	0.025	C
2	0-20	0.009	0.054	0.013	1.09	2.79	8.79	0.019	C
	20-40	0.011	0.040	0.027	0.96	2.52	7.65	0.012	C
3	0-20	0.020	0.134	0.035	2.05	2.51	6.50	0.036	C
	20-40	0.020	0.077	0.032	1.93	2.36	6.29	0.027	C
4	0-20	0.027	0.033	0.048	2.11	2.68	7.24	0.030	C
	20-40	0.028	0.023	0.014	2.13	2.33	7.34	0.024	C
5	0-20	0.041	0.259	0.027	5.45	2.25	5.26	0.038	C
	20-40	0.028	0.251	0.039	6.21	2.29	5.97	0.039	C
6	0-20	0.014	0.029	0.020	2.59	2.09	5.00	0.014	C
	20-40	0.015	0.030	0.038	2.92	2.40	5.81	0.022	C
7	0-20	0.018	0.152	0.024	2.19	2.91	6.87	0.018	SiC
	20-40	0.017	0.057	0.034	1.66	2.54	6.33	0.017	C
8	0-20	0.014	0.048	0.042	1.81	2.79	7.64	0.022	C
	20-40	0.012	0.033	0.013	1.70	2.66	7.36	0.011	C
9	0-20	0.019	0.039	0.037	1.84	2.77	3.67	0.043	C
	20-40	0.016	0.026	0.017	2.05	2.89	4.06	0.042	C
10	0-20	0.011	0.167	0.012	1.66	2.95	9.97	0.022	C
	20-40	0.011	0.067	0.047	1.47	2.68	11.58	0.026	C
11	0-20	0.021	0.137	0.030	1.93	3.05	6.94	0.023	C
	20-40	0.024	0.317	0.076	2.16	3.28	6.92	0.031	C
12	0-20	0.015	0.055	0.038	1.27	2.60	6.32	0.023	SiC
	20-40	0.013	0.026	0.052	0.93	2.51	7.35	0.016	SiC
13	0-20	0.012	0.035	0.026	0.89	2.93	6.66	0.024	SiC
	20-40	0.010	0.040	0.015	1.08	2.85	7.11	0.012	SiC
14	0-20	0.019	0.239	0.015	2.08	3.75	6.37	0.027	SiC
	20-40	0.020	0.132	0.023	1.98	3.74	8.16	0.029	SiC
15	0-20	0.016	0.064	0.034	1.66	2.17	3.06	0.054	C
	20-40	0.014	0.042	0.027	1.15	1.95	2.80	0.055	C
16	0-20	0.016	0.028	0.026	1.22	2.86	7.46	0.015	C
	20-40	0.016	0.016	0.039	1.13	3.42	8.84	0.016	SiC
17	0-20	0.011	0.016	0.024	0.90	3.13	6.92	0.013	C
	20-40	0.011	0.013	0.130	0.86	3.12	7.07	0.014	C
18	0-20	0.019	0.030	0.120	1.25	3.58	8.26	0.019	C
	20-40	0.018	0.011	0.041	0.92	3.28	7.75	0.006	SiC

19	0-20	0.020	0.060	0.022	1.29	1.48	5.08	0.017	CL
	20-40	0.019	0.035	0.023	1.27	1.48	4.95	0.018	CL
20	0-20	0.026	0.043	0.026	1.64	1.78	9.67	0.014	CL
	20-40	0.027	0.046	0.020	1.71	1.86	11.64	0.016	CL
21	0-20	0.019	0.239	0.015	1.20	1.11	3.63	0.011	CL
	20-40	0.019	0.233	0.064	1.07	1.16	3.84	0.009	CL
22	0-20	0.019	0.024	0.012	1.35	1.96	11.03	0.019	SiC
	20-40	0.019	0.032	0.025	1.44	1.98	10.22	0.022	SiC
23	0-20	0.021	0.062	0.023	1.51	2.87	7.99	0.101	C
	20-40	0.021	0.055	0.029	1.50	2.79	8.55	0.100	SiC
24	0-20	0.021	0.020	0.028	1.59	3.35	13.97	0.024	C
	20-40	0.022	0.021	0.022	1.64	3.24	14.30	0.024	C
25	0-20	0.022	0.048	0.032	1.01	3.59	7.84	0.008	C
	20-40	0.021	0.032	0.031	1.03	3.51	8.10	0.019	C
26	0-20	0.022	0.032	0.013	0.79	3.38	6.64	0.009	C
	20-40	0.024	0.057	0.035	0.90	3.53	7.04	0.011	C
27	0-20	0.024	0.119	0.187	1.89	2.56	5.24	0.024	SiC
	20-40	0.022	0.106	0.030	1.62	2.48	3.82	0.019	C
28	0-20	0.022	0.027	0.031	1.43	2.15	5.20	0.008	SiC
	20-40	0.023	0.028	0.033	1.31	2.13	5.28	0.011	SiC
29	0-20	0.014	0.034	0.008	0.80	2.14	5.07	0.013	CL
	20-40	0.015	0.113	0.031	1.30	2.33	5.09	0.018	CL
30	0-20	0.019	0.034	0.037	1.48	3.40	11.89	0.023	CL
	20-40	0.018	0.044	0.030	1.62	3.77	15.09	0.021	CL
Min		0.009	0.011	0.008	0.787	1.11	2.80	0.006	
Max		0.041	0.317	0.187	6.211	3.77	15.09	0.101	
Ort. (Av.)	**0-20**	0.019	0.077	0.034	1.653	2.70	7.16	0.024	
Ort. (Av.)	**20-40**	0.018	0.068	0.039	1.648	2.69	7.51	0.025	
	Ort. (Av.)	0.019	0.076	0.038	1.710	2.69	7.39	0.025	

Nikel

Çalışma alanı tarım topraklarının bütününün değişebilir nikel içeriği en düşük 0.787 mg/kg iken, en yüksek 6.211 mg/kg olarak belirlenmiştir. Toprakların 0-20 cm derinliğindeki örneklerinin ortalama değişebilir Nikel içeriği 1.653 mg/kg iken 20-40 cm derinliklerde ise 1.653 mg/kg olup, her iki derinlikte ortalama 1.710 mg/kg olarak bulunmuştur (Tablo 2.). Farklı bir bölgede yapılan çalışmada, Taş ve Demir (2023) Bingöl ovası tarım topraklarının verimlilik düzeyi ile bazı ağır metal içeriklerinin belirlenmesini amaçladıkları çalışma sonucunda toprakların Ni içeriği yönünden ortalama 7.22 mg/kg seviyelerde olduğunu belirleyerek benzer sonuçlar ortaya koymuşlardır. Aynı zamanda, Tüfekçi ve ark. (2019) tarafından yapılan bir çalışma, Türkiye'nin bazı bölgelerindeki tarım topraklarında nikel seviyelerini incelemiştir. Bu çalışmada da, tarım topraklarının genel olarak orta düzeyde nikel içeriğine sahip olduğu tespit edilmiş olup yapılan çalışma ile benzer sonuçlar ortay koymuştur.

Bakır

Kırıkhan-Reyhanlı bölgesi tarım toprakların bakır içeriği örneklerde en düşük 1.11 mg/kg iken, en yüksek bakır 3.77 mg/kg olarak belirlenmiştir. Toprakların 0-20 cm derinliğindeki örneklerinin ortalama bakır içeriği 2.70 mg/kg iken 20-40 cm derinlikteki örneklerde ise 2.69 mg/kg olup iki derinlikte ortalama olarak 2.69 mg/kg bulunmuştur.

Toprak örneklerinin alınabilir bakır içeriği yönünden Linsay ve Norvell (1978) bildirdiği sınır değerler ele alındığında toprakların % 15'inin yetersiz düzeyde (<2 mg/kg) olduğu belirlenir iken geri kalan toprakların % 85'inin ise alınabilir bakır içeriği bakımından yeterli düzeyde (>2 ppm) olduğu görülmüştür (Tablo 2.). Benzer bir çalışmada, Kırat ve Savcı (2023) Ulutaş Köyü (Erzurum) bölgesindeki topraklarda ağır metal kirliliğinin belirlenmesini araştırdıkları çalışma sonuçlarına göre, toprakların Cu içeriğinin 14.10-49.40 mg/kg değerleri arasında yüksek düzeyde belirleyerek benzer sonuçlar ortaya koymuşlardır. Aynı zamanda, Al-Adham ve ark. (2016) tarafından Konya Havzası'ndaki tarım topraklarının bakır içeriği incelenmiştir. Araştırma sonuçlarına göre, Konya Havzası'ndaki tarım topraklarının bakır içeriği genellikle düşük ila orta düzeyde bulunmuştur. Bu bulgu, Kırıkhan-Reyhanlı bölgesindeki tarım topraklarının bakır içeriği bulgularıyla benzerlik göstermektedir.

Demir

Çalışma alanının topraklarının alınabilir demir içerikleri örneklerde en düşük 2.80 mg/kg iken, en yüksek demir içeriği 15.09 mg/kg olarak belirlenmiştir. Toprakların 0-20 cm derinliğindeki örneklerinin ortalaması demir içeriği 7.16 mg/kg iken 20-40 cm derinlikteki örneklerde ise 7.51 mg/kg olup her iki derinliğin ortalaması olarak 7.39 mg/kg olarak bulunmuştur. Toprak örneklerinin Viets ve Lindsay (1973)'in ortaya koyduğu sınır değerlere göre net bir şekilde demir noksanlığı (<2.5 mg/kg) gösteren topraklar belirlenememiştir. Kritik demir noksanlığı gösterme olasılığı bulunan (2.5-4.5 mg/kg) topraklar % 11.66 iken % 88.34'ü ise alınabilir demir açısından iyi (>4.5 mg/kg) durumda topraklardır (Tablo 2.). Benzer bir çalışmada, Alkayın ve Yıldız (2023) Doğu Karadeniz yöresinde üretilen bazı çayların mineral beslenme durumunu belirledikleri çalışma sonucunda toprakların Fe içeriğinin % 93 oranında yüksek ve yeterli düzeyde belirleyerek benzer sonuçlar ortaya koymuşlardır. Aynı zamanda, Güneş ve ark. (2007) tarafından Türkiye'nin farklı bölgelerindeki tarım topraklarının demir içeriği incelenmiştir. Araştırma sonuçlarına göre, Türkiye genelindeki tarım topraklarının demir içeriği çeşitli bölgelerde farklılık göstermekle birlikte genellikle orta düzeyde bulunmuştur. Bu bulgu, çalışma alanındaki toprakların demir içeriği bulgularıyla uyumlu görünmektedir.

Molibden

Kırıkhan-Reyhanlı alanı tarım topraklarının alınabilir molibden içeriği örneklerde en düşük 0.006 µg/kg iken, en yüksek molibden 0.101 µg/kg olarak belirlenmiştir. Toprakların 0-20 cm derinliğindeki örneklerinin ortalaması molibden içeriği 0.024 µg/kg iken 20-40 cm derinlikteki örneklerde ise 0.025 µg/kg olup her iki derinliğin ortalaması olarak 0.025 µg/kg olarak bulunmuştur. Kırıkhan-Reyhanlı bölgesi tarım topraklarının hepsinin alınabilir molibden içerikleri Viets ve Lindsay (1973)'e göre yeterli düzeyde (>1 ppm) olduğu görülmüştür (Tablo 2.). Aynı bölgede yapılan bir çalışmada, Yalçın ve Çimrin (2019) Kırıkhan-Reyhanlı çayır mera toprakların molibden içeriği yönünden yapılan çalışma ile benzer sonuçlar ortaya koymuşlardır. Özçelik ve ark. (2010) tarafından Türkiye'nin bazı bölgelerindeki tarım topraklarının molibden içeriği incelenmiştir. Araştırma sonuçlarına göre, Türkiye genelinde tarım topraklarının molibden içeriği düşük düzeyde bulunmuştur. Bu bulgu, Kırıkhan-Reyhanlı alanındaki toprakların molibden içeriği bulgularıyla uyumlu görünmektedir.

3.3.Alınabilir Molibden İçeriği ile Diğer Bazı Toprak Ağır Metal Özellikleri Arasındaki İlişkiler

Araştırma konusu toprakların ağır metal içerikleri ile alınabilir molibden arasındaki ilişkiler Tablo 3'de verilmiştir. Tablonun incelenmesinden de anlaşılacağı gibi toprakların Mo ile Co (r: 0.11*; Şekil 2) ve Ni (r: 0.25*; Şekil 3) içerikleri arasında pozitif önemli ilişkiler belirlenir iken Mo ile Cr (r: -0.03*; Şekil 4) içerikleri arasında ise negatif önemli ilişki belirlenmiştir. Aynı bölge topraklarında yaptıkları çalışmada, Yalçın ve Çimrin (2019) Kırıkhan-Reyhanlı çayır mera topraklarının Ni ve Co yönünden pozitif korelasyon gösterdiğini belirleyerek benzer sonuçlar ortaya koymuşlardır. Yu ve ark. (2018) tarafından yapılan bir çalışma, Mo, Co, Ni ve Cr gibi elementlerin topraklardaki ilişkilerini incelemiştir. Bu çalışma, Mo'nin Co ve Ni ile pozitif korelasyon gösterdiğini ve Cr ile negatif korelasyon gösterdiğini bulmuştur. Bu bulgular, Kırıkhan-Reyhanlı bölgesindeki toprakların element içerikleri arasındaki ilişkilerle uyumlu görünmektedir. Ayrıca toprakların Cd içeriği ile Co (r: 0.57***) ve Ni (r: 0.53***) içerikleri arasında oldukça önemli pozitif ilişkiler belirlenmiştir. Arıkan ve ark. (2019) tarafından yapılan bir çalışma, tarım topraklarında Cd ile Co ve Ni arasında pozitif ilişkiler olduğunu göstermiştir. Bu bulgular, verilerin bu çalışmadaki sonuçlarla uyumlu olduğunu göstermektedir. Toprakların Co içeriği ile Ni (r: 0.53***) içeriği arasında pozitif önemli ilişki belirlenirken Co içeriği ile Fe (r: -0.27*) içeriği arasında ise negatif önemli ilişki belirlenmiştir. Karaca ve ark. (2020) tarafından yapılan bir çalışma, tarım topraklarında Co ile Ni arasında pozitif ilişkiler ve Co ile Fe arasında negatif ilişkiler olduğunu göstermiştir. Bu bulgular, verilerin bu çalışmadaki sonuçlarla uyumlu olduğunu göstermektedir. Bununla birlikte Cu içeriği ile Fe (r: 0.44***) içeriği arasında önemli pozitif ilişkiye belirlenmiştir. Canlı ve ark. (2020) tarafından yapılan bir çalışma, tarım topraklarında Cu ile Fe arasında pozitif bir ilişki olduğunu göstermiştir. Bu bulgu, verilerin bu çalışmadaki sonuçlarla uyumlu olduğunu göstermektedir.

Tablo 3. Kırıkhan-Reyhanlı bölgesi tarım topraklarının molibden ile bazı toprak ağır metal içerikleri arasındaki korelasyon katsayıları (r)

	Mo mg/kg	Cd mg/kg	Co mg/kg	Cr mg/kg	Ni mg/kg	Cu mg/kg
Cd mg/kg	0.16					
Co mg/kg	0.11*	0.36***				
Cr mg/kg	-0.03*	-0.01	0.07			
Ni mg/kg	0.25*	0.53***	0.53***	0.01		
Cu mg/kg	0.03	-0.15	-0.13	0.18	-0.10	
Fe mg/kg	-0.06	-0.03	-0.27*	-0.05	-0.11	0.44***

* 0.05 düzeyinde önemli, *** 0.001 düzeyinde önemli

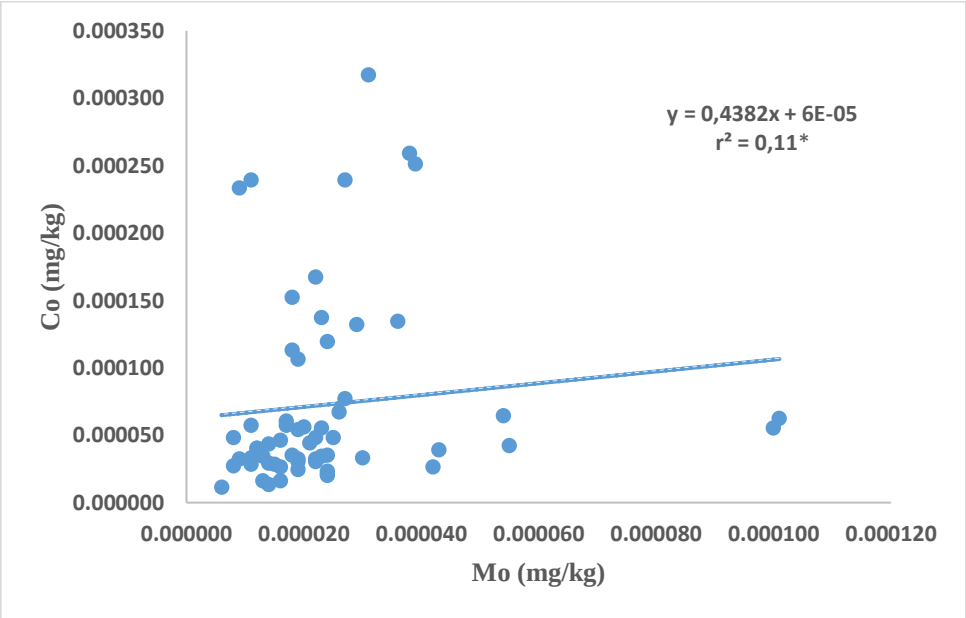

Şekil 2. Toprak öneklerinin yarayışlı Mo ile Co içerikleri arasındaki ilişki

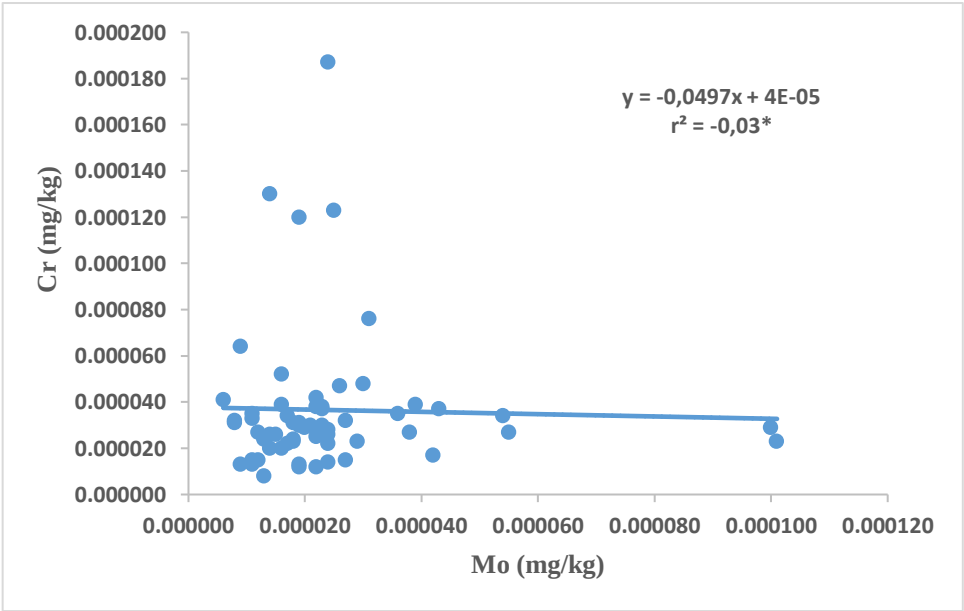

Şekil 3. Toprak öneklerinin yarayışlı Mo ile Cr içerikleri arasındaki ilişki

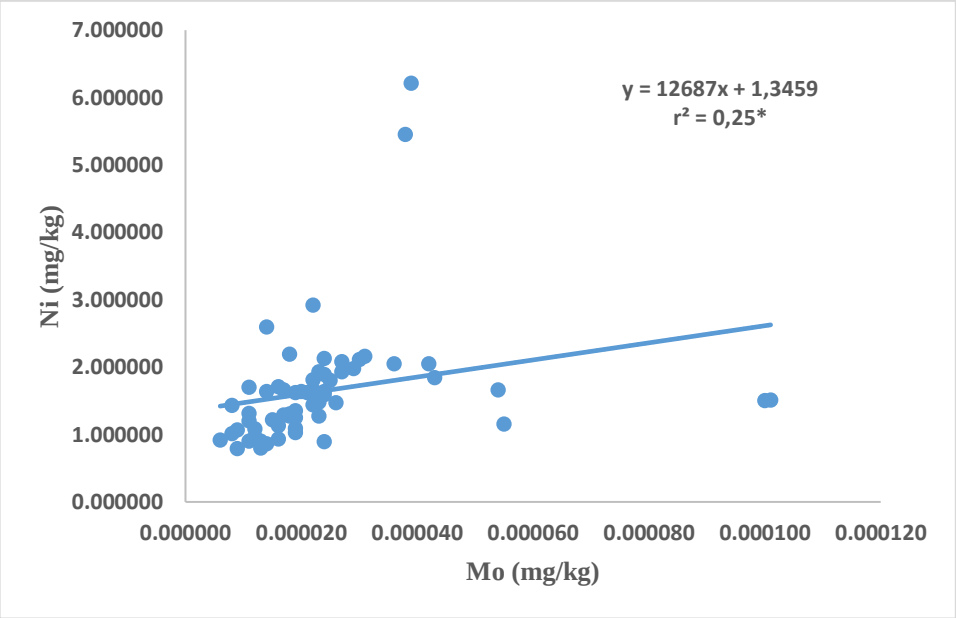

Şekil 4. Toprak öneklerinin yarayışlı Mo ile Ni içerikleri arasındaki ilişki

4.Sonuç

Hatay ili Kırıkhan-Reyhanlı bölgesi tarım topraklarının yarayışlı molibden durumu incelenmiş ve topraktaki bazı ağır metal içerikleriyle ilişkisi belirlenmeye çalışılmıştır. Bu görüş doğrultusunda, araştırma sonucunda elde edilen Kırıkhan-Reyhanlı tarım toprakları örneklerine ait değerlerin Türkiye ve Dünya'da toprakta izin verilen ağır metal sınır değerleri ile karşılaştırıldığında; çalışma alanı topraklarında ağır metal birikiminin kabul edilebilir sınır değeri içerisinde olduğu görülmüştür. Bu çalışma bize göstermiştir ki; topraklardaki tarımsal ve endüstriyel faaliyetlerin neden olduğu ağır metal kirliliğinin özellikle insanların sağlığı açısından meydana getirebileceği zararın en düşük seviyede olduğu görülmüştür. Araştırma bölgesi tarım topraklarının insan ve hayvan sağlığı açısından zararlı seviyelerde bulunmayan ağır metal içeriklerinin sınır değerlerin üzerine çıkmaması için gerekli tedbirlerin bir an önce alınması oldukça önemlidir. Özellikle çalışma alanı tarım topraklarına yakın bulunan sanayi ve endüstri alanlarında yer alan işletmelerin ve fabrikaların çok sıkı şekilde denetlenmesi kaçınılmaz bir sonuçtur.

Kaynaklar

Acir N, Günal H. 2020. Spesifik yüzey alanı belirlenmesinde organik madde, kireç ve demir oksitlerin uzaklaştırılmasının önemi. TTDB, 7(1):205-211.

Akyıldız M, Karataş B. 2018. Adana şehir merkezindeki topraklarda ağır metal kirliliğinin araştırılması. Ç.Ü. Müh. Fak. Dergisi, 33(2):199-214.

Al-Adham A, Tüfekçi N, Aydın M, Yıldız A. 2016. Determination of heavy metal pollution in Konya Basin agricultural soils. FEB, 25(9):3544-3551.

Alkayın M, Yıldız N. 2023. Doğu Karadeniz yöresinde üretilen bazı çayların mineral beslenme durumunun değerlendirilmesi. EJOSAT, 50:162-170.

Arıkan B, Çakmakçı G, Akıncı İE, Güler C. 2019. Gaziantep ili tarım topraklarında ağır metal kirliliği ve bitki-gübre toprak ilişkisi. ANAJAS, 34(3):365-374.

Barceloux DG. 1999. Molybdenum. J Toxicol Clin Toxicol, 37(2):231-237.

Bouyoucos GJ. 1952. A Recalibration of the hydrometer for making mechanical analysis of soil. Agronomy Journal, 43(9): 434-438.

Breus D, Yevtushenko O. 2022. Modeling of trace elements and heavy metals content in the steppe soils of Ukraine. JEE, 23(2):159–165.

Canlı S, Şener E, Özbek M. 2020. Determination of heavy metal content in some soils used for agricultural purposes in Trabzon province. TURJAF, 8(5):1087-1091.

Düzgüneş O, Kesici T, Kavuncu O, Gürbüz F. 1987. Araştırma deneme metotları (istatistik metotları-II). Ankara Üniversitesi Ziraat Fak. Yay. 1021:381s.

Güneş A, Alpaslan M, İnal A, Çakmak İ, Öztürk L. 2007. Mineral contents of some staple foodstuffs grown in Turkey. Food Chemistry, 101(1):490-499.

Horneck DA, Hart JM, Topper K, Koepsell B. 1989. Methods of soil analysis used in the soil testing laboratory at Oregon State University. P 1-21. Agr. Exp. Sta. Oregon, USA.

Karaaslan MA, Sönmez İ, Yaman M. 2014. Kadmiyum ve kurşun kirliliği açısından Türkiye tarım topraklarının durumu. SDÜFBED, 18(2):162-170.

Karaca A, Başkaya HS, Ay Y, Güngör A, Arslan M. 2020. An investigation of the relationship between heavy metal contents of soils and crops in Mardin Province, Turkey. Jour of Agri Sci, 26(2):251-260.

Kırat G, Savcı S. 2023. Ulutaş köyü (Erzurum) bölgesindeki topraklarda ağır metal kirliliğinin araştırılması. TTDB,10(2): 223–233.

Küçük C, Karaoğlu M. 2021. Iğdır ili 080 devlet karayolu boyunca tarım topraklarında ağır metal kirliliği. EJOSAT, 25:325-333.

Lindsay WL, Norwel WA. 1978. Development of a DTPA test for zinc. iron. manganese and copper. J. Soil Sci. Am. 42:421-428.

İpek H. 2003. Molibden. YYÜ Veterinerlik Fak Der, 14(1):73-76.

McDowell LR. 1992. Copper and molybdenum minerals. Ani and Hum Nutr. 22(3):176- 204.

Nelson RE. 1982. Carbonate and gypsum. methods of soil analysis part 2. chemical and microbiological properties second edition. Agronamy. No: 9 Part 2. Edition P: 191- 197.

Nelson DW, Sommers LE. 1982. Organic matter methods of soil analysis part 2. chemical and microbiological properties second edition. Agronamy, No: 9 Part 2. Edition P: 574- 579.

Özçelik H, Kaya Z, İnan H. 2010. Determination of heavy metals in soils and vegetables in the vicinity of a textile mill. Environ Monit Assess 163(1-4):651-659.

Özkan F, Demir Y. 2023. Rize ilinde geleneksel ve organik çay tarımı yapılan alanların topraklarında bazı verimlilik parametreleri ile ağır metal içeriklerinin karşılaştırılması. Iğdır Üniversitesi FBED, 13(2):1405-1417.

Rhoades JD. 1982. Cation exchange capacity methods of soil analysis part 2. chemical and microbiological properties second edition. Agronamy, No: 9 Part 2. Edition P: 149- 157.

Şahin Ü, Aydın M, Yılmaz V. 2013. Türkiye'nin bazı tarım topraklarında krom seviyeleri. E.Ü. Ziraat Fak Derg, 50(1):33-40.

Şahin Ü, Orhan Y, Akıncı G. 2016. Türkiye'de bazı tarım topraklarında kobalt seviyeleri. SDÜFBED, 20(1):166-172.

Şimşek T, Kalkancı N, Büyük G. 2021. Tarım topraklarındaki ağır metallerin kirlilik düzeylerinin belirlenmesi: Osmaniye örneği. MKU. Tar. Bil. Derg, 26 (1):106-116.

Taş R, Demir Y. 2022. Bingöl ovası tarım topraklarının verimlilik düzeyi ile bazı ağır metal içeriklerinin belirlenmesi ve haritalanması. DÜOD, 18(2):296-315.

Tolunay D. 1992. Toprak kirlenmesi ve yanlış arazi kullanımının yarattığı sorunlar ile çözüm önerileri. FORESTIST, 42(2):155-167.

Tüfekçi M, Yaşar S, Büyükgüngör H. 2019. İç anadolu bölgesi'nde tarım arazilerinin değişebilir ağır metal içeriği ve faktör analizi ile kirlilik durumunun belirlenmesi. TÜTAD, 6(1):55-61.

Yu X, Sun B, Zhou J, Wang Y. 2018. Distribution and relationship of molybdenum, cobalt, nickel and chromium in typical Chinese soils. Env Sci and Pollu Resea, 25(8):7970-7979.

Viets FG, Lindsay WL. 1973. Testing soils for zinc. Copper. Managanese and iron. Soil Soc. Of Amer. Inc. Madison Wisconcin USA. 153-172.

Yalçın M. 2023. Hatay İli Kırıkhan-Reyhanlı Bölgesi Tarımsal Toprakların Bor Durumunun Belirlenmesi. MAS JAPS 8(2): 202–212.

Yalçın M, Çimrin KM. 2019. Determination of molybdenum contents and relation of some heavy metals in the soil of meadow-pasture terraces between Kırıkhan-Reyhanlı. TURJAF, 7(1):13-21, 2019

Yerli C, Çakmakçı T, Şahin Ü, Tüfenkçi Ş. 2020. Ağır metallerin toprak, bitki, su ve insan sağlığına etkileri. TDFD, 9:103-114.

RESEARCH ARTICLE
Eurasian J Bio Chem Sci, 6(2):73-76, 2023
https://doi.org/10.46239/ejbcs.1291057

EJBCS

Eurasian Journal of Biological and Chemical Sciences

Journal homepage: www.dergipark.org.tr/ejbcs

Contributions to the fauna of Geometridae in the north eastern provinces

Mürşit Ömür Koyuncu[1*], Murat Kütük[2], Mehmet Yaran[2]
*[*1]Gaziantep University, Araban Vocational School, Department of Veterinary, Gaziantep, Turkey*
[2]Gaziantep University, Faculty of Science and Arts, Department of Biology, Gaziantep, Turkey

*Corresponding author : mursitkoyuncu@gantep.edu.tr
Orcid No: https://orcid.org/ 0000-0002-0789-6925

Received : 02/05/2023
Accepted : 14/08/2023

Abstract: This article is based on Geometridae species collected from Ardahan, Bayburt, Erzincan, Erzurum, Gumushane and Kars provinces in Türkiye in 2021. Geometridae species were collected using insect net and light traps. All collected samples were prepared and diagnosed in the laboratory. As a result, 4 subfamilies, 23 genera and 27 species were determined. Photos of all diagnosed species and material examined were presented. In addition, 7 from Ardahan, 8 from Bayburt, 5 from Erzincan, 5 from Erzurum, 8 from Gümüşhane and 3 from Kars were determined for the first time in this study Geometridae species.

Keywords: Geometridae, fauna, Lepidoptera, Türkiye

1. Introduction

This study depends on Geometridae species which were collected from the eastern north east provinces of Türkiye in the summer of 2021 (Ardahan, Bayburt, Erzincan, Erzurum, Gümüshane, Kars).

Adult period, it feeds on water and pollen and thus helps pollination. However, since the larva feeds on the green parts and fruits of the lice, it damages the plants. Geometridae species are known to damage low-rise plants, forest trees, and cultivated plants (Koyuncu and Kütük 2020).

In terms of the number of species in the Lepidoptera order, the second most crowded family is Geometridae. The Geometridae family is represented by more than 23,000 species in the world (Scoble and Hausmann 2007), 988 in Europe (Hausmann et al. 2007), and 687 species in Türkiye (Koçak and Kemal 2018).

This study aimed to contribute to the distribution of Geometridae in Türkiye. and as a result, four subfamilies, 23 genera and 27 Geometridae species were determined.

2. Materials and Method

Geometridae species were collected from the eastern north east provinces in the summer of 2021 (Figure 1). Insect net was used for Diurnal Geometridae species and a curtain light trap was used for nocturnal species. Obtained adult species were taken into the killing jar and the deceased species were deposited with their label information.

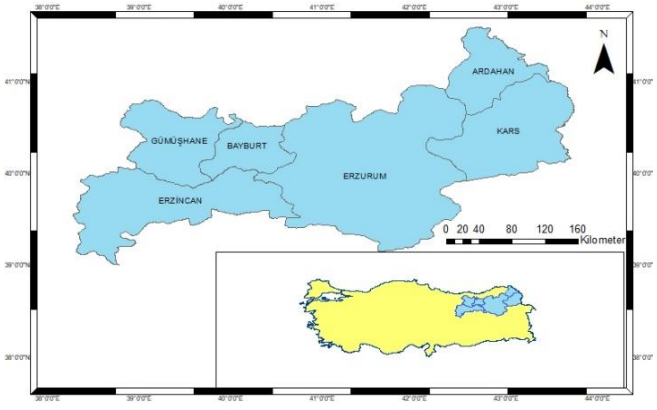

Fig. 1. Research area of collected specimens.

Fresh adult species were prepared in the laboratory. Dry species were relaxed according to Koyuncu and Kütük 2022 and then prepared. Labelling and diagnosis were made for all of the prepared species. Also genital preparations of all species were made for diagnosis. Species were diagnosed using following literatures: Hausmann 2001: Mironov 2003; Hausmann 2004; Redondo at al. 2009; Leraut 2009; Hausmann and Viidalepp 2012; Skou and Sihvonen 2015; Müller at al. 2019;, Koyuncu and Kütük 2021.

3. Results

This article presents new contributions to the fauna of the eastern north east provinces of Türkiye. As a result of the study, 4 subfamilies, 23 genera and 27 species were

determined (Table 1). Photographs of all species (Figure B), reviewed material and individual numbers were presented. All species listed alphabetical order.

Table 1. List of Geometridae Species

Subfamily	Genus	Species
Ennominae	*Alcis*	*Alcis repandata*
	Chiasmia	*Chiasmia clathrata*
	Cabera	*Cabera pusaria*
	Ematurga	*Ematurga atomaria*
	Isturgia	*Isturgia murinaria*
	Macaria	*Macaria notata*
Geometrinae	*Aplasta*	*Aplasta ononaria*
	Thalera	*Thalera fimbrialis*
	Thetidia	*Thetidia smaragdaria*
Larentiinae	*Aplocera*	*Aplocera annexata*
	Camptogramma	*Camptogramma bilineata*
	Epirrhoe	*Epirrhoe alternata*
	Odezia	*Odezia atrata*
	Philereme	*Philereme transversata*
	Schistostege	*Schistostege nubilaria*
	Scotopteryx	*Scotopteryx chenopodiata*
	Thera	*Thera obeliscata*
	Triphosa	*Triphosa taochata*
Sterrhinae	*Cleta*	*Cleta filacearia*
	Idaea	*Idaea aureolaria*
		Idaea aversata
		Idaea ochrata
		Idaea rufaria
		Idaea rusticata
	Lythria	*Lythria purpuraria*
	Rhodostrophia	*Rhodostrophia auctata*
	Scopula	*Scopula decorata*

Alcis repandata (Linnaeus, 1758) Fig. 2-1
Material examined: 1♂, 1♀, **Ardahan**, Center, Universty Campus,, 41°07'35 N, 42°47'00 E, 1941m, 10.07.2021.

Aplasta ononaria (Fuessly, 1783) Fig. 2-2
Material examined: 3♂♂, **Erzincan**, Refahiye, Center, 39°53'47 N, 38°51'53 E, 1686m, 07.07.2021; 1♂, Gümüşhane Ahmetli, 39°52'25 N, 39°20'54 E, 2045m, 08.07.2021. 1♂, **Erzurum**, Center, Karagöbek, 40°09'29 N, 41°25'58 E, 1997m, 09.07.2021.

Aplocera annexata (Freyer, 1830) Fig. 2-3
Material examined: 3♀♀, **Bayburt**, Kop Mountain, Şehitlik, 40°01'56 N, 40°30'57 E, 2433m, 08.07.2021.

Cabera pusaria (Linnaeus, 1758) Fig. 2-4
Material examined: 1♂, **Bayburt**, Kop Mountain, Şehitlik, 40°01'56 N, 40°30'57 E, 2433m, 08.07.2021. 1♀, **Erzurum**, Center, Karagöbek, 40°09'29 N, 41°25'58 E, 1997m, 09.07.2021; 2♂♂, Pasinler, Center, 39°58'40 N, 41°37'35 E, 1630m, 11.07.2021. 3♂♂, 1♀, **Gümüşhane**, Center, Çimenli, 38°57'12 N, 39°24'40 E, 1722m, 08.07.2021.

Camptogramma bilineata (Linnaeus, 1758) Fig. 2-5
Material examined: 4♂♂, 5♀♀, **Erzurum**, Oltu, Tahtaköy, 40°39'55 N, 42°22'29 E, 1339m, 09.07.2021; 5♂♂, Pasinler, Center, 39°58'40 N, 41°37'35 E, 1630m, 11.07.2021. 1♂, **Gümüşhane**, Center, Çimenli, 38°57'12 N, 39°24'40 E, 1722m, 08.07.2021.

Chiasmia clathrata (Linnaeus, 1758) Fig. 2-6
Material examined: 2♂♂, **Ardahan**, Center, Universty Campus,, 41°07'35 N, 42°47'00 E, 1941m, 10.07.2021.

Cleta filacearia (Herrich-Schäffer, 1847) Fig. 2-7
Material examined: 7♂♂, 3♀♀, **Bayburt**, Kop Mountain, Şehitlik, 40°01'56 N, 40°30'57 E, 2433m, 08.07.2021.

Ematurga atomaria (Linnaeus, 1758) Fig. 2-8
Material examined: 2♂♂, **Erzincan**, Refahiye, Arpayazı, 39°49'51 N, 38°44'50 E, 1880m, 07.07.2021.

Epirrhoe alternata (Müller, 1764) Fig. 2-9
Material examined: 1♂, 1♀, **Bayburt**, Kop Mountain, Şehitlik, 40°01'56 N, 40°30'57 E, 2433m, 08.07.2021.

Idaea aureolaria (Denis & Schiffermüller, 1775) Fig. 2-10
Material examined: 1♂, **Ardahan**, Center, Çamlıçatak, 41°05'35 N, 42°49'05 E, 2034m, 10.07.2021.

Idaea aversata (Linnaeus, 1758) Fig. 2-11
Material examined: 2♂♂, **Gümüşhane**, Center, Çimenli, 38°57'12 N, 39°24'40 E, 1722m, 08.07.2021.

Idaea ochrata (Scopoli, 1763) Fig. 2-12
Material examined: 4 ♂♂, **Bayburt**, Center, 40°05'26 N, 39°43'11 E, 1774m, 08.07.2021; 2♂♂, Kop Mountain, Şehitlik, 40°01'56 N, 40°30'57 E, 2433m, 08.07.2021. 3♂♂, 1♀, **Erzincan**, Refahiye, Arpayazı, 39°49'51 N, 38°44'50 E, 1880m, 07.07.2021; 2♀♀, Refahiye, Center, 39°53'47 N, 38°51'53 E, 1686m, 07.07.2021. 2♂♂, **Gümüşhane**, Center, Çimenli, 38°57'12 N, 39°24'40 E, 1722m, 08.07.2021. 3♂♂, 2♀♀, **Kars**, Susuz, Kırkpınar, 42°52'06 N, 43°01'33 E, 2157m, 10.07.2021.

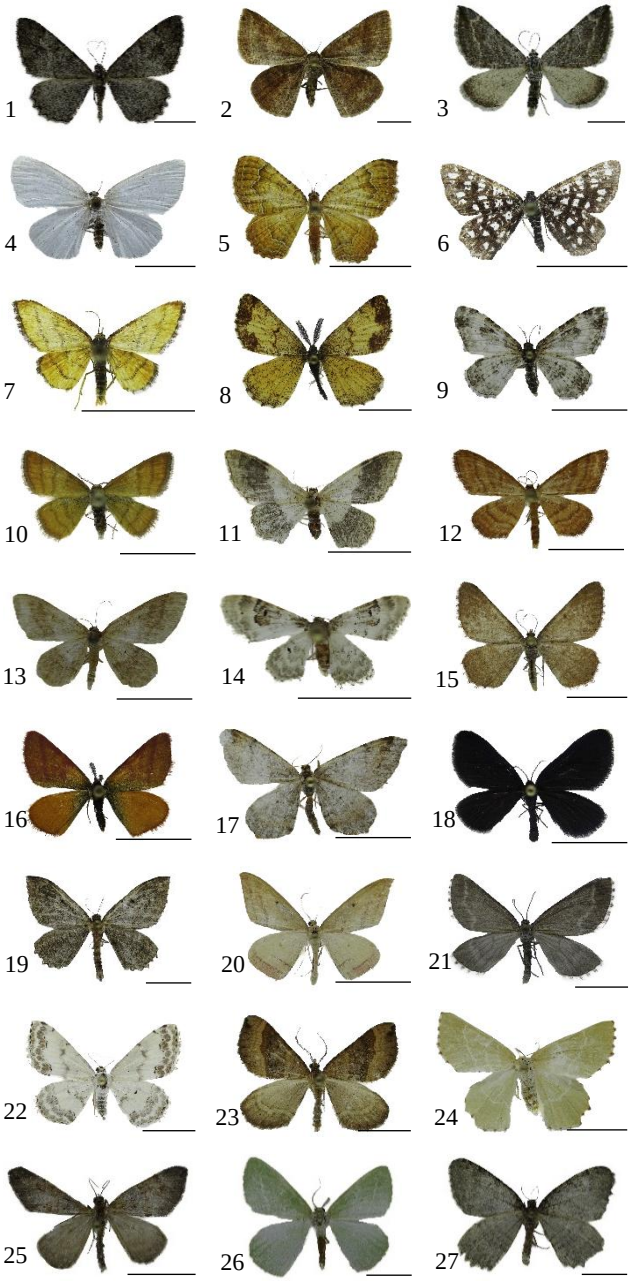

Fig. 2. Geometridae species: 1. *Alcis repandata*, 2. *Aplasta ononaria*,3. *Aplocera annexata*, 4. *Cabera pusaria*, 5. *Camptogramma bilineata*, 6. *Chiasmia clathrata*, 7. *Cleta filacearia*, 8. *Ematurga atomaria*, 9. *Epirrhoe alternata*, 10. *Idaea aureolaria*, 11. *I. aversata*, 12. *I. ochrata*, 13. *I. rufaria*, 14. *I. rusticata*, 15. *Isturgia murinaria*, 16. *Lythria purpuraria*, 17. *Macaria notata*, 18. *Odezia atrata*, 19. *Philereme transversata*, 20. *Rhodostrophia auctata*, 21. *Schistostege nubilaria*, 22. *Scopula decorata*, 23. *Scotopteryx chenopodiata*, 24. *Thalera fimbrialis*, 25. *Thera obeliscata*, 26. *Thetidia smaragdaria*, 27. *Triphosa taochata*. (Scale bar: 1cm)

Idaea rufaria (Hübner, [1799]) Fig. 2-13
Material examined: 1♂, **Ardahan**, Center, Çamlıçatak, 41°05'35 N, 42°49'05 E, 2034m, 10.07.2021. 1♂, **Erzincan**, Gümüşhane Ahmetli, 39°52'25 N, 39°20'54 E, 2045m, 08.07.2021. 1♂, **Gümüşhane**, Center, Çimenli, 38°57'12 N, 39°24'40 E, 1722m, 08.07.2021.

Idaea rusticata (Denis & Schiffermüller, 1775) Fig. 2-14
Material examined: 2♀♀, **Erzurum**, Oltu, Tahtaköy, 40°39'55 N, 42°22'29 E, 1339m, 09.07.2021. 3♂♂, **Gümüşhane**, Center, Çimenli, 38°57'12 N, 39°24'40 E, 1722m, 08.07.2021.

Isturgia murinaria ([Denis & Schiffermüller], 1775) Fig. 2-15
Material examined: 1♀, **Bayburt**, Kop Mountain, Şehitlik, 40°01'56 N, 40°30'57 E, 2433m, 08.07.2021. 1♂, **Erzurum**, Center, Karagöbek, 40°09'29 N, 41°25'58 E, 1997m, 09.07.2021.

Lythria purpuraria (Linnaeus, 1758) Fig. 2-16
Material examined: 4♂♂, **Ardahan**, Center, Universty Campus,, 41°08'01 N, 42°46'45 E, 1966m, 10.07.2021; 1♂, Center, Çamlıçatak, 41°05'35 N, 42°49'05 E, 2034m, 10.07.2021. 1♂, **Erzurum**, Pasinler, Üğümü, 39°59'20 N, 40°43'49 E, 1689m, 11.07.2021. 1♂, **Gümüşhane**, Center, Çimenli, 38°57'12 N, 39°24'40 E, 1722m, 08.07.2021. 6♂♂, 2♀♀, **Kars**, Susuz, Kırkpınar, 42°52'06 N, 43°01'33 E, 2157m, 10.07.2021.

Macaria notata (Linnaeus, 1758) Fig. 2-17
Material examined: 2♂♂, **Ardahan**, Center, Universty Campus,, 41°07'35 N, 42°47'00 E, 1941m, 10.07.2021.

Odezia atrata (Linnaeus, 1758) Fig. 2-18
Material examined: 5♂♂, 4♀♀, **Bayburt**, Kop Mountain, Şehitlik, 40°01'56 N, 40°30'57 E, 2433m, 08.07.2021.

Philereme transversata (Hufnagel, 1767)) Fig. 2-19
Material examined: 2♂♂, **Ardahan**, Center, Universty Campus,, 41°07'35 N, 42°47'00 E, 1941m, 10.07.2021

Rhodostrophia auctata Staudinger, 1887 Fig. 2-20
Material examined: 1♂, **Erzincan**, Gümüşhane Ahmetli, 39°52'25 N, 39°20'54 E, 2045m, 08.07.2021. 2♂♂, **Bayburt**, Kop Mountain, Şehitlik, 40°01'56 N, 40°30'57 E, 2433m, 08.07.2021.

Schistostege nubilaria (Hübner, 1799) Fig. 2-21
Material examined: 6♂♂, 2♀♀, **Kars**, Susuz, Kırkpınar, 42°52'06 N, 43°01'33 E, 2157m, 10.07.2021.

Scopula decorata (Denis & Schiffermüller, 1775) Fig. 2-22
Material examined: 2♂♂, **Bayburt**, Kop Mountain, Şehitlik, 40°01'56 N, 40°30'57 E, 2433m, 08.07.2021.

Scotopteryx chenopodiata (Linnaeus, 1758) Fig. 2-23
Material examined: 11♂♂, 7♀♀, **Ardahan**, Center, Universty Campus,, 41°07'35 N, 42°47'00 E, 1941m, 10.07.2021.

Thalera fimbrialis (Scopoli, 1763) Fig. 2-24
Material examined: 2♂♂, **Erzincan**, İliç, Bozçalı, 39°42'58 N, 38°36'37 E, 1400m, 07.07.2021. 2♂♂, **Erzurum**, Pasinler, Üğümü, 39°59'20 N, 40°43'49 E, 1689m, 11.07.2021. 1♂, **Gümüşhane**, Center, Çimenli, 38°57'12

N, 39°24'40 E, 1722m, 08.07.2021. 1♂, **Kars**, Susuz, Kırkpınar, 42°52'06 N, 43°01'33 E, 2157m, 10.07.2021.

Thera obeliscata (Hübner, 1787) Fig. 2-25
Material examined: 2♂♂, **Ardahan**, Center, Universty Campus,, 41°07'35 N, 42°47'00 E, 1941m, 10.07.2021.

Thetidia smaragdaria (Fabricius, 1787) Fig. 2-26
Material examined: 2♂♂, **Bayburt**, Kop Mountain, Şehitlik, 40°01'56 N, 40°30'57 E, 2433m, 08.07.2021.

Triphosa taochata Lederer, 1870 Fig. 2-27
Material examined: 2♂♂, **Ardahan**, Center, Universty Campus,, 41°07'35 N, 42°47'00 E, 1941m, 10.07.2021.

4. Discussion

According to the literatures, some Geometridae species reported previously from the eastern north east provinces (Koçak ve Kemal 2018). There were reported 51 species from Ardahan, 15 from Bayburt, 26 from Erzincan, 70 from Erzurum, 27 from Gümüşhane and 59 from Kars.

In this article, 10 species were determined from Ardahan province, 7 of which were reported for the first time (*Idaea aureolaria*, *Idaea rufaria*, *Lythria purpuraria*, *Macaria notata*, *Philereme transversata*, *Thera obeliscata* *Triphosa taochata*). 10 species were determined from Bayburt province, 8 of which were reported for the first time (*Cabera pusaria*, *Cleta filacearia*, *Epirrhoe alternata*, *Idaea ochrata*, *Isturgia murinaria*, *Odezia atrata*, *Scopula decorata*, *Thetidia smaragdaria*) in this study. 6 species were determined from Erzincan province, 5 of which were reported for the first time (*Aplasta ononaria*, *Ematurga atomaria*, *Idaea ochrata*, *Idaea rufaria*, *Thalera fimbrialis*) in this study. 7 species were determined from Erzurum province, 6 of which were reported for the first time (*Aplasta ononaria*, *Cabera pusaria*, *Camptogramma bilineata*, *Isturgia murinaria*, *Lythria purpuraria*, *Thalera fimbrialis*) in this study. 8 species were determined from Gümüşhane province, 8 of which were reported for the first time (*Cabera pusaria*, *Camptogramma bilineata*, *Idaea aversata*, *Idaea ochrata*, *Idaea rufaria*, *Idaea rusticata*, *Lythria purpuraria*, *Thalera fimbrialis*) in this study. 4 species were determined from Kars province, 3 of which were reported for the first time (*Idaea ochrata*, *Lythria purpuraria*, *Thalera fimbrialis*) in this study (Table 2).

The order of insects has a wide distribution worldwide and is essential both ecologically and agriculturally. Thus, it is thought that faunistic studies on insects should be increased and agriculturally damaging species should be determined in our country. In addition, this study provides new faunistic contribution for Geometridae fauna of Türkiye.

Table 2. Distribution of Geometridae species in provinces

Geometridae species / Provinces	Species count before this study	Determined species in this study	New record for provinces	Species count after this study
Ardahan	51	10	7	58
Bayburt	15	10	8	23
Erzincan	26	6	5	31
Erzurum	70	7	6	75
Gümüşhane	27	8	8	35
Kars	59	4	3	62

Authors' contributions:

MÖK**:** Sample collection, Preparation, Identification MK: sample collection MY: Sample collection, Identification

Conflict of interest disclosure:
The authors declare no conflict of interests

References

Hausmann A, Viidalepp J. 2012. The Geometrid Moths of Europe. Volume 3. Apollo Books, Stenstrup, Denmark.

Hausmann A. 2001. The Geometrid Moths of Europe. Volume 1. Apollo Books, Stenstrup, Denmark

Hausmann A. 2004. The Geometrid Moths of Europe. Volume 2. Apollo Books, Stenstrup, Denmark.

Hausmann A, Mironov V, Viidalepp J. 2007. Fauna Europaea: Experts. Avaliable from http//www.faunaeur.org/experts.php?group id=63) (accessed 14 September 2007).

Koçak AÖ, Kemal M. 2018. A synonymous and distributional list of the species of the Lepidoptera of Turkey, Ankara, Türkiye, Priamus, 8:1-487.

Koyuncu MÖ, Kütük M. 2020. Ennominae, Geometrinae and Larentiinae (Lepidoptera: Geometridae) Fauna in Gaziantep province, Turkey. Commun Fac Sci Univ Ank Series C. 29(1):50-60.

Koyuncu MÖ, Kütük M. 2021. Research on the Geometridae (Lepidoptera) fauna of Adıyaman, Malatya and Şanlıurfa provinces. Fresenius Environ Bull. 30(6):7309-7320.

Koyuncu MÖ, Kütük M. 2022. A New System for Relaxing the Dry Insects. KSU J Agric Nat. 25(1):127-132.

Leraut P. 2009. Moths of Europa Geometridae Volume II.

Mironov V. 2003. The Geometrid Moths of Europe. Vol. 4: Larentiinae II (Subfamily Sterrhinae II). Apollo Books, Stenstrup, Denmark.

Müller B, Erlacher S, Hausmann A, Rajaei H, Sihvonen P, Skou P. 2019. The Geometrid Moths of Europe.Volume 6. Apollo Books, Stenstrup, Denmark.

Redondo V, Gastón FJ, Gimeno R. 2009. Geometridae Ibericae. Apollo Books, Stenstrup.

Scoble MJ, Hausmann A. 2007. Online list of valid and available names of the Geometridae of the World, http://www. lepbarcoding. org/geometridae/species_checklists. Page visited (19 March 2015).

Skou P, Sihvonen P. 2015. The Geometrid moths of Europe. Volume 5. Apollo Books, Stenstrup, Denmark.

RESEARCH ARTICLE
Eurasian J Bio Chem Sci, 6(2):77-80, 2023
https://doi.org/10.46239/ejbcs.1215182

EJBCS

Eurasian Journal of Biological and Chemical Sciences

Journal homepage: www.dergipark.org.tr/ejbcs

Peroxidase mimicking activity of macroporous carbon

Bekir Çakıroğlu*

**Sakarya University, Biomedical, Magnetic and Semiconductor Materials Research Center (BIMAS-RC), Sakarya, Turkey.*

*Corresponding author : bekircakiroglu@sakarya.edu.tr
Orcid No: https://orcid.org/0000-0001-5989-4545

Received : 06/12/2022
Accepted : 31/08/2023

Abstract: This study looked into the peroxidase-like activity of macroporous carbon produced using a silica template. Macroporous carbon's nanozyme activity was compared to that of commercial graphene oxide. The macroporous microstructure of carbon was visible in the field emission scanning electron microscopy image. By catalytically oxidizing the chromogenic substrate 2,2'-azino-bis(3-ethylbenzothiazoline-6-sulfonic acid (ABTS) in the presence of hydrogen peroxide, the nanozyme activity was investigated. The oxidized form of ABTS, which has a green color, can be seen by the eye. The synthetic macroporous carbon developed a green hue without functionalization or enzyme use, indicating peroxidase activity. This is likely because of the enormous surface area and numerous active sites that are present on the surface. As active sites, the oxygen-containing functional groups created during carbonization can be crucial to the peroxidase-mimicking action.

Keywords: Nanozyme, Carbonaceous material, ABTS, Peroxidase-like activity, Sustainability

Makro gözenekli karbonun peroksidaz mimik aktivitesi

Özet: Bu çalışmada, silika şablonu kullanılarak üretilen makro gözenekli karbonun peroksidaz mimik aktivitesi araştırılmıştır. Makro gözenekli karbonun nanozim aktivitesi, ticari grafen oksit ile karşılaştırıldı. Karbonun alan emisyon taramalı elektron mikroskobu görüntüsü, makro gözenekli morfolojiyi ortaya çıkardı. Nanozim aktivitesi, kromojenik substrat 2,2'-azino-bis(3-etilbenzotiazolin-6-sülfonik asidin (ABTS) hidrojen peroksit varlığında katalitik oksidasyonu yoluyla incelenmiştir ve yeşil renkli ABTS'nin oksitlenmiş formu gözle görülebilecek şekilde oluştu. İşlevselleştirme ve enzim kullanımı olmadan, elde edilen makro gözenekli karbon yeşil renk gelişimi gösterdi, bu da muhtemelen geniş yüzey alanı ve dolayısıyla yüzeyde bulunan bol miktarda aktif bölge nedeniyle peroksidaz aktivitesini gösteriyor. Karbonizasyon sırasında oluşan oksijen içeren fonksiyonel gruplar, aktif bölgeler olarak davranabilir ve peroksidazı taklit eden aktivitede çok önemli bir rol oynayabilir.

Anahtar Kelimeler: Nanozim, karbonlu malzeme, ABTS, peroksidaz mimik aktivite, sürdürülebilirlik

1. Introduction

Enzymes have been extensively utilized owing to their efficient and specific catalytic activity on substrates under mild conditions (Hanefeld et al. 2013). However, some inherent problems with enzymes exist, such as expensive purification and poor working and storage stability (Q. Wang et al. 2021). They are also sensitive to pH, temperature, ionic strength, surfactants, and organic solvents, and their broad use is hampered by proteases' digestion (Wu et al. 2020). Since the exciting discovery of Fe_3O_4 MNPs with peroxidase-like activity in 2007(Gao et al. 2007), researchers have paid much attention to researching effective artificial enzymes "nanozymes" with intrinsic enzyme-like activities, to solve these problems (Q. Wang et al. 2018). Due to their impressive advantages, nanozymes have been at the forefront as a potential substitute to help with analyte detection (Ren et al. 2022). These include satisfying catalytic activity, high medium resistance, easy surface modification, cheap cost, and simple manufacturing (Liang and Yan 2019). However, unlike enzymes, nanozymes could not catalyze one substrate with high selectivity(Robert and Meunier, 2022). One possible challenging will be increasing the asymmetric selectivity of nanozymes (Yang et al. 2021). To date, morphology, heterogeneous atomic doping, particle size adjustment, and surface modification have all been used to modify the catalytic activity and selectivity of nanozymes (Jiang et al. 2019). The increased activity is a result of the bigger surface area exposing more active sites and the preferential exposure of catalytically active atoms. Surface defects including ledges, adatoms, vacancies, and kinks strongly attract substrates because they are coordinatively unsaturated reactive sites (Wang et al. 2016).

2. Materials and Method

Graphene oxide (GO), sucrose, tetraethyl orthosilicate (TEOS), 25% ammonia solution, hydrofluoric acid, 98% sulfuric acid, and absolute ethanol were purchased from Sigma-Aldrich. 2,2'-azino-bis(3-ethylbenzothiazoline-6-sulfonic acid (ABTS) was purchased from Roche Diagnostics (Germany). Hydrogen peroxide solution (30%) was purchased from Merck. Acetate buffer solution (ABS) was prepared using glacial acetic acid (Merck) and sodium acetate (Sigma-Aldrich).

2.1. Preparation of SiO_2 Templates

SiO_2 (silica) NPs were synthesized via the classical Stöber Method (Han et al. 2017). Briefly, 1 mL of TEOS, 50 mL of ethanol, 1 mL of DW, and 5 mL of ammonia solution were magnetically stirred in a flask at 250 rpm and 25 °C in a water bath. After 6 h, SiO_2 NPs were purified by twice centrifugation at 10000 rpm for 20 min. The sedimented SiO_2 NPs were resuspended in ethanol (Figure 1), and the suspension was evaporated in an oven at 70 °C to obtain templates (Figure 2).

2.2. Preparation of Macroporous Carbon

The precursor of carbonaceous material contains 1.4 g of sucrose, 3.2 mL of deionized water, 14 mL of ethanol, and 40 µL of 98% sulfuric acid. The infiltration was carried under the vacuum by dropping carbon precursor solution onto the silica template at room temperature. The infiltration was repeated several times to fill the voids of the silica template. The sucrose-soaked templates were heated at 160 °C for 5 h in the air for the carbonization of sucrose catalyzed by sulfuric acid and annealed. Macroporous carbon was left behind by etching away silica templates with 4% HF solution overnight.

2.3. Peroxidase-like Activity Measurements

2.5 mL of 0.4 mM ABTS solutions were prepared in 100 mM ABS pH 3.8 with 4 mg of macroporous carbon. 30 µL of hydrogen peroxide (30%) was added to the above mixture and incubated for 10 min at room temperature. Then, macroporous carbon was removed from the reaction medium, and the absorbance spectra were recorded.

2.4. Characterization

The morphological features of nanozyme components were characterized by field emission scanning electron microscopy (FESEM) recorded on an FEI Quanta FEG 450. UV visible (UV-Vis) absorbance spectra were recorded using a Shimadzu UV-2600 spectrophotometer at 200-800 nm. The particle size distribution of silica NPs was obtained on a Nano Plus (Micromeritics). The functional group investigation of the nanocomposites was carried out by Perkin Elmer Fourier transform infrared (FTIR) Spectrometer (Spectrum Two).

3. Results

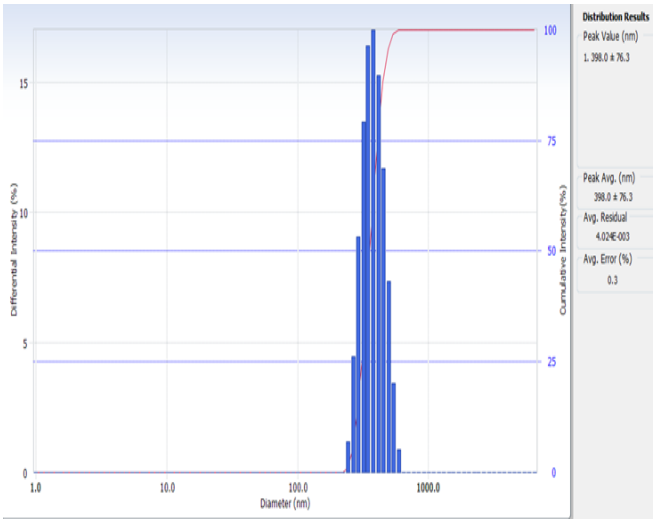

Fig. 1 Particle Size Dispersion of Silica NPs

Fig. 2 Silica Template for Macroporous Carbon Fabrication

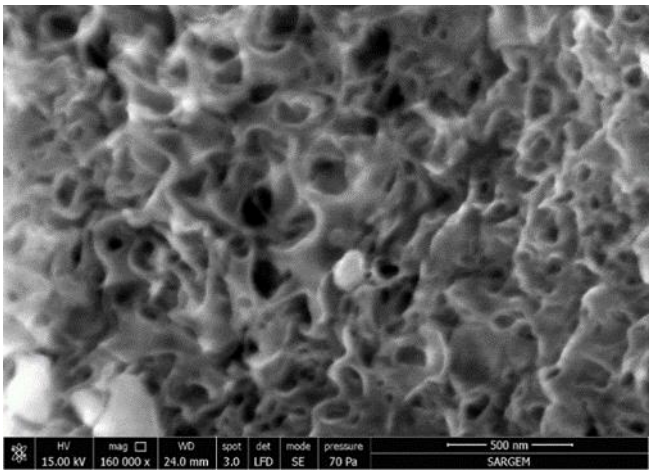

Fig. 3 FESEM Image of Macroporous Carbon

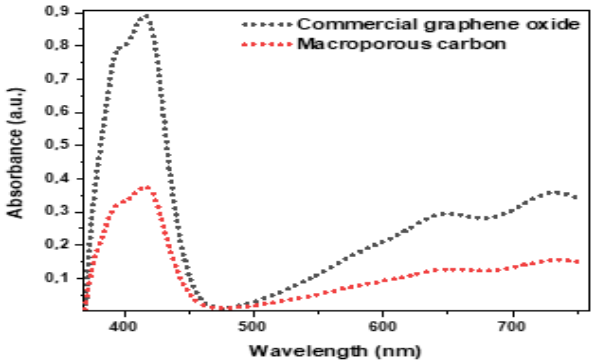

Fig. 4 Absorbance Spectrum of Oxidized ABTS Generated by Commercial Graphene Oxide and Macroporous Carbon

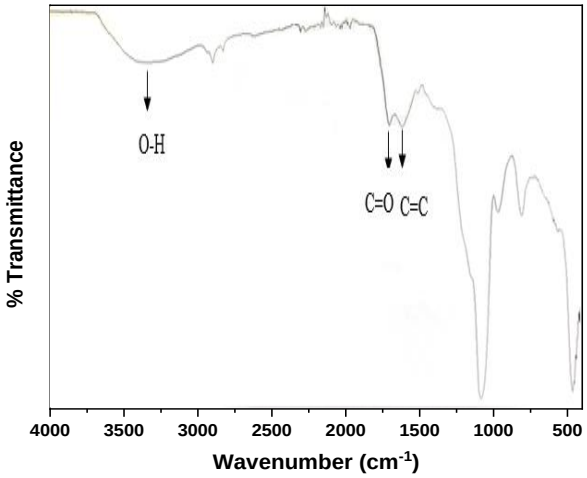

Fig. 5 FTIR Spectrum of Macroporous Carbon

4. Discussion

Carbon-based materials with enzyme-like activity have garnered great attention by researchers. Hitherto, numerous carbon-based nanozymes, including graphene oxide (Wang et al. 2020), carbon nanotubes (H. Wang et al. 2018), fullerenes (Hong et al. 2022), graphene quantum dots(Devi et al. 2021), and carbonaceous metal organic frameworks(Zhao et al. 2022), have been manufactured to investigate enzyme-mimicking activities. Carbon-based nanozymes, in contrast to natural enzymes, exhibit considerable potential in biomedical applications due to their plentiful active sites, outstanding stability, and good biological safety (X. Wang et al. 2021). In this context, low-cost carbonaceous nanozyme manufacturing is of great significance for the catalytic applications. This study reported the fabrication of an efficient carbon-based nanozyme as a peroxidase substitute.

Particle size distribution of silica NPs was exhibited in Figure 1. The average diameter of silica NPs was found to be 398 nm with a narrow particle distribution value. Figure 2 shows the opalescence of silica NPs deposition owing to its opal photonic crystal behavior.

The FESEM image of carbon material revealed a porous morphology, which implies abundant active sites (Chen et al. 2020) (Figure 3). Up to now, carbonaceous materials have mirrored peroxidase, oxidase, superoxide dismutase and catalase-like activities (Sun et al. 2018). Depending on their morphology and active groups, the enzyme mimicking activities have been found to change. Fullerenes with ball-shape morphology display SOD-like activity, while graphene oxide with leaf-like morphology mostly displayed substantial peroxidase mimicking activity.

Peroxidase mimicking activities were investigated using chromogenic substrate ABTS in the presence of hydrogen peroxide (Figure 4). Graphene oxide is a well-known peroxidase-like nanozyme in the literature owing to its carboxyl groups, which play a crucial role in the catalytic oxidation of chromogenic substrates in hydrogen peroxide containing solution (Song et al. 2010). Commercial graphene oxide revealed peroxidase-like activity that can oxidase ABTS in the presence of H_2O_2 by producing a green-colored product. On the other hand, the macroporous carbon has also demonstrated peroxidase-mimicking activity, although it led to less absorbance intensity than graphene oxide. At the absorbance wavelength of 646 nm, the fabricated carbon showed half the absorbance intensity generated by graphene oxide (Figure 4). FTIR analysis revealed the existence of O-H (3395 cm^{-1}) and C=O (1720 cm^{-1}) functional groups (Çakıroğlu et al. 2018), implying that carboxyl groups are introduced on the microporous carbon during carbonization (Figure 5). The peroxidase-like catalytic activity of carbon can be attributed to the carboxyl groups (-COOH) on the surface (Wang et al. 2020).

According to the literature, the reaction mechanism of peroxidase mimicking activity was realized by reduction of hydrogen peroxide on carboxylic acid moiety with the concomitant oxidation of ABTS, as can be seen in the equations below (Lin et al. 2019).

$$\mathbf{H_2O_2 + ABTS \rightarrow 2\,H_2O + oxABTS}$$

Herein, radicals are probably formed during nanozyme catalysis, and these radicals can facilitate the oxidation of ABTS on the active sites of carbonaceous material (X. Wang et al. 2021).

Thus, it is confirmed in this study that oxygen containing functional groups on carbonaceous material are responsible for the chromogenic substrate oxidation in the presence of hydrogen peroxide.

5. Conclusion

In this study, a macroporous carbon was reported for peroxidase-mimicking activity. Its peroxidase-like activity was examined in the presence of a chromogenic substrate ABTS. Carbon material was synthesized with favorable morphology for reactants and products. The rational design of material grants access to abundant catalytically active sites and enhances the catalytic activity. This study may find its unique niche in the sensor area as a biomimic peroxidase for hydrogen peroxide monitoring.

Acknowledgements

The author would like to thank Prof. Dr. Ayşe Ogan and Assoc. Prof. Dr. Emrah Bulut for their valuable contributions.

References

Çakıroğlu B, Çiğil-Beyler A, Ogan A, Kahraman MV, Demir S. 2018. Covalent immobilization of acetylcholinesterase on a novel polyacrylic acid-based nanofiber membrane. Eng Life Sci. 18:254-262

Chen Y, Jiao L, Yan H, Xu W, Wu Y, Wang H, Gu W, Zhu C. 2020. Hierarchically Porous S/N Codoped Carbon Nanozymes with Enhanced Peroxidase-like Activity for Total Antioxidant Capacity Biosensing. Anal Chem. 92:13518–13524

Devi M, Das P, Boruah PK, Deka MJ, Duarah R, Gogoi A, Neog D, Dutta HS, Das MR. 2021. Fluorescent graphitic carbon nitride and graphene oxide quantum dots as efficient nanozymes: Colorimetric detection of fluoride ion in water by graphitic carbon nitride quantum dots. J Environ Chem Eng. 9:104803

Gao L, Zhuang J, Nie L, Zhang J, Zhang Y, Gu N, Wang T, Feng J, Yang D, Perrett S, Yan X. 2007. Intrinsic peroxidase-like activity of ferromagnetic nanoparticles. Nat Nanotechnol. 2:577–583

Hanefeld U, Cao L, Magner E. 2013. Enzyme immobilisation: fundamentals and application. Chem Soc Rev. 42:6211–6212

Hong SJ, Chun H, Hong M, Han B. 2022. N- and B-doped fullerene as peroxidase- and catalase-like metal-free nanozymes with pH-switchable catalytic activity: A first-principles approach. Appl Surf Sci. 598:153715

Jiang D, Ni D, Rosenkrans ZT, Huang P, Yan X, Cai W. 2019. Nanozyme: new horizons for responsive biomedical applications. Chem Soc Rev. 48:3683–3704

Liang M, Yan X. 2019. Nanozymes: From New Concepts, Mechanisms, and Standards to Applications. Acc Chem Res. 52:2190–2200

Lin S, Zhang Y, Cao W, Wang X, Qin L, Zhou M, Wei H. 2019. Nucleobase-mediated synthesis of nitrogen-doped carbon nanozymes as efficient peroxidase mimics. Dalt Trans. 48: 1993–1999

Ren X, Chen D, Wang Y, Li H, Zhang Y, Chen H, Li X, Huo M. 2022. Nanozymes-recent development and biomedical applications. J Nanobiotechnology. 20:92

Robert A, Meunier B. 2022. How to Define a Nanozyme. ACS Nano. 16:6956–6959

Song Y, Qu K, Zhao C, Ren J, Qu X. 2010. Graphene Oxide: Intrinsic Peroxidase Catalytic Activity and Its Application to Glucose Detection. Adv Mater. 22:2206–2210

Sun H, Zhou Y, Ren J, Qu X. 2018. Carbon Nanozymes: Enzymatic Properties, Catalytic Mechanism, and Applications. Angew Chemie Int Ed. 57:9224–9237

Wang D, Song X, Li P, Gao XJ, Gao X. 2020. Origins of the peroxidase mimicking activities of graphene oxide from first principles. J Mater Chem B. 8:9028–9034

Wang H, Li P, Yu D, Zhang Y, Wang Z, Liu C, Qiu H, Liu Z, Ren J, Qu X. 2018. Unraveling the Enzymatic Activity of Oxygenated Carbon Nanotubes and Their Application in the Treatment of Bacterial Infections. Nano Lett. 18:3344–3351

Wang Q, Liu S, Tang Z. 2021. Recent progress in the design of analytical methods based on nanozymes. J Mater Chem B. 9:8174–8184

Wang Q, Wei H, Zhang Z, Wang E, Dong S. 2018. Nanozyme: An emerging alternative to natural enzyme for biosensing and immunoassay. TrAC Trends Anal Chem. 105:218–224

Wang X, Hu Y, Wei H. 2016. Nanozymes in bionanotechnology: from sensing to therapeutics and beyond. Inorg Chem Front. 3:41–60

Wang X, Wang H, Zhou S. 2021. Progress and Perspective on Carbon-Based Nanozymes for Peroxidase-like Applications. J Phys Chem Lett. 12:11751–11760

Wu W, Huang L, Wang E, Dong S. 2020. Atomic engineering of single-atom nanozymes for enzyme-like catalysis. Chem Sci. 11:9741–9756

Yang W, Yang X, Zhu L, Chu H, Li X, Xu W. 2021. Nanozymes: Activity origin, catalytic mechanism, and biological application. Coord Chem Rev. 448:214170

Zhao J, Gong J, Wei J, Yang Q, Li G, Tong Y, He W. 2022. Metal organic framework loaded fluorescent nitrogen-doped carbon nanozyme with light regulating redox ability for detection of ferric ion and glutathione. J Colloid Interface Sci. 618:11–21

RESEARCH ARTICLE
Eurasian J Bio Chem Sci, 6(2):81-87, 2023
https://doi.org/10.46239/ejbcs.1251033

EJBCS

Eurasian Journal of Biological and Chemical Sciences

Journal homepage: www.dergipark.org.tr/ejbcs

Comparison of glutathione peroxidase-1 in free divers with their counterparts: A model study for sports informatics

Levent Çavaş[1*], Elif Cireli[2], Osman Ateş[3]
*[*1]Dokuz Eylül University, Faculty of Science, Department of Chemistry, Biochemistry Division, Tınaztepe Campus, İzmir-Türkiye*
[2]541 sok. Anıt Apt. C-Blok, No:4, Kat 4, D.8 İzmir/Türkiye
[3]İstanbul University-Cerrahpaşa, Faculty of Sports Science, İstanbul, Türkiye

*Corresponding author : levent.cavas@deu.edu.tr
Orcid No: *https://orcid.org/*0000-0003-2136-6928

Received : 15/02/2023
Accepted : 18/10/2023

Abstract: Free diving is a popular sport because there are many features of free diving such as sustainability, eco-friendly and challenges to nature. Due to increased interest on this sport in recent years, the number of competitions is also increasing gradually. On the other hand, the scientific reports on the understanding of breath-holding mechanisms and metabolism are still unclear. To provide contributions on this phenomenon, glutathione peroxidase (GPX) was selected as a model enzyme because of its critical importance in breath-holding. The GPX enzymes from human and free diving animals were compared by using bioinformatics tools such as ProtParam, Swiss-Model, Clustal Omega and the results are discussed in the present paper. In conclusion, the specific amino acid sequences can be considered in the selection of elite free divers for international competitions to get the best results. However, it should be noted that special training methods should also be applied to have better breath-holding capacities.

Keywords: apnea, free diving, glutathione peroxidase, GPX-1

1. Introduction

Free diving is a physical exercise based on breath-holding under the water without a SCUBA apparatus. Free diving for air-breathing vertebrates requires important adaptations such as overcoming increasing pressure under the water, decreased visibility, and temperature of the water. Mankind has long been interested in free diving due to many purposes such as hunting, military purposes or sports. There are many different sports disciplines nowadays such as spearfishing, underwater hockey, underwater rugby, synchronized swimming and apnea which require strong breath-holding capacity. The athletes under these disciplines always search for alternative techniques to develop their breath-holding capacities. Unfortunately, very limited information exists in the scientific literature for the techniques to develop breath-holding time. There are only seven papers when the keyword "free diver" is searched in Pubmed on 15.02.2023 (Wilkinson, 2009; Ioannidis et al., 2015; Cormack et al., 2017; Rich et al.,2019; Bart and Lau, 2021; Annen et al., 2021; Scott et al., 2021). Since there is a great need for scientific studies on increasing the breath-holding capacity, we wanted to propose sample and basic bioinformatics based selection for suitable athletes for international competitions organized by international federations such as Confédération Mondiale des Activités Subaquatiques (CMAS).

In silico techniques in biology provide important contributions for life sciences such as medicine, biochemistry, molecular biology, and genetics. The tools developed under bioinformatics are now a necessary part of analyzing bio-based data such as protein and DNA sequences. After the completion of human genome project, many different tools have so far been developed to evaluate the big data in the life sciences. The data banks on protein and DNA sequences provide big contributions for understanding of biological phenomena in various dimensions. From this perspective, important metabolism-based features from well-adapted animals can be extracted to be used in the selection of best athletes. Glutathione peroxidase-1 (hereafter GPX-1) was selected as a model enzyme due to its vital importance for the protection of hemoglobin in free diving (Rousseau et al., 2002). GPX-1 has a special role in the decomposition of hydrogen peroxide and lipid hydroperoxide in the metabolism. Since GPX-1 is an important enzyme oxygen metabolism, we wanted to compare the structure of GPX-1 in human and breath-holding animals. Moreover, GPX-1 sequences can also be available for well-adapted breath-holding animals in ocean ecosystems to compare with human GPX-1. These

species are *Delphinapterus leucas, Physeter macrocephalus, Balaenoptera acutorostrata scammoni, Callorhinus ursinus, Neomonachus schauinslandi, Leptonychotes weddellii, Zalophus californianus, Neophocaena asiaeorientalis asiaeorientalis, Lipotes vexillifer* and, *Tursiops truncatus*. These animals have significantly higher breath-holding times compared to *Homo sapiens*. Therefore, in this study, it is aimed to compare GPX enzymes from human and breath-holding animals by using bioinformatics tools.

2. Materials and Method

2.1 Retrieval of GPX-1 Enzyme sequences

Total of 11 GPX-1 enzyme sequences belonging to different species were retrieved from UniProt which is publicly available at (http://www.uniprot.org) (Uniprot Consortium, 2021). Accession IDs of the related enzymes are listed in Table 1.

2.2 Multiple sequence alignment

The GPX-1 enzyme sequences in Table 1 are aligned by using Clustal Omega (Sievers et al., 2011). Multiple sequence alignment of the GPX-1 enzymes is shown in Figure 1.

2.3 Construction of phylogenetic tree

Phylogenetic tree is constructed by using the using Clustal omega (Sievers et al., 2011).

2.4 Amino acid composition and protein parameters of GPX-1 enzymes

ProtParam tool (Gasteiger et al., 2005) is used for analysis of amino acid compositions and chemical properties such as pI, net charge, instability index of the related enzymes.

2.5 3-Dimensional modeling of GPX-1

3-D models of the GPX-1 enzyme belonging to different species are constructed by using Swiss-Model protein structure homology-modelling server (Waterhouse et al., 2018; Studer et al., 2020).

3. Results

3.1 GPX-1 protein retrieval

Sports informatics may provide important contributions to sports science. In this study, we compared amino acid sequences of the GPX-1 enzymes from free diving animals including human. The accession IDs of GPX-1 enzyme, length, and the name of the organisms are given in Table 1.

3.2 Multiple sequence alignment of the selected proteins

Multiple sequence analysis of the studied enzymes is compared in Figure 1. The sequence belonging to *Physeter macrocephalus* is removed because of the incompleteness of the sequence. Regardless of this species, the amino acid sequence of the all studied enzymes starts with Met-Cys-Ala-Ala except for *Balaenoptera acutorostrata scammoni*. It could be said that this tetrapeptide must be conserved. After that there is a gap with 6 amino acid residues. These residues differ from species to species. The gap in *Homo sapiens* is longer than other studied animals. After this gap, polyalanine residues are generally observed. It is interesting to note that leucine is one of the amino acids within these polyalanine residues. Since alanine is a hydrophobic amino acid, it could be said that these polyalanine residues can be in the inner region of the GPX-1 enzymes in the study.

Table 1. Accession IDs and length of the retrieved GPX-1 proteins from different species.

Entry name	Organism	Length
P07203	*Homo sapiens* (Human)	203
A0A455ATU6	*Physeter macrocephalus* (Sperm whale)	139
A0A2Y9GTM2	*Neomonachus schauinslandi* (Hawaiian monk seal)	209
A0A2U3Z8Z4	*Leptonychotes weddellii* (Weddell seal)	209
A0A341AVW4	*Neophocaena asiaeorientalis asiaeorientalis* (Yangtze finless porpoise)	206
A0A2Y9N3R9	*Delphinapterus leucas* (Beluga whale)	206
A0A384BFI6	*Balaenoptera acutorostrata scammoni* (North Pacific minke whale)	238
A0A3Q7RKY4	*Callorhinus ursinus* (Northern fur seal)	208
A0A340YI12	*Lipotes vexillifer* (Yangtze river dolphin)	206
A0A6J2CIH9	*Zalophus californianus* (California sea lion)	208
A0A2U3VAH2	*Tursiops truncatus* (Atlantic bottle-nosed dolphin)	206

```
B.acutorostrata       MTPVARLLKGGASRTPCSSSPRLSPVSLGTHTMCAAQRS---AAALAAAAPRSVYAFSAR  57
N.asiaeorientalis     ------------------------------MCAAQRS---AAALAAAAPRSVYAFSAR  25
D.leucas              ------------------------------MCAAQRS---AAALAAAAPRSVYAFSAR  25
T.truncatus           ------------------------------MCAAQRS---AAALAAAAPRSVYAFSAR  25
L.vexillifer          ------------------------------MCAAQRS---AAALAAAAPRSVYAFSAR  25
H.sapiens             ------------------------------MCAARLAA------AAAAAQSVYAFSAR  22
N.schauinslandi       ------------------------------MCAAPLAAAAAAAAAAAAAPRSVYAFSAR  28
L.weddellii           ------------------------------MCAAPLAAAAAVADAAAAPRSVYAFSAR  28
C.ursinus             ------------------------------MCAAPLATAAA-ALGAAAPRSVYAFSAR  27
Z.californianus       ------------------------------MCAAPLATAAA-AVGAAAPRSVYAFSAR  27
                                                     ****  :       .*** :********

B.acutorostrata       PLAGGEPVNLGSLRGKVLLIENVASLUGTTVRDYTQMNDLQRRLGPQGLVVLGFPCNQFG  117
N.asiaeorientalis     PLAGGEPVNLGSLRGKVLLIENVASLUGTTVRDYTQMNDLQRRLGPRGLVVLGFPCNQFG  85
D.leucas              PLAGGEPVNLGSLRGKVLLIENVASLUGTTVRDYTQMNDLQRRLGPRGLVVLGFPCNQFG  85
T.truncatus           PLAGGEPVNLGSLRGKVLLIENVASLUGTTVRDYTQMNDLQRRLGPRGLVVLGFPCNQFG  85
L.vexillifer          PLAGGEPVNLGSLRGKVLLIENVASLXGTTVRDYTQMNDLQRRLGPRGLVVLGFPCNQFG  85
H.sapiens             PLAGGEPVSLGSLRGKVLLIENVASLUGTTVRDYTQMNELQRRLGPRGLVVLGFPCNQFG  82
N.schauinslandi       PLAGGEPLSLGSLRGKVLLIENVASLUGTTVRDYTQMNELQRRLGPRGLVVLGFPCNQFG  88
L.weddellii           PLAGGEPLSLGSLRGKVLLIENVASLUGTTVRDYTQMNELQRRLGPRGLVVLGFPCNQFG  88
C.ursinus             PLAGGEPLSLGSLRGKVLLIENVASLUGTTVRDYTQMNELQRRLGPRGLVVLPFPCNQLG  87
Z.californianus       PLAGGEPLSLGSLRGKVLLIENVASLUGTTVRDYTQMNELQRRLGPRGLVVLGFPCNQFG  87
                      *******:.***************** ***********:*******:***** *****:*

B.acutorostrata       HQENAKNEEILNCLKYVRPGGGFEPNFMLFEKCEVNGEKAHPLFAFLREALPTPSDDATA  177
N.asiaeorientalis     HQENAKNEEILNCLKYVRPGGGFEPNFMLFEKCEVNGEKAHPLFTFLREALPTPSDDATA  145
D.leucas              HQENAKNEEILNCLKYVRPGGGFEPNFMLFEKCEVNGEKAHPLFTFLREALPTPSDDATA  145
T.truncatus           HQENAKNEEILNCLKYVRPGGGFEPNFMLFEKCEVNGEKAHPLFTFLREALPTPSDDATA  145
L.vexillifer          HQENAKNEEILNCLKYVRPGGGFEPNFMLFEKCEVNGEKAHPLFTFLREALPTPSDDATA  145
H.sapiens             HQENAKNEEILNSLKYVRPGGGFEPNFMLFEKCEVNGAGAHPLFAFLREALPAPSDDATA  142
N.schauinslandi       HQENAKNEEILNSLKYVRPGGGFEPNFTLFEKCEVNGAQAHPLFAFLRESLPAPSDDATA  148
L.weddellii           HQENAKNEEILNSLKYVRPGGGFEPNFTLFEKCEVNGAQAHPLFAFLRESLPAPSDDATA  148
C.ursinus             HQENAKNAEILNSLKYVRPGDGFEPNFTLFEKCEVNGAQAHSLFAFLRESLPAPSDDATA  147
Z.californianus       HQENAKNEEILNSLKYVRPGGGFEPNFTLFEKCEVNGAQAHPLFAFLRESLPAPSDDATA  147
                      ******* ****.*******.****** *********  ** **:****:**:*******

B.acutorostrata       LMTDPKFITWSPVCRNDVAWNFEKFLVGPDGVPVRRYSRRFLTIDIEPDIEALLSQGPSC  237
N.asiaeorientalis     LMTDPKFITWSPVCRNDVAWNFEKFLVGPDGVPVRRYSRRFLTIDIEPDIEALLSQGPSC  205
D.leucas              LMTDPKFITWSPVCRNDVAWNFEKFLVGPDGVPVRRYSRRFLTIDIEPDIEALLSQGPSC  205
T.truncatus           LMTDPKFITWSPVCRNDVAWNFEKFLVGPDGVPVRRYSRRFLTIDIEPDIEALLSQGPSC  205
L.vexillifer          LMTDPKFITWSPVCRNDVAWNFEKFLVGPDGVPVRRYSRRFLTIDIEPDIEALLSQGPTC  205
H.sapiens             LMTDPKLITWSPVCRNDVAWNFEKFLVGPDGVPLRRYSRRFQTIDIEPDIEALLSQGPSC  202
N.schauinslandi       LMTDPKFITWSPVCRNDIAWNFEKFLVGPDGVPVRRYSRRFPTINIEPDIEALLSQGPSS  208
L.weddellii           LMTDPKFITWSPVCRNDIAWNFEKFLVGPDGVPVRRYSRRFPTINIEPDIEALLSQGPSS  208
C.ursinus             LMTDPKFIIWSPVCRNDIAWNFEKFLVGPDGVPVRRYSRRFPTIDIEPDIEALLSQGPSS  207
Z.californianus       LMTDPKFIIWSPVCRNDIAWNFEKFLVGPDGVPVRRYSRRFPTIDIEPDIEALLSQGPSS  207
                      ******:* ********:***************:******* **:*************:.

B.acutorostrata       A 238
N.asiaeorientalis     A 206
D.leucas              A 206
T.truncatus           A 206
L.vexillifer          A 206
H.sapiens             A 203
N.schauinslandi       A 209
L.weddellii           A 209
C.ursinus             A 208
Z.californianus       A 208
                      *
```

Fig 1. Multiple sequence alignment results for the GPX-1 enzymes of selected breath-holding animals.

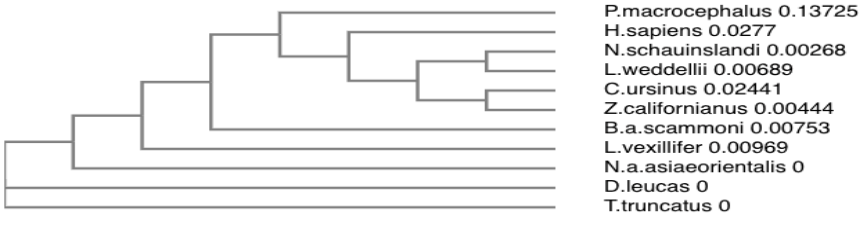

Fig 2. Phylogenetic tree based on GPX-1 enzymes of the selected aquatic organisms.

3.3 Phylogenetic tree construction

Phylogenetic relationship was also studied in this paper. Clustal omega based phylogenetic tree was shown in Figure 2. *Tursiops truncatus, Delphinapterus leucas, Neophocaena asiaeorientalis asiaeorientalis*, and *Lipotes vexillifer* are located different clades (Figure 2).

3.4 ProtParam protein composition analysis

Protein parameters of the analyzed enzymes were studied by using the ProtParam tool (Gasteiger et al., 2005). The amino acid lengths of the enzymes are revealed in Table 1. According to the results, the maximum number of amino acids observed in *Balaenoptera acutorostrata scammoni* is 238. The minimum length was found to be 139 and it is in *Physeter macrocephalus.* The amino acid percentages and numbers are given in Table 2. The results show that the enzymes can be clustered based on maximum amino acid percentages. The amino acid with maximum percentage is found for alanin in *Homo sapiens, Physeter macrocephalus, Neomonachus schauinslandi, Leptonychotes weddelliii, Callorhinus ursinus* and *Zalophus californianus*. On the other hand, leucine is maximum in *Neophocaena asiaeorientalis asiaeorientalis, Delphinapterus leucas, Balaenoptera acutorostrata scammon* and *Lipotes vexillifer.* ProtParam tool also gives important characteristics of the proteins such as theoretical pI, total number of negatively and positively charged residues, net charges and instability index. The results of these parameters are tabulated in Table 3. The diving depth and breath holding capacities of the mammals with apnea ability are given in Table 4 for comparison. According to Table 4, *Physeter macrocephalus* dives the deepest following with *Delphinapterus leucas.*

Table 2. Amino acid numbers and percentages in the GPX-1 enzymes in the study.

	Homo sapiens		*Neomonachus schauinslandi*		*Leptonychotes weddellii*		*Neophocaena asiaeorientalis asiaeorientalis*		*Delphinapterus leucas*		*Balaenoptera acutorostrata scammoni*		*Callorhinus ursinus*		*Lipotes vexillifer*		*Zalophus californianus*		*Tursiops truncatus*	
	#	%	#	%	#	%	#	%	#	%	#	%	#	%	#	%	#	%	#	%
Ala(A)	24	11.8	28	13.4	26	12.4	21	10.2	21	10.2	24	10.1	25	12.0	21	10.2	24	11.5	21	10.2
Arg(R)	14	6.9	14	6.7	14	6.7	15	7.3	15	7.3	17	7.1	14	6.7	15	7.3	14	6.7	15	7.3
Asn(N)	10	4.9	11	5.3	11	5.3	11	5.3	11	5.3	11	4.6	10	4.8	11	5.3	10	4.8	11	5.3
Asp(D)	8	3.9	7	3.3	8	3.8	9	4.4	9	4.4	9	3.8	9	4.3	9	4.4	8	3.8	9	4.4
Cys(C)	5	2.5	4	1.9	4	1.9	6	2.9	6	2.9	7	2.9	4	1.9	6	2.9	4	1.9	6	2.9
Gln(Q)	7	3.4	6	2.9	6	2.9	6	2.9	6	2.9	7	2.9	6	2.9	6	2.9	6	2.9	6	2.9
Glu(E)	13	6.4	13	6.2	13	6.2	13	6.3	13	6.3	13	5.5	12	5.8	13	6.3	13	6.2	13	6.3
Gly(G)	17	8.4	16	7.7	16	7.7	16	7.8	16	7.8	19	8.0	15	7.2	16	7.8	17	8.2	16	7.8
His(H)	2	1.0	2	1.0	2	1.0	2	1.0	2	1.0	3	1.3	2	1.0	2	1.0	2	1.0	2	1.0
Ile(I)	6	3.0	7	3.3	7	3.3	6	2.9	6	2.9	6	2.5	8	3.8	6	2.9	8	3.8	6	2.9
Leu(L)	23	11.3	22	10.5	22	10.5	22	10.7	22	10.7	26	10.9	24	11.5	22	10.7	22	10.6	22	10.7
Lys K)	6	3.0	6	2.9	6	2.9	7	3.4	7	3.4	8	3.4	6	2.9	7	3.4	6	2.9	7	3.4
Met(M)	4	2.0	3	1.4	3	1.4	4	1.9	4	1.9	5	2.1	3	1.4	4	1.9	3	1.4	4	1.9
Phe(F)	11	5.4	12	5.7	12	5.7	12	5.8	12	5.8	12	5.0	11	5.3	12	5.8	12	5.8	12	5.8
Pro(P)	15	7.4	18	8.6	18	8.6	16	7.8	16	7.8	20	8.4	18	8.7	16	7.8	18	8.7	16	7.8
Ser(S)	11	5.4	13	6.2	13	6.2	10	4.9	10	4.9	16	6.7	14	6.7	9	4.4	13	6.2	10	4.9
Thr(T)	7	3.4	8	3.8	8	3.8	9	4.4	9	4.4	12	5.0	8	3.8	10	4.9	8	3.8	9	4.4
Trp(W)	2	1.0	2	1.0	2	1.0	2	1.0	2	1.0	2	0.8	2	1.0	2	1.0	2	1.0	2	1.0
Tyr(Y)	4	2.0	4	1.9	4	1.9	4	1.9	4	1.9	4	1.7	4	1.9	4	1.9	4	1.9	4	1.9
Val(V)	13	6.4	12	5.7	13	6.2	14	6.8	14	6.8	16	6.7	12	5.8	14	6.8	13	6.2	14	6.8
Pyl(O)	0	0.0	0	0.0	0	0.0	0	0.0	0	0.0	0	0.0	0	0.0	0	0.0	0	0.0	0	0.0
Sec(U)	1	0.5	1	0.5	0	0.0	1	0.5	1	0.5	1	0.4	1	0.5	0	0.0	1	0.5	1	0.5

Table 3. Protein parameters in the GPX-1 enzymes of selected breath-holding animals.

Species	#aa	Mw (Kda)	Theoretical pI	Negatively Charged Residues (Asp+Glu)	Positively Charged Residues (Arg+Lys)	Net Charge	Instability Index
Homo sapiens	203	22088.17	6.15	21	20	-1	47.96
Neomonachus schauinslandi	209	22566.64	6.74	20	20	0	51.55
Leptonychotes weddellii	209	22600.00	6.15	21	20	-1	50.27
Neophocaena asiaeorientalis asiaeorientalis	206	22651.85	6.73	22	22	0	50.50
Delphinapterus leucas	206	22651.85	6.73	22	22	0	50.50
Balaenoptera acutorostrata scammoni	238	25841.54	8.50	22	25	+3	51.78
Callorhinus ursinus	208	22562.69	6.14	21	20	-1	49.55
Lipotes vexillifer	206	22627.16	6.73	22	22	0	47.10
Zalophus californianus	208	22552.66	6.15	21	20	-1	49.54
Tursiops truncatus	206	22651.85	6.73	22	22	0	50.50

Table 4. Reported maximum breath-holding times of the animals in the study.

Organism	Breath holding time (min)	Deep diving depth (m)	References
Homo sapiens (Human)	10.45	100	www.cmas.org
Physeter macrocephalus (Sperm whale)	<138	<2000	Watkins et al., 1993
Neomonachus schauinslandi (Hawaiian monk seal)	20	<550	NOAA fisheries, 2018
Leptonychotes weddellii (Weddell seal)	<70	<600	Kooyman, 1966; Zaopol et al.,1979
Neophocaena asiaeorientalis asiaeorientalis (Yangtze finless porpoise)	2	20	Bi et al., 2015
Delphinapterus leucas (Beluga whale)	<20	20- 900	Heide-Jørgensen et al., 1998
Balaenoptera acutorostrata scammoni (North Pacific minke whale)	9.6	106	Gales et al., 2013
Callorhinus ursinus (Northern fur seal)	5	175	Zeppelin et al., 2019
Lipotes vexillifer (Yangtze river dolphin)	5	20	Zhou et al., 1979
Zalophus californianus (California sea lion)	12	536	Steven et al., 1989
Tursiops truncatus (Atlantic bottle-nosed dolphin)	5	450	Leigh et al., 2007

3.5 3-Dimensional modelling of the protein structures

Three-dimensional model of human GPX was modeled by using the Swiss Model (Figure 3) (Waterhouse et al., 2018; Studer et al., 2020). Swiss Model created the model by using the template coded 1gp1.1.A. The sequence identity was found to be 90.16%. The resolution of the model was given as 0.2 nm. GMQE and QMEANDisCo Global values were found as 0.89 and 0.90 ± 0.05, respectively. In this study, we also wanted to see 3-D structural differences between the GPX-1of *Homo sapiens* and *Tursiops truncatus* (Atlantic bottle-nosed dolphin). We wanted to select *T.truncatus* since it can dive greater than 450 m. *T.truncatus* was selected in this study since it is one of the common animals. The complete enzyme sequence for *Physeter macrocephalus* does not exist in Uniprot database. The 3-dimensional structure of *T.truncatus* was also shown in Figure 3b. From the Swiss model parameters, it could be said that the GPX-1enzymes found in these organisms are quite similar. Due to the high similarities, GPX-1enzymes are house-keeping enzymes and therefore, highly conserved sequences among the species. Possible mutations observed within these sequences may affect the diving times.

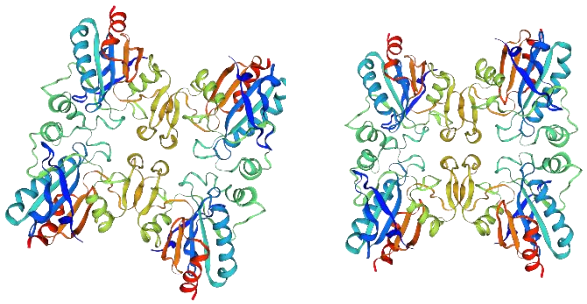

a) *Homo sapiens* b) *Tursiops truncatus*

Fig 3. Swiss-Models of GPX-1 enzymes from *Homo sapiens* (a) and *Tursiops truncatus* (b) (template: 1gp1.1.A).

In protein data bank (rcsb.org), 3-D structures of different GPX-1 enzymes can also be accessible. For example, crystal structure of the selenocysteine to glycine mutant of human glutathione peroxidase 1 is also accessible through the code of 2F8A.

4. Discussion

GPX-1 is of great importance in detoxification of hydrogen peroxide which is formed as a product of many metabolic processes in human metabolism. Effects of physical exercise on GPX is complicated. According to a very recent meta-analysis, physical exercise has no effect on GPX in human (Wang et al., 2023). In this paper, GPX-1 from breath-holding animals were compared and it is found that the sequence of this enzyme is mostly conserved in all animals due to its critical function in the metabolism.

According to Uniprot.org, the human GPX-1enzyme reveals important amino acid modifications. The modifications such as phosphoserine, N6-acetyllysine, N6-succinyllysine are observed at the residues 34, 88, 114, 148, 197 and 201. From this research, it could be said that whatever the breath holding species is in the paper, the amino acid sequence of GPX-1 is highly conserved.

In this report, we also compared the diving times and also depth of some of the breath holding animals (Table 5). The diving time and depth for *Homo sapiens* (human) is reported as 10.45 min and 100 meters, respectively (www.cmas.org). Maximum diving time and depth were found as 138 min and deeper than 2000 m, respectively, from *Physeter macrocephalus* (Sperm whale) (Watkins et al., 1993). Other samples of the animals are also given in Table 4. Based on the mutations in the amino acid sequence sports informatics methods can be developed for the selection of athletes for apnea competitions. This is a sample basic research of GPX-1 enzyme among different species. The anatomical structures of the species analyzed are not investigated which also play a role in dive depth and breath holding e.g. lung size presence of tail and special traits for swimming and diving. Further studies based on different enzymes should be conducted especially on human breath-holding times. Since bioinformatics tools may reveal interesting outputs. After the availibility of GPX-1 sequence data among humans, the selection of the athletes would be possible based on diferences in amino acid sequences.

5. Conclusion

Sports informatics is a new field in sports science. The biological data in bioinformatics databases such as DNA and protein sequences related to performances can effectively be used in sport sciences for many purposes such as talent selection, prevention of sport injuries and development of special trainings. This paper shows that amino acid sequences of GPX-1 from different breath holding animals are highly conserved. Therefore, GPX-1enzyme activities, mRNA levels and its sequence can be checked in athletes who are interested in breath holding sports such as apnea, spear fishing, underwater hockey and underwater rugby.

Acknowledgements

This paper was presented in 5th International Eurasion Conference on Biological and Chemical Sciences, 23-25 November 2022, Ankara-Türkiye.

Authors' contributions:

L.C. conceived of the presented idea. L.C., E.C. and O.A. developed to the design and implementation of the research, to the analysis of the results and to the writing of the manuscript. All authors agreed to submit the paper to the Eurasian Journal of Biological and Chemical Sciences.

Conflict of interest disclosure:

The authors declare that they have no known competing financial interests or personal relationships that could have appeared to influence the work reported in this paper

References

Annen J, Panda R, Martial C, Piarulli A, Nery G, Sanz LR, Valdivia-Valdivia JM, Ledoux D, Gosseries O. Laureys S. 2021. Mapping the functional brain state of a world champion freediver in static dry apnea. Brain Struc Func. 226: 2675-2688.

Bart RM, Lau H. 2022. Shallow Water Blackout. In StatPearls. StatPearls Publishing. Treasure Island (FL).

Bi J, Hu B, Zheng J, Wang J, Xiao W, Wang D. 2015. Characterization of the hypoxia-inducible factor 1 alpha gene in the sperm whale, beluga whale, and Yangtze finless porpoise. Mar Biol 162(6):1201-1213

Cormack J. R., Gott J., Kondogiannis S. 2017. Profound Hypopnea With Xenon Anesthesia in a Free Diver. A&A Practice, 8(4): 90

Feldkamp SD, DeLong RL, Antonelis GA. 1989. Diving patterns of California sea lions, *Zalophus californianus*. Can J Zool. 67(4):872-883

Gales N, Bowers M, Durban JW, Friedlaender AS, Nowacek DP, Pitman RL, Read AJ, Tyson RB. 2013. Advances in non-lethal research on Antarctic minke whales: biotelemetry, photo-identification and biopsy sampling. Paper SC/65a/IA12 presented to the IWC Scientific Committee.

Gasteiger E, Hoogland C, Gattiker A, Wilkins MR, Appel RD, Bairoch A. 2005. Protein identification and analysis tools on the ExPASy server. The Proteomics Protocols Handbook 571-607

Heide-Jørgensen MP, Richard PR, Rosing-Asvid A. 1998. Dive Patterns of Belugas (*Delphinapterus lencas*) in Waters near Eastern Devon Island. Arctic. 17-26

Ioannidis G, Lazaridis G, Baka S, Mpoukovinas I, Karavasilis V, Lampaki S, Kioumis I, Pitsiou G, Papaiwannou A, Karavergou A, Katsikogiannis N, Sarika E, Tsakiridis K, Korantzis I, Zarogoulidis K, Zarogoulidis P. 2015. Barotrauma and Pneumothorax. J Thorac Dis. 7(1):S38–S43

Klatsky LJ, Wells RS, Sweeney JC. 2007. Offshore bottlenose dolphins (*Tursiops truncatus*): Movement and dive behavior near the Bermuda Pedestal. J Mammal. 88(1): 59-66

Kooyman, GL. 1966. Maximum diving capacities of the Weddell seal, *Leptonychotes weddelli*. Science 151(3717):1553-1554

NOAA Fisheries. 2022. Hawaiian Monk Seal. https://www.fisheries.noaa.gov/species/hawaiian-monk-seal. Accessed 1 Nov 2022

Rich C., McAteer K., Leytin V., Binder W. 2019. A free diver with hemoptysis and chest pain. Rhode Island Med J 102(1):33-36

Scott T., van Waart H., Vrijdag X. C., Mullins D., Mesley P., Mitchell S. J. 2021. Arterial blood gas measurements during deep open-water breath-hold dives. J Appl Physiol. 130(5): 1490-1495

Sievers F, Wilm A, Dineen D, Gibson TJ, Karplus K, Li W, Lopez R, McWilliam H, Remmert M, Söding J, Thompson JD. 2011. Fast, scalable generation of high-quality protein multiple

sequence alignments using Clustal Omega. Mol Syst Biol. 7(1):539

Studer G, Rempfer C, Waterhouse AM, Gumienny R, Haas J, Schwede T. 2020. QMEANDisCo—distance constraints applied on model quality estimation. Bioinformatics 36(6):1765-1771

Uniprot Consortium. 2021. UniProt: the universal protein knowledgebase in 2021. Nucleic Acids Res 49 no. D1 (2021): D480-D489

Wang Y, Luo D, Jiang H, Song Y, Wang Z, Shao L, Liu Y. 2023. Effects of physical exercise on biomarkers of oxidative stress in healthy subjects: A meta-analysis of randomized controlled trials. Open Life Sci. 18(1):20220668

Waterhouse A, Bertoni M, Bienert S, Studer G, Tauriello G, Gumienny R, Heer FT, de Beer TA, Rempfer C, Bordoli L, Lepore R. 2018. SWISS-MODEL: homology modelling of protein structures and complexes. Nucleic Acids Res. 46(W1):W296-W303

Watkins WA, Daher MA, Fristrup KM, Howald TJ, Di Sciara GN. 1993. Sperm whales tagged with transponders and tracked underwater by sonar. Mar Mammal Sci 9(1):55-67

Wilkinson A. 2009. The deepest dive: how far down can a free diver go? New Yorker 24:24-30

Zapol WM, Liggins GC, Schneider RC, Qvist J, Snider MT, Creasy RK, Hochachka PW. 1979. Regional blood flow during simulated diving in the conscious Weddell seal. J Appl Physiol. 47(5): 968-973

Zeppelin T, Pelland N, Sterling J, Brost B, Melin S, Johnson D, Lea MA, Ream R. 2019. Migratory strategies of juvenile northern fur seals (*Callorhinus ursinus*): bridging the gap between pups and adults. Sci Rep. 9(1):1-16

Zhou K, Pilleri G, Li Y. 1979. Observations on the baiji (*Lipotes vexillifer*) and the finless porpoise (*Neophocaena asiaeorientalis*) in the Changjiang (Yangtze) River between Nanjing and Taiyangzhou, with remarks on some physiological adaptations of the baiji to its environment. Investig Cetacea. 10:109-20

RESEARCH ARTICLE
Eurasian J Bio Chem Sci, 6(2):88-93, 2023
https://doi.org/10.46239/ejbcs.1373150

EJBCS

Eurasian Journal of Biological and Chemical Sciences

Journal homepage: www.dergipark.org.tr/ejbcs

Application of a new inhibitor for the corrosion of iron in acidic solution: Electrochemical effect of a scorpion venom

Demet Özkır[1]*, Osman Seyyar[2]

*[*1]Niğde Ömer Halisdemir University, Faculty of Arts & Sciences, Department of Chemistry, Niğde, 51240, Türkiye*
[2]Niğde Ömer Halisdemir University, Faculty of Arts & Sciences, Department of Biology, Niğde, 51240, Türkiye

*Corresponding author : dozkir@ohu.edu.tr
Orcid No: https://orcid.org/0000-0002-8096-5755

Received : 09/10/2023
Accepted : 05/11/2023

Abstract: In this study, the venom of the species *Leiurus abdullahbayrami*, known as the yellow scorpion from the Buthidae family, was applied for the first time as a natural corrosion inhibitor for iron in hydrochloric acid solution. The effectiveness of scorpion venom as an eco-friendly and natural inhibitor was determined by electrochemical methods such as electrochemical impedance spectroscopy (EIS), potentiodynamic polarization (Tafel extrapolation method) and linear polarization resistance (LPR) after an hour of immersion. Four different concentrations were determined for the green and natural inhibitor scorpion venom in 1.0 M HCl, and it was observed that the corrosion of iron in these solutions was significantly inhibited. In general, the inhibition efficiency was above 80%. According to the potentiodynamic polarization data, it has been determined that the *Leiurus abdullahbayrami* venom acts as a cathodic-type inhibitor on the Fe surface. Finally, the surface images of the iron electrodes in 1.0 M HCl solutions without and with *Leiurus abdullahbayrami* venom after 1 h immersion were examined by field emission scanning electron microscope (FE-SEM), it was concluded that the surface containing scorpion venom had a flatter compared to the uninhibited surface.

Keywords: Scorpion venom, *Leiurus abdullahbayrami*, Acidic corrosion, Green inhibitor, Adsorption, EIS

1. Introduction

One of the most important problems experienced today is corrosion and its consequences. Corrosion is an inevitable natural disaster and an important phenomenon that must be struggled. In the industrial field, when considered in terms of production costs of metallic materials, it causes significant losses (Fang et al. 2019). All technical metals actually exist in nature as their oxides and sulphides, called ores. In this state, they are in their most stable state in nature, with minimum energy and maximum disorder. Since everything in nature is stable with the lowest energy and highest disorder, all metals spontaneously try to return to their stable state in nature when left uncontrolled. In fact, this rotation phenomenon is another expression of corrosion (Erbil 2012). The most commonly used metal in industry and architecture is iron, and the alloy is steel. They are highly preferred due to both their physical and chemical properties and cost. However, the biggest problem that limits the use of these materials is corrosion.

One of the methods of preventing corrosion, and the most preferred especially in cleaning processes with acidic solutions, is inhibitor applications. By means of various inhibitor compounds added to the corrosive solution, the interaction between the metal and the solution is interrupted, and these substances are physically and/or chemically adsorbed to the metal surface by the effect of the electric field formed at the interface (Doğru Mert 2017). The effectiveness of inhibitor substances is related to their chemical structures, and it is known that heteroatomic organic substances containing functional groups such as -OH, -COOH, -CN, -SN, double/triple bonds or unshared electron pairs will easily interact with the metal surface (Özkır 2019a). Unfortunately, chemicals known as corrosion inhibitors harm the environment due to their ecological side effects. However, in recent years, new and non-toxic inhibitors that cover the metallic surface strongly, are both highly efficient and environmentally safe, have attracted the attention of researchers (Srivastava et al. 2017; Nazlıgül et al. 2022).

Scorpions are predatory and living fossils that have existed on Earth for 430 million years by adapting very effectively to their natural habitat (Gomes and Gomes 2015). There are many harmful scorpions belonging to the Buthidae family in Türkiye, and one of the most poisonous Turkish scorpion species is known as *Leiurus abdullahbayrami* (Fig. 1). Scorpion venoms are the main sources that provide

promising bioactive peptide molecules, especially in the discovery and development of new drugs in the field of medicine. Scorpion venoms consist of a complex mixture of small organic molecules and ions, bioactive peptides and proteins for the development of defense mechanisms (Numanoğlu Çevik and Kanat 2022). Scorpion venom incorporates both non-proteinaceous components consisting of water, mucosa, nucleotides, mucopolysaccharide, lipids, metals and inorganic compounds, and proteinaceous components consisting of enzymes and peptides (Tobassum et al. 2020).

The most important idea in this study emerged from the fact that scorpion venoms can play a role as an effective inhibitor in preventing metallic corrosion, as they have a molecular structure suitable for corrosion inhibitors, as they are known to contain molecules such as bioactive peptides and proteins. In the light of this idea, in this study, the effect of venom from the *Leiurus abdullahbayrami* species as an environmentally friendly green inhibitor on the corrosion of iron (mild steel) electrodes kept in 1.0 M HCl solution for one hour was investigated by some electrochemical methods. This study is also noteworthy because there is no previous study in the literature showing that scorpion venom has been used as an inhibitor to prevent metallic corrosion.

Fig. 1 Photograph of the yellow scorpion *Leiurus abdullahbayrami*, whose venom was used in the study (original)

2. Materials and Method

2.1. Leiurus abdullahbayrami venom

Leiurus abdullahbayrami venom was obtained from Niğde Ömer Halisdemir University Arachnology Museum (NOHUAM).

2.2. Determination of concentration of stock Leiurus abdullahbayrami venom solution and preparation of working solutions

The mass of scorpion venom obtained from NOHUAM was 0.1733 g. For this reason, the actual concentration of the stock scorpion venom solution was calculated as 0.3466% (w/v). After the stock solution concentration, the working concentrations for electrochemical experiments were determined as 0.160% (w/v); 0.100% (w/v); 0.050% (w/v); 0.020% (w/v) and 0.010% (w/v), respectively, from the most concentrated solution to the most dilute. Electrochemical experiments were carried out in 1.0 M HCl solution.

2.3. Electrochemical experimental processes

Iron (mild steel) was tapped as the working electrode with the following percentage composition (wt.%) such as 0.06030% Cr, 0.00222% Nb, 0.07890% Ni, 0.01100% V, 0.01100% P, 0.01040% Mo, 0.08400% C, 0.21700% Cu, 0.40900% Mn, 0.01900% S, 0.01620% Sn, 0.00198% Co, 0.10200% Si and 98.977% Fe. The electrode surfaces were added in a cylindrical mould including mixture of polyester and surface area of Fe electrode was 0.5024 cm^2 exposed to the HCl solution. The Fe electrode' surfaces were smoothed with 150, 600 grids of emery paper. The Fe electrodes' surfaces were polished with acetone and distilled water. The conventional three-electrode technique was applied utilizing the computer-integrated CHI-660B electrochemical analyzer device in experiments. The working test electrode is iron was utilized. The Pt plate is a counter electrode with a surface area of 2.0 cm^2, and the reference electrode is Ag/AgCl. All potentials are given by reference electrode.

Electrochemical experiments were conducted by LPR, EIS and Tafel extrapolation methods. These methods were performed in 1.0 M HCl solution without and with four different *Leiurus abdullahbayrami* venom concentrations. Before starting all electrochemical experiments, the Fe electrodes were immersed in the hydrochloride acid solution for one-hour in order to balance the system at 298 K for the open circuit potential (E_{corr}). EIS experiments were carried out on the E_{corr} at a frequency range of 10^5 to $5x10^{-3}$ Hz with 5 mV amplitude practised to the corrosion system. The Tafel extrapolation measurements were conducted with ±0.350 V anodic/cathodic potential from E_{corr}, respectively. It is practised at a scan rate of 1.0 mV s^{-1}. LPR method as the third experiment was conducted at a scan rate of 0.1 mV s^{-1} ±10 mV from E_{corr} and polarization resistance (R_p) was calculated from the potential slope versus current.

2.4. Surface examinations of iron electrodes

The images of Fe surfaces were examined by FE-SEM (Zeiss GeminiSEM 500 with computer controlled) technique in aggressive blank solution with and without 0.160% (w/v) *Leiurus abdullahbayrami* venom after 1 hour of duration at 298 K.

3. Results and Discussion

3.1. Evaluation of electrochemical data for Leiurus abdullahbayrami venom

It is important that the method to be applied to determine the corrosion rate does not essentially change the natural structure of the metal surface. For this reason, alternative current impedance, which is an electrochemical method and is thought to change the nature of the metal at a minimum level, is one of the most preferred methods (Erbil, 2012). Therefore, measurements were made and evaluated with EIS, LPR and Tafel extrapolation methods end of an hour of immersion in 1.0 M HCl solutions with and without four different concentrations of scorpion venom as inhibitor, in order to determine the electrochemical corrosion behavior of iron. The two types of equivalent circuits of the corrosion

process were composed from the EIS data by using Zview2 software. Two types of electrical equivalent circuit models in Figure 2 and 3 for blank and all inhibited solutions, respectively were indicated in process.

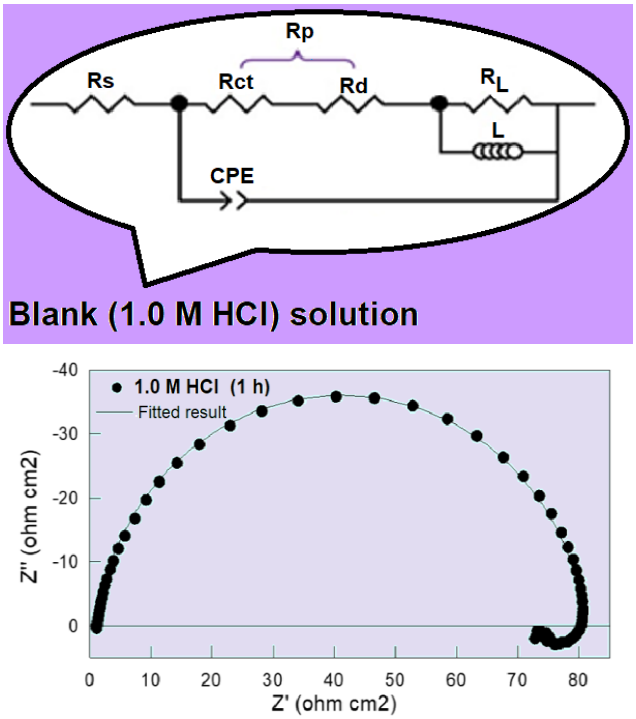

Fig. 2 Electrical equivalent circuit proposed and impedance diagram for blank solution after 1 h immersion

It will be seen that in Fig. 2 and 3, the two circuits proposed are dissimilar from each other. The most logical separation for solutions containing the scorpion venom is the inhibitor film composed on the Fe electrode surface and the resistance (R_{film}) it forms (Fig. 3). Film resistance results from the adsorption of complex organic molecules such as peptides and proteins in the scorpion venom, directed to the Fe electrode surface in the acidic solution. When four different concentrations of scorpion venom are added to the aggressive 1.0 M HCl electrolyte, it can be followed that the corrosion of Fe electrodes declines more plainly in the impedance diagram in Figure 3 (Özkır 2019b; Özkır 2021a). *Leiurus abdullahbayrami* venom adsorbed on the surface of iron in fact hinders the corrosion by forming a protective film layer on the Fe surface. In addition, this situation is clearly understood from the increasing radius as the inhibitor is added to the solution.

Impedance diagrams generally consist of two parts: High and low frequency regions. While the corrosion process consists of the total of these two frequency regions, charge transfer (R_{ct}) and diffuse layer (R_d) processes occur in the high frequency region. The low frequency region is basically the important part affected by the inhibitor. In other words, surface protection occurs with the film layer (R_f) formed due to total adsorption from the scorpion venom, as well as the products (R_a) accumulated on the surface due to corrosion.

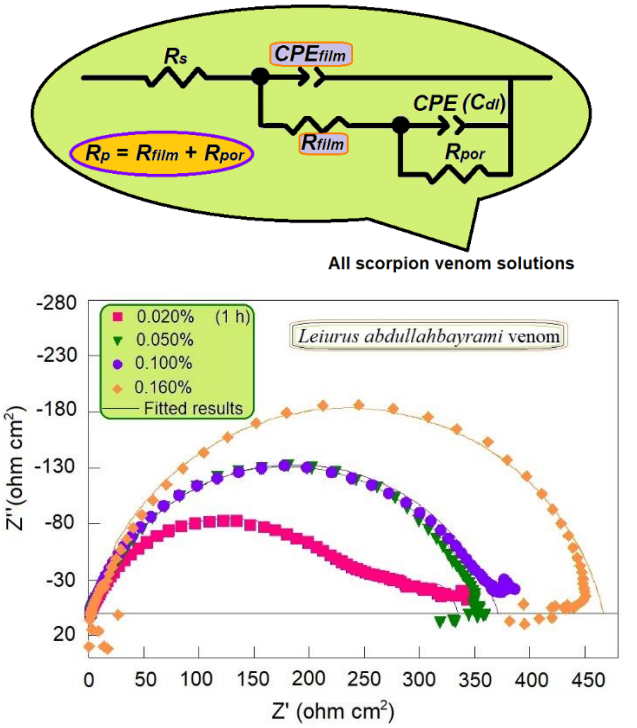

Fig. 3 Electrical equivalent circuit proposed and impedance diagrams in containing four different concentrations of *L. abdullahbayrami* venom

Looking at Fig. 3, the equivalent circuit proposed for the inhibited system consists of two constant phase elements: Double layer capacitance (CPE_{dl}), which refers to the double layer between the Fe metal and the solution, and film capacitance (CPE_{film}), which results from the adsorption of the scorpion venom on the surface of the Fe metal.

The polarization resistance (R_p) values obtained from the EIS, LPR and Potentiodynamic polarization experiments are indicated in Table 1.

Table 1 Electrochemical experiment data in solutions without and with *L. abdullahbayrami* venom

Scorpion venom	**EIS**				
***C* (w/v %)**	**Blank**	**0.020**	**0.050**	**0.100**	**0.160**
E_{corr} **(V/Ag/AgCl)**	-0.474	-0.530	-0.522	-0.520	-0.514
R_s **(Ω cm²)**	1.2	1.3	1.5	1.4	1.3
***CPE* (μF cm⁻²)**	110	84	80	69	57
n	0.94	0.85	0.81	0.80	0.76
R_L **(Ω cm²)**	8	-	-	-	-
***L* (*H*)**	4	-	-	-	-
R_p **(Ω cm²)**	72	335	356	370	466
η (%)	-	**78.5**	**79.8**	**80.5**	**84.5**
Scorpion venom	***LPR**				
$^{*}E_{corr}$ ***(V/Ag/AgCl)***	-0.475	-0.530	-0.529	-0.526	-0.523
$^{*}R_p$ **(Ω cm²)**	71	351	355	392	435
$^{*}\eta$ **(%)**	-	**79.8**	**80.0**	**81.9**	**83.7**
Scorpion venom	****Potentiodynamic polarization**				
$^{**}E_{corr}$ ***(V/Ag/AgCl)***	-0.475	-0.531	-0.528	-0.530	-0.523
$-\beta_c$ **(*mV* dec⁻¹)**	108	108	105	111	111
i_{corr} **(*μA* cm⁻²)**	265	62	55	51	41
$^{**}\eta$ **(%)**	-	**76.6**	**79.2**	**80.8**	**84.5**

At the end of the one-hour immersion period, the η% values calculated from the R_p values by the EIS method increased as scorpion venom was added to the solution medium. The distribution range of η% values was 78.5–84.5%. While the *CPE* value in blank solution was 110 $\mu F/cm^2$, it was monitored that it dominated when scorpion venom was added to the HCl solution. The distribution range of CPE values is 84–57 $\mu F/cm^2$. While the corrosion potential value (E_{corr}) was –0.474 V in HCl electrolyte, it shifted to more negative (cathodic) potentials in solutions containing *L. abdullahbayrami* venom (Table 1). According to the LPR method data, the $^{*}R_p$ value was 71 $\Omega\ cm^2$ in 1.0 M HCl solution without inhibitor, but it rised when scorpion venom was added to the acidic solution. $^{*}\eta$% values calculated from $^{*}R_p$ values increased as scorpion venom base was added to the HCl solution and the distribution range became 79.8–83.7%. The inhibitory efficiency results of the *L. abdullahbayrami* venom calculated by both electrochemical methods were highly consistent with each other (Özkır 2021b). The dissolution process parameters of iron electrode calculated by the Tafel extrapolation method, which is another electrochemical method, are shown in **Table 1. Potentiodynamic polarization curves of working electrodes in HCl solution for four different *L. abdullahbayrami* venom concentrations at 298 K are offered in Figure 4. While the corrosion current density (i_{corr}) value in the blank solution was 265 μA/cm^2, these values gradually dimunated as scorpion venom was added to the HCl solution.

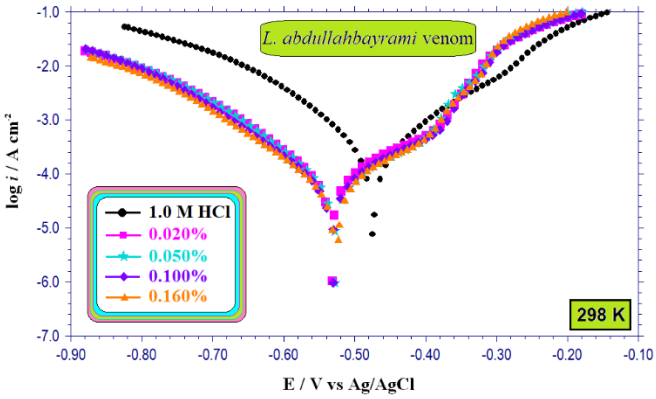

Fig. 4 Potentiodynamic polarization plots of Fe electrode in HCl solution for four concentrations of *L. abdullahbayrami* venom

In all experimental solutions, as the scorpion venom concentration enhanced, corrosion current density (i_{corr}) values decreased and inhibition efficiency values rised. While the cathodic Tafel constant ($-\beta_c$) was 108 mV/dec in the blank solution, it varied between 97 mV/dec and 102 mV/dec in the solutions with inhibitor. The fact that the cathodic Tafel constants calculated in solutions containing and without scorpion venom did not change much indicates that the hydrogen formation mechanism was not affected by the inhibitor scorpion venom studied. As can be seen from the semi-logarithmic current-potential curves and Table 1, the $^{**}E_{corr}$ values of Fe electrode read directly from the CHI device were -0.475 V at 298 K in an uninhibited solution, while the $^{**}E_{corr}$ values shifted to more negative (cathodic) potentials when scorpion venom solutions were added to the medium. The maximum potential change in solutions without and containing inhibitors is 56 mV. In the solution with scorpion venom, in contrast to the blank solution, the $^{**}E_{corr}$ values shift very slightly to negative values, and all of the shifts of the E_{corr} values are less than 85 mV (Wen et al. 2023). Looking at the cathodic curves in Figure 4, the contribution of scorpion venom significantly reduced the current density in 1.0 M HCl solution. For this reason, it was thought that the scorpion venom used acted as a cathodic inhibitor in 1.0 M HCl solution (Policarpi and Spinelli 2020; Akkoç et al. 2023). The results obtained with the three experimental methods applied were both supportive of each other and it was concluded that the adsorption of *L. abdullahbayrami venom* on the Fe surface is inevitable and it can also be used as a green inhibitor because it does not have an environmentally friendly effect.

A visual graphic summary of the electrochemical experiment data in Table 1 is presented in Figure 5.

3.2. Surface examinations by FE-SEM analysis

Since FE-SEM is a field emission scanning electron microscope, it provides the opportunity to perform much clearer surface analysis with high resolution (Singh et al. 2018). Detailed surface examinations were carried out by FE-SEM analysis to determine the surface morphologies of the Fe electrodes that were kept at 298 K for one hour in 1.0 M HCl solutions containing *L. abdullahbayrami* venom at the highest (0.160% w/v) concentration and without inhibitor. FE-SEM images were monitored in Figure 6.

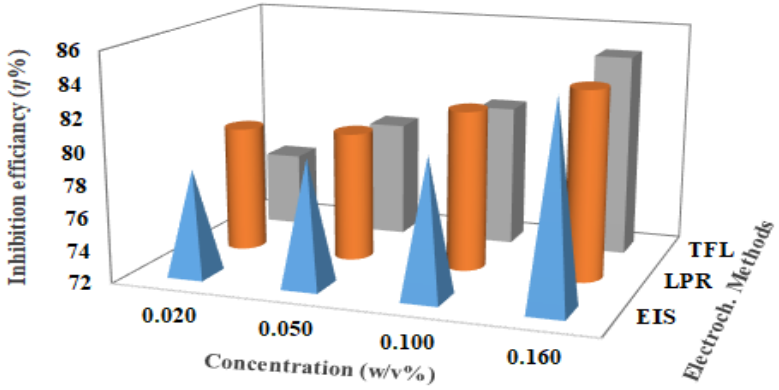

Fig. 5 Variation of inhibition efficiency values according to experimental methods and concentration

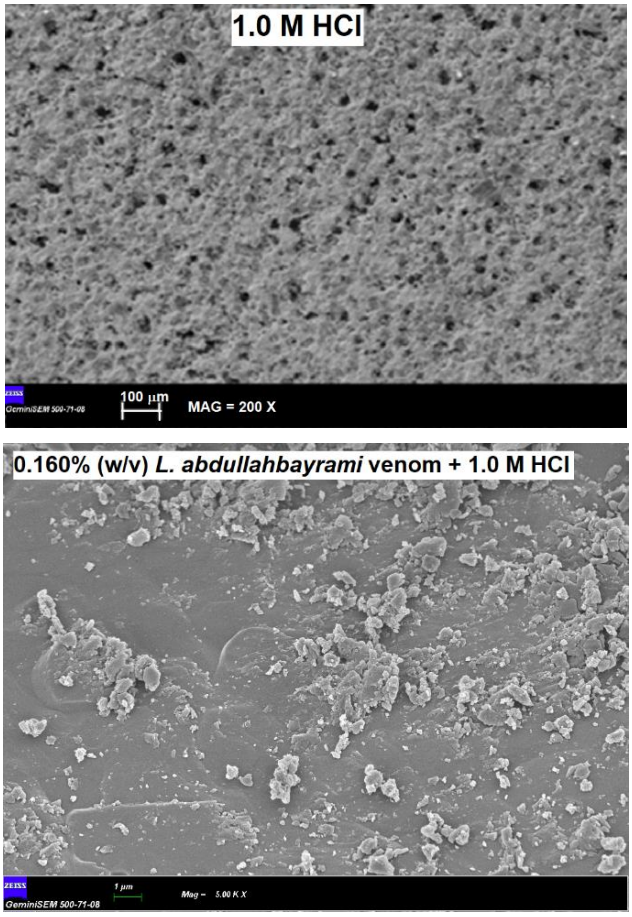

Fig. 6 FE-SEM images of the Fe electrodes for 1 h immersion at 298 K

It was observed that the surface of the Fe electrode, which was immersed in the solution without inhibitor, was indented and in the appearance of pits, the electrode kept in the solution with *L. abdullahbayrami* venom was flatter and the pits both diminuated in number and became smaller (Özkır and Kayakırılmaz 2020).

5. Conclusion

According to the results obtained with EIS, LPR and potentiodynamic polarization curves, it was observed that the inhibition efficiency values enhanced as the *Leiurus abdullahbayrami* venom concentration rised. Even in the solution containing the highest concentration of scorpion venom, Fe electrode is protected with approximately 85% inhibition after 1 hour of immersion time. Scorpion venom affected the corrosion of iron electrode in acidic solution as a cathodic-type inhibitor. In addition, FE-SEM micrographs clearly show that scorpion venom prevents corrosion of Fe surface by forming a protective inhibitor film on the metal surface.

This study stands out for the first application of *Leiurus abdullahbayrami* venom from the family Buthidae as an eco-friendly and green inhibitor for Fe electrode in 1.0 M HCl solution. The main sources of scorpion venom are bioactive peptide molecules. It has been reported that the main components in scorpion venom consist of a complex mixture of non-proteinaceous and proteinaceous components. Considering these main components and the results obtained, these properties are among the main reasons for the high inhibitory effectiveness in preventing metallic corrosion. The use of such compounds as corrosion inhibitors is a very important study in terms of both industrial processes and the development of a different application area, since they are biodegradable and do not contain harmful compounds.

Authors' contributions: DÖ, obtaining data & principle investigation & experimental measurements & editing & writing; OS, obtaining data & principle investigation & editing & writing.

Conflict of interest disclosure: The authors declare no conflict of interest on the written article.

References

Akkoç S, Özkır D, Başaran E, Kaya S, Berisha A. 2023. A combined experimental and theoretical approach effect of a benzimidazolium salt as a new corrosion inhibitor on mild steel in HCl solution. Ionics, 29:3813–3827.

Doğru Mert B. 2017. Yumuşak Çeliğin Korozyon Davranışı. Çukurova Üniversitesi Mühendislik Mimarlık Fakültesi Dergisi, 32(2):145-152.

Erbil M. 2012. Korozyon İlkeler – Yöntemler, Korozyon Derneği Yayını, Poyraz Ofset, Ankara.

Fang Y, Suganthan B, Ramasamy RP. 2019. Electrochemical characterization of aromatic corrosion inhibitors from plant extracts. J Electroanal Chem. 840:74-83.

Gomes A, Gomes A. 2015. Scorpion Venoms. In: Gopalakrishnakone P. et al (eds.) Scorpion Venom Research Around the World: Heterometrus Species, Springer Dordrecht Heidelberg New York.

Nazlıgül H, Güllü E, Mert ME, Doğru Mert B. 2022. Investigation of Inhibition Performance of Epdantoin for Mild Steel Protection in HCl Solution: Electrochemical and Quantum Theoretical Approaches. Tr J Nature Sci. 11(4):70-78.

Numanoğlu Çevik Y, Kanat MA. 2022. Comparative analysis of peptides and proteins in two congeneric (Leiurus abdullahbayrami; Buthidae) scorpion venoms by MALDI-TOF MS. Biological Diversity and Conservation, 15(2):186-194.

Özkır D. 2019a. A Newly Synthesized Schiff Base Derived from Condensation Reaction of 2,5-dichloroaniline and benzaldehyde: Its Applicability through Molecular Interaction on Mild Steel as an Acidic Corrosion Inhibitor by Using Electrochemical Techniques. Journal of Electrochemical Science and Technology, 10(1):37–54.

Özkır D. 2019b. The Electrochemical Variation of a Kind of Protein Staining and Food Dye as a New Corrosion Inhibitor on Mild Steel in Acidic Medium. Int J Electrochem. (Article ID 5743952), 2019:1–11.

Özkır D, Kayakırılmaz K. 2020. The Inhibitor Effect of (E)-5-[(4-(benzyl(methyl)amino)phenyl) diazenyl]-1,4-dimethyl-1H-1,2,4-triazol-4-ium zinc(II) Chloride, an Industrial Cationic Azo Dye, onto Reducing Acidic Corrosion Rate of Mild Steel. J Electrochem Sci Technol. 11(3):257-272.

Özkır D. 2021a. The role of *Lavandula* sp. extract for effective inhibiting the mild steel corrosion in the hydrochloric acid solution. Int J Chem Technol. 5(2):125-132.

Özkır D. 2021b. An Overview of *Plagiochila porelloides* (Marchantiophyta) as a New Environmentally Sustainable Green Corrosion Inhibitor for Mild Steel in Acidic Solution. Anatolian Bryol. 7(2):119-130.

Policarpi EdB, Spinelli A. 2020. Application of *Hymenaea stigonocarpa* fruit shell extract as eco-friendly corrosion inhibitor for steel in sulfuric acid. J Taiwan Inst Chem Eng. 116:215-222.

Singh DK, Ebenso EE, Singh MK, Behera D, Udayabhanu G, John RP. 2018. Non-toxic Schiff bases as efficient corrosion inhibitors for mild steel in 1 M HCl: Electrochemical, AFM, FE-SEM and theoretical studies. J Mol Liq. 250:88-99.

Srivastava M, Tiwari P, Srivastava SK, Prakash R, Ji G. 2017. Electrochemical investigation of Irbesartan drug molecules as an inhibitor of mild steel corrosion in 1 M HCl and 0.5 M H 2 SO 4 solutions. J Mol Liq. 236:184-197.

Tobassum S, Tahir HM, Arshad M, Zahid MT, Ali S, Ahsan MM. 2020. Nature and applications of scorpion venom: An overview. Toxin Rev. 39(3):214-225.

Wen J, Zhang X, Liu Y, Shang B, He J, Li L. 2023. Exploration of imidazol-4-methylimine thiourea as effective corrosion inhibitor for mild steel in hydrochloric medium: Experimental and theoretical studies. Colloids Surf A: Physicochem Eng Asp. 674:131895.

RESEARCH ARTICLE
Eurasian J Bio Chem Sci, 6(2):94-103, 2023
https://doi.org/10.46239/ejbcs.1377815

Eurasian Journal of Biological and Chemical Sciences

Journal homepage:www.dergipark.org.tr/ejbcs

Endüstriyel amaçlı kullanılan bazı boyar maddelerin mutajenik etkilerinin *Drosophila* kanat benek testi ile *in vivo* olarak belirlenmesi

Hatice Çelik[1], Handan Uysal [2*]
*[*1]Atatürk Üniversitesi, Fen Bilimleri Enstitüsü, Erzurum,Türkiye*
[2]Atatürk Üniversitesi, Fen Fakültesi, Biyoloji Bölümü, Erzurum,Türkiye

*Corresponding author : hauysal@atauni.edu.tr
Orcid No: https://orcid.org/0000-0002-4290-8223

Received : 18/10/2023
Accepted : 05/112023

Özet: Sentetik boyar maddeler tekstil, kozmetik, gıda, mobilya, ilaç ve otomotiv endüstrisi gibi yaygın kullanım alanları nedeniyle ticari öneme sahip endüstriyel ürünlerdir. Birçok ülkede kullanılan bu boyaların yaklaşık 10.000 çeşidi bulunmaktadır. Yıllık 700.000 ton üretim hacmine sahip olan boyar maddeler, tüm endüstriyel atık miktarının önemli bir kısmını (1/5) oluşturmaktadırlar. Tekstil endüstrisine ait deşarjların tarım alanlarına ve su kaynaklarına karışması toprak gözeneklerinin tıkanıp verimin düşmesine, içme ve sulama suyunun insan tüketimi için elverişsiz hale gelmesine neden olmaktadır. Bu çalışmada üç farklı tekstil boyasının (Süperfix Black NNX (SBNNX), Syanacryl Black XFDL (SBXFDL) ve Reaktive Blue 19 (RB19) mutajenik ve rekombinojenik etkileri *in vivo* olarak *Drosophila* kanat benek testi ile belirlenmiştir.Bu amaçla distile su negatif ve EMS pozitif kontrol grupları hazırlanmıştır. Ayrıca uygulama grupları için de farklı dozlarda her üç tekstil boyası (150, 300 ve 450 ppm) kullanılmıştır. Elde edilen verilere göre, tüm tekstil boyaları hem mutajenik hem de rekombinojenik etkili bulunmuştur. Uygulama gruplarına ait veriler, distile su kontrol grubu ile karşılaştırıldığında aralarındaki fark istatistiki olarak anlamlıdır (p<0,05). Kullanılan boyaların genotoksisitesi için de dominansi sırası SBNNX > SBXFDL > RB19 olarak belirlenmiştir.

Anahtar Kelimeler: model organizma, somatik mutasyon, tekstil boyası

In vitro determination of the mutagenic effects of some dyestuffs used for industrial purposes using the Drosophila wing spot test.

Abstract: Synthetic dyes are industrial products of commercial importance due to their widespread use in the textile, cosmetics, food, furniture, pharmaceutical and automotive industries. There are approximately 10.000 types of these paints used in many countries. With an annual production volume of 700.000 tons, dyestuffs constitute a significant portion (1/5) of all industrial waste.The mixing of the discharges from the textile industry into agricultural areas and water resources causes the soil pores to become clogged, resulting in a decrease in productivity and making drinking/irrigation water unsuitable for human consumption.In this study, the mutagenic and recombinogenic effects of three different textile dyes (Superfix Black NNX (SBNNX), Syanacryl Black XFDL (SBXFDL) and Reactive Blue 19 (RB19) were determined *in vivo* by *Drosophila* wing spot test. For this purpose, distilled water negative and EMS positive control groups were prepared.In addition, different doses of all three textile dyes (150, 300 and 450 ppm) were used for the application groups.According to the data obtained, all textile dyes were found to be both mutagenic and recombinogenic.When the data of the application groups are compared with the distilled water control group, the difference between them is statistically significant (p<0.05).For the genotoxicity of the dyes used, the dominance order was determined as SBNNX > SBXFDL > RB19.

Keywords: model organism, somatic mutation, textile dye

*Bu makale Atatürk Üniversitesi, Fen Bilimleri Enstitüsü,, Biyoloji Ana Bilim dalında, Prof. Dr. Handan UYSAL danışmanlığında hazırlanmış olan Hatice ÇELİK'in " *Drosophila* kanat hücrelerinde bazı sentetik tekstil boyalarına bağlı mitotik rekombinasyonların *in vivo* olarak belirlenmesi " isimli yüksek lisans tezinden çıkarılmıştır.

1.Giriş

Yaşadığımız dünya düzeninde hızlı değişmenin ve küreselleşmenin getirdiği rekabete ayak uydurabilmenin en önemli etkeni teknolojidir. Dünya nüfusundaki artışa paralel olarak teknolojinin ilerlemesiyle sanayi kuruluşları, fabrikalar ve diğer endüstriyel üretimlerde de artış söz konusudur. Türkiye ise sanayisi gelişmekte olan bir ülkedir ve son yıllarda Türkiye'de sanayinin hızla gelişmesine paralel olarak tekstil endüstrisinde de dev adımlar atılmaktadır (Mercimek 2007). Tekstil ve hazır giyim sektörü, elyaf ve ipliği kullanım eşyasına dönüştürecek süreçleri kapsayan işlemleri içermektedir (Sarıoğlu ve Kayadibi 2012). Tekstil endüstrisinde özellikle daha küçük ölçekli ve alt yapı bakımından yetersiz tesislerin varlığı da kontrolsüz büyümeyi beraberinde getirmiştir. Ayrıca bu sektörde kullanılan elyafın elde edilme işlemleri, iplik yapımı, dokuma ve terbiye hazırlık aşamalarında kuru ve ıslak prosesler oldukça önemlidir. İplik yapımı ve dokuma hazırlık aşamaları, kuru işlemler diye tanımlanan süreçleri kapsarken terbiye işlemi (haşıl dökme, yıkama, pişirme, merserizasyon, boyama, apreleme) bol miktarda suyun kullanıldığı ıslak proseslerden meydana gelmektedir.En çok su harcanan işlemlerden birisi ise boyamadır. Tekstil endüstrisi deşarjları, kullanılan boyar maddenin yapısına göre çözünmüş halde ya da kolloyidal yapıda bulunabilen çok renkli atık suları içermekte ve bu atık suların bulunduğu alanlarda ise çevresel bakımdan çok önemli olan endüstriyel kirlenme meydana gelmektedir (Tünay ve ark. 1996; Ölmez 1999).

Cisimleri renkli hale getirmek için kullanılan maddelere boyar madde denir. Boyar madde, herhangi bir nesneye renk vermek veya onu korumak için uygulanan kaplama amaçlı maddeler olarak da tanımlanmaktadır. Boya ile korumadaki temel amaç, uygulama alanının su veya hava ile temasının kesilmesidir. Boyalar sanat, tasarım ve endüstriyel amaçlı kullanıldıkları gibi örneğin karayollarında şerit çizgilerinin çekilerek güvenli ulaşımın sağlanması gibi farklı alanlarda da kullanılmakta ve oldukça farklı malzemelere uygulanabilmektedir.

Boyar maddelerin sürekli kullanıldığı bir diğer sektör tekstildir. Boyar maddeler, organik bileşikler olup boyanacak materyalle kimyasal veya fiziko-kimyasal etkileşime girerek cisimleri renkli hale getirirler. Rengarenk hazırlanan tekstil ürünleri çeşitli işlemlerden geçerek boyanmaktadır. Boyar madde kullanarak değiştirilen malzemelerin boyandıktan sonraki ilk haline tekrar dönmesi de mümkün olamamaktadır.

Tarihsel süreçte insanların cisimlere ve kendisine özel bir görünüm kazandırmak istemesi ile boyar maddelere ihtiyaç doğmuş ve ilk çağdan beri doğal ürünlerden birçok boyar madde elde edilmiştir. Doğal boyar maddeler maya ve bakteri gibi mikroorganizmalardan, bitkilerin kök, kabuk, tohum, meyve, çiçek kısımlarından, bazı böcekler ve balıklardan, hayvanların deri ve salgı bezlerinden basit bir takım işlemler sonucu elde edilmektedir. Örneğin; Fabaceae familyasından *Indigofera tinctoria* (indigo ağacı) bitkisi mavi, Kermesidea (Insecta)'ya ait *Kermes ilicis* (kermes böceği) kırmızı, *Janthinobacterium lividum* bakterisi mor, bir çeşit mantar olan *Aspergillus niger* de siyah renk eldesi için kaynak teşkil etmektedir (Başer ve İnanıcı 1990; Önal 2000; Hunger 2003; Gürcüm ve Öneş 2018). Fakat sanayi devriminden sonra birçok sektörün gelişmesi ile doğal boyar maddelere olan ihtiyaç ve kullanım artmış ve doğal ürünlerden elde edilen boyar maddelerin elde edilmesinin zor, pahalı ve miktar olarak az olması, renk skalasının dar, kalitelerinin de düşük oluşu, artan nüfus ve gelişen teknoloji gibi nedenlerden dolayı yetersiz kalmıştır. Bu nedenle sentetik boyar madde arayışına geçilmiştir. 1856 yılında İngiliz kimyager William Henry Perkintarafından anilin yağından tesadüfen elde edilmiş olan anilin moru, ilk sentetik boya olarak bilinmektedir (Kant 2012).

Dünyada endüstrinin gelişmesiyle birlikte daha fazla kullanılan boyar maddelere çeşitli canlılar ve özellikle insanlar dolaylı ya da dolaysız olarak maruz kalmaktadır. Giysilerimizin, ev ve ofis mobilyalarımızın çoğu sentetik veya doğal boyalarla renklendirilmektedir. Ancak doğal boyar maddelerin üretilmesinin uzun, maliyetli ve elde edilmesinin zor olması nedeniyle sentetik boyar maddeler tercih edilmektedir. Kullanılan sentetik boyalar, bulundukları ortamdaki tüm canlı türleri üzerinde olumsuz etki yaratabilirler. Farklı endüstriyel alanlara ait sentetik boyar maddelerin üretildiği ve kullanıldığı yerlere ait atıkların, alıcı ortamları arasında içme suyu kanalları, nehirler, göller, denizler gibi sucul ekosistemler ve bu suların geçtiği ve sulama yapılan tarlalar gibi kara ekosistemleri bulunmaktadır. Bu tip kirliliğe maruz kalmış alanlardan alınan atık su örnekleri ile yapılan mutajenite testleri, boyar maddelere ait atıkların farklı canlı gruplarında orta dereceli risk oluşturabildiklerini göstermiştir. Carmen ve Daniela (2012) tarafından yapılan bir çalışmada, Reactive Blue 19 tekstil boyasının sucul ortamlarda 25ºC'de ve pH: 7.0'de yaklaşık 46 yıllık yarılanma ömrüne ve yüksek çevresel kalıcılığa sahip olduğu gösterilmiştir. Gottlieb ve ark. (2003)'a göre *Vibrio fischeri* ile yapılan çalışmada Reactive Black 5 tekstil boyasının toksik etkili olduğu tespit edilmiştir. Novotný ve ark. (2006)'a göre ise Reactive Orange 16 azo boyası *Salmonella typhimirium*'da nokta mutasyona neden olmuştur. Ayrıca sentetik boyar maddeler konjenital malformasyonlara (doğumsal kusurlara) ve gıda sektöründeki kullanımlarına dayalı olarak gıda güvenliği sorunlarına yol açabilen, kanserojenik etki gösterebilen genotoksik ajanlar olarak da değerlendirilmektedir (Öztürk ve Uysal 2021; 2022). Gıda endüstrisinde kullanılan tatrazin (sarı), amaranth (kırmızı), sunset yellow (gün batımı sarısı) ve ponceau 4R (kırmızı) gibi azo boyalarının *D. melanogaster* Oregon-R'nin yabanıl soyunda ömür uzunluğu üzerine etkileri Uysal ve ark. (2017) tarafından araştırılmış ve bu boyaların *D. melonogaster*'in hem dişi hem de erkek popülasyonunda ortalama ve maksimum yaşam süresini azalttığı belirlenmiştir.

Yine besin zinciri yoluyla günlük besinlerle birlikte alımı ve vücutta birikime bağlı olarak üreme ve merkezi sinir sistemi, beyin, böbrek, karaciğer gibi organlarda fonksiyon bozukluklarının şiddetlenmesine de neden olabilmektedirler. Üreme ve merkezi sinir sistemi, beyin, böbrek, karaciğer gibi organlardaki fonksiyon bozukluklarının şiddetlenmesine de neden olabilmektedirler (Guo ve ark. 2019). Benzidin (sentetik boyaların üretiminde kullanılan kimyasal bir türev) Dünya Sağlık Örgütü tarafından kanserojen etkilerinin yanı sıra DNA hasarına da yol açan genotoksik ajanlardan birisi olarak kabul edilmiştir. Das ve ark. (1994), benzidine maruz kalan farelerin lenfosit hücrelerinde kromozomal aberasyonların oranında artış gözlemiştir. Bu maddeye soluma, yutma veya enjeksiyon yoluyla maruz kalma sonucunda kemirgenlerin karaciğer ve böbreğinde ağırlık azalması, şişlik, dalakta büyüme ve idrarda kan gibi komplikasyonlar da gözlenmiştir (Choudhary 1996; Ching Chen ve ark. 2011; Chen ve ark. 2014). Benzer bir başka çalışma da Lentz ve ark. (2010) tarafından yapılmış ve kronik benzidin maruziyeti yaşayan *Gambusia affinis* (sivrisinek balığı)'de apoptoz ile insan karaciğer dokusunda tümör oluşumu görülmüştür. Zebra balığı embriyolarının benzidine maruz bırakılması ile de doz-süre etkileşimine bağlı olarak beynin telencephalon bölgesinde malformasyonlar, beyin ve dorsal nöronlarda yaygın apoptoz, embriyo gelişiminde yavaşlama ve embriyonal anomaliler gözlenmiştir.

Tüm bu sistemik disfonksiyonlara bağlı olarak boyar maddeler, hem güçlü bir çevresel kirleticihem de canlılardaki metabolik süreçler için "ket vurucu toksikantlar" olarak tanımlanabilirler. Özellikle kanserleşmenin potansiyel kaynağı olan aromatik aminler, su ortamına bırakılan ve bu ortamda biyodegredasyona uğrayan boyar maddelerden evrilebilmektedir (Majcen-Le Marechal ve ark. 1997; Şenel 2006). Doğada biyolojik parçalanma özelliği göstermeyen aromatik aminler, biyobirikim göstererek kanseojenik olabilmektedirler (Keşkek Karabulut 2020).

Daha önce yapılan çalışmalarda tekstil boyalarının çeşitli organizmalarda biyotoksik etkili olduğu görülmüştür.. Sunulan bu çalışmada, tekstil endüstrisinde kullanılan, Süperfix Black NNX (SBNNX), Syanacryl Black XFDL (SBXFDL) ve Reaktive Blue 19 (RB19) sentetik boyalarının genotoksik etkili olup/olmadığı genetik denemeler için önemli bir model organizma olan *D. melanogaster*'de kanat benek testi (Somatik Mutasyon ve Rekombinasyon Testi /SMART) ile araştırılmıştır.

2. Materyal ve Metot

2.1. Kullanılan Kimyasal Maddeler

Çalışmada genotoksik etkilerinin belirlenmesi için kullanılan Süperfix Black NNX (SBNNX), Synacryl Black XFDL (SBXFDL) ve Reaktive Blue 19 (RB19) tekstil boyaları ile mutajenik etkili olan ve genotoksisite çalışmalarında pozitif kontrol olarak tercih edilen etil metansülfonat (EMS: CAS No.62-50-0) Sigma-Aldrich Şirketi'nden (St Louis, Missouri, ABD), *Drosophila* Instant Medium (DIM, Formül 4-24) ise Carolina Biyolojik Tedarik Şirketi'nden (2700 York Road, Burlington, ABD) satın alınmıştır. Çalışma kapsamında stok kültürlerin beslenmesi için kullanılan Standart *Drosophila* besiyerinin (SDB) içeriğini oluşturan ve kanat preparatlarının hazırlanması için gerekli olan agar agar, dietil eter, propionik asit, gliserol, kloral hidrat, arap zamkı, entellan, etil alkol gibi kimyasal maddeler de yine Sigma-Aldrich (St. Louis, MO, USA) şirketinden temin edilmiştir.

2.2. Kullanılan Drosophila Soyları

Mendel genetiği alanında sürdürülen genotoksisite çalışmaları, farklı model organizmalar ile yapılmaktadır. Bu organizmaların en önemlilerinden birisi olan *Drosophila melanogaster* (meyve/sirke sineği) Atatürk Üniversitesi, Fen Fakültesi, Biyoloji Bölümü, Genetik Araştırma Laboratuvarı'nda uzun yıllardan beri kendileştirilmiş genetik olarak homozigot, hiçbir mutant karakter taşımayan yabanıl bir laboratuvar stoğudur. Bu çalışmada kullanılan mutant soylar ise *D. melanogaster*'in normal metabolik aktiviteye sahip multiple wing hair (*mwh*) ile *flare (flr^3)* soylarıdır ve diğer yabanıl soylar gibi Genetik Araştırma Laboratuvarı'nda uzun yıllardan beri kendileştirilerek yaşatılmaktadır. *mwh* mutant soyunda bulunan *mwh* resesif geni, III. kromozomun telomere yakın kısmında (3–0.3) bulunmaktadır. *flr^3* geni de yine III. kromozomda sentromere yakın (3- 38.8) yer almaktadır ve bu gen homozigot resesif durumda embriyoda letaliteye sebep olduğu için ergin bireyler oluşamamaktadır. *flr^3* geninin embriyonik letal etkisinden dengeleyici bir kromozom olan TM3 kromozomu ile heterozigotluk sağlanarak korunulmakta ve embriyonun kanat imajinal disklerinden mutant kanat hücrelerinin gelişimi sağlanmaktadır. Ayrıca dengeleyici *TM3* kromozomunda bulunan *BdS* geni, mutant bireyin kanat kenarlarının testere dişi şeklinde fenotip göstermesine neden olmaktadır. Fenotipik olarak yuvarlak-kırmızı gözlü, uzun kanatlı ve kahverengi vücutlu olan mutant soylarda (Şekil 1a ve 1b) resesif belirleyici genler kanat kıllarının (trikom) şeklinde değişikliğe sebep olmaktadır. *mwh* geni, fenotipte normal kanat (Şekil 1a) ve hücre başına bir kanat kılı yerine çoklu kanat kıllarını oluştururken (Şekil 2a) *flr^3* geni sineklerin testere dişi şeklinde kanatlara (Şekil 1b) ve kanatlarındaki normal, düz ve uzun kıllar yerine körelmiş, amorfik kıl (Şekil 2b) oluşmasına sebep olmaktadır (Graf ve ark. 1998).

Şekil 1a. *mwh* genotipli bireylerde normal kanat yapısı, **b.** *flr*^{3} genotipli bireylerde testere dişi kanat yapısı (10x40)

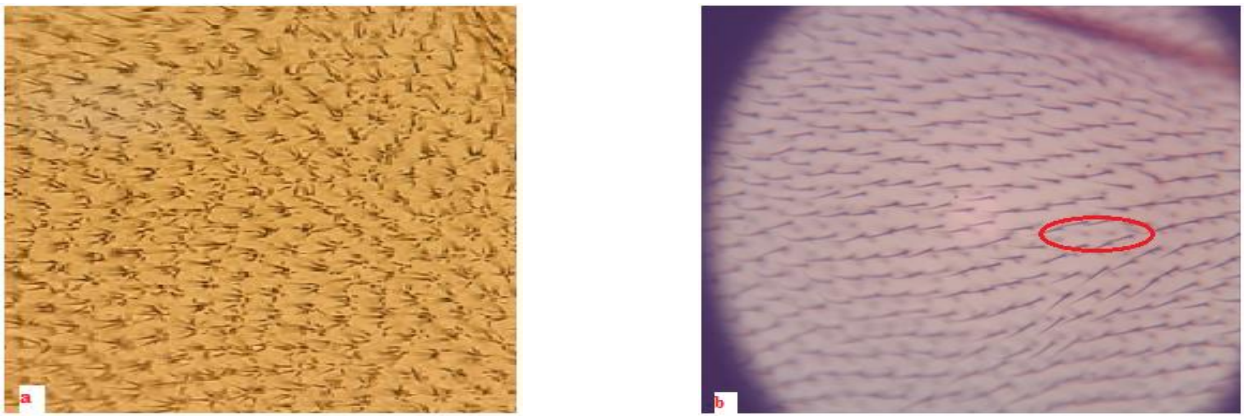

Şekil 2a. *mwh* genotipli bireylerde çoklu kanat kılları (10x40), **b.** *flr*^{3} genotipli bireylerde körelmiş kanat kılları (10x40)

2.3. Kanat Benek Testinin Yapılışı

Bir diğer bilinen adıyla **"**Somatik Mutasyon ve Rekombinasyon Testi" (SMART) için öncelikle *mwh* ve *flr*^{3}mutant türlerine ait erkek ve dişi bireylerin sayılarının artırılması gereklidir. Bu amaçlahazırlanan kültür şişelerine *flr*^{3} ve *mwh* türleri ayrı ayrı konulmuş ve her iki tür için çok sayıda ön çaprazlamalar yapılmıştır. Çaprazlamalar sonucunda metamorfozu tamamlayan 1-3 günlük (yaklaşık 72±4 saatlik) aynı yaşlı *flr*^{3} ve *mwh* ergin bireyleri, 4'er saatlik periyotlar halinde henüz çiftleşmeden yine ayrı ayrı toplanmıştır. Daha sonra çalışma kapsamında kullanılacak olan trans-heterozigot larvaların elde edilmesi için 20 *flr*^{3} dişi ve 20 *mwh* erkek kullanılarak yeni çaprazlamalar yapılmıştır.

SMART için kontrol ve uygulama grubu olmak üzere iki farklı deney seti hazırlanmıştır. İlk deney seti, distile su negatif kontrol grubu ile 1 ppm etil metansülfonat (EMS) içeren pozitif kontrol grubundan oluşmaktadır. Diğer deney seti ise üç farklı tekstil boyasının farklı konsantrasyonlarını içeren (150, 300 ve 450 ppm) uygulama gruplarıdır. Yapılan ön denemelerde 150 ppm'den daha düşük uygulamalarda genotoksik etki gözlenmezken 450 ppm'den yüksek uygulamalarda larvaların yaşama oranı düştüğü için kanat preparatı hazırlayacak kadar ergin birey elde edilememiştir. Bu nedenle 150 ppm'den daha düşük ve 450 ppm'den daha yüksek konsantrasyonlar ile çalışılamamıştır. Kontrol ve uygulama gruplarına ait kültür şişelerine, 100'er adet 3. evre trans-heterozigot larva konulmuş ve larvalar metamorfozu tamamlayıp erginleşinceye kadar ısıtmalı-soğutmalı etüvlerde (25±1˚C) muhafaza edilmiştir. Larvalardan hayat devrini tamamlayıp ergin hale gelen bireyler normal kanatlı ve testere dişli kanatlı ayrımı yapılarak toplanmış ve kanat preparatları hazırlanıncaya kadar %70'lik etil alkol içeren ependorf tüpleri içerisinde +4˚C'de muhafaza edilmiştir.

2.4. Kanat Preparatlarının Hazırlanması

Trans-heterozigot larvalardan elde edilen ergin sineklere ait kanat preparatlarının hazırlanması için erginlerönce likle çukur lamda bulunan faure solüsyonuna alınmışlardır. Nikon marka binoküler mikroskop altında ince uçlu pensler ile ergin bireylereait kanatlar vücuda bağlandığı

yerden ayrılarak kanat preparatları hazırlanmıştır. Her bir bireyin kanatları çiftler halinde yan yana gelecek şekilde lam üzerinde belirli aralıklarla dizilmiş ve lam üzerine ortalama 40 çift kanat yerleştirildikten sonra preparatlar bir gün kurumaya bırakılmıştır. Kuruyan preparatlara 1-2 damla entellan damlatılarak üzerlerine lamel kapatılıp daimi preparatlar hazırlanmıştır. Tüm preparatlar Boeco marka digital kameralı trinoküler ışık mikroskobu ile incelenmiş ve belirlenen mutant hücre klonları tekli ve ikili benekler şeklinde gruplandırılmıştır. Elde edilen sonuçların tümüne ait istatistiksel analiz, Microsta bilgisayar programı ile yapılmıştır ve hesaplanan orijinal ve alternatif hipotezlerin sonuçları, Frei ve Würgler (1988)'in çoklu karar prosedürüne göre değerlendirilmiştir.

3. Bulgular

Çalışma kapsamında hem uygulama hem de pozitif ve negatif kontrol gruplarına ait kanat preparatları, mutant klon oluşup oluşmadığı yönüyle incelenmiştir.Uygulama gruplarında kullanılan boyar maddelerin sebep olduğu somatik mutasyonlar ile gerçekleşen genotoksik etkilerin göstergesi olan mutant klonlar; küçük tek tip (KTT, Şekil 3), büyük tek tip (BTT, Şekil 4) ve ikiz klon (Şekil 5) olmak üzere üçe ayrılmaktadır. Bu mutant klonlar, normal ve serrat kanatlara ait tüm kanat sektörleri (Şekil 6) için ayrı ayrı olmak üzere sayılarak kaydedilmiş ve istatistiki değerlendirmeler yapılmıştır. İstatistiksel değerlendirmeler, öncelikle kontrol grubunu oluşturan distile su negatif kontrol grubu ile EMS pozitif kontrol grubu arasında ve daha sonra tüm uygulama gruplarına ait sonuçlar ile distile su kontrol grubu arasında yapılmıştır.

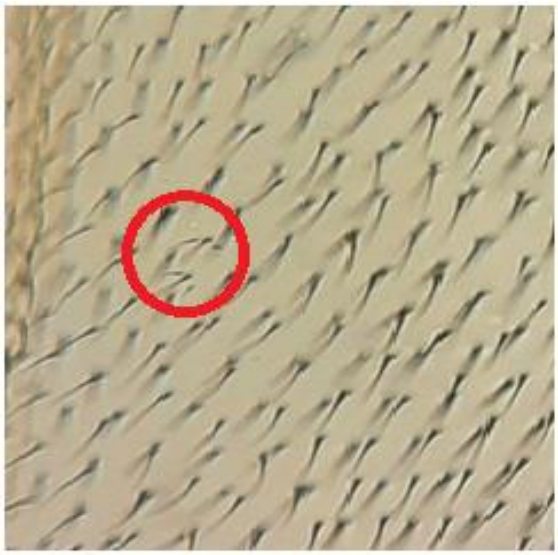

Şekil 3. Küçük tek tip *mwh* mutant klonların mikroskobik görüntüsü (10x40)

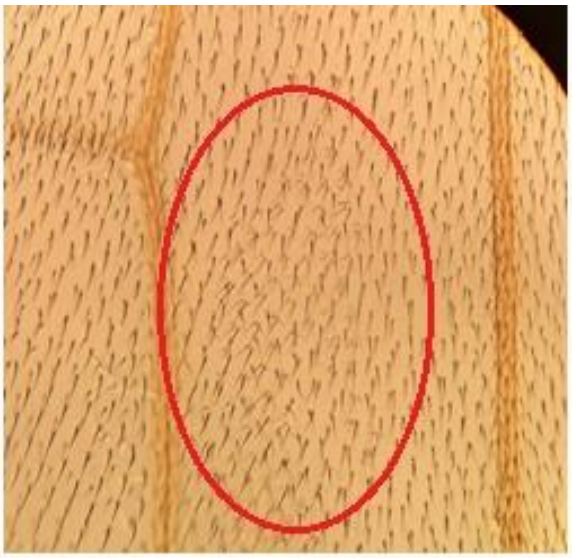

Şekil 4. Büyük tek tip *mwh* mutant klonların mikroskobik görüntüsü (10x40)

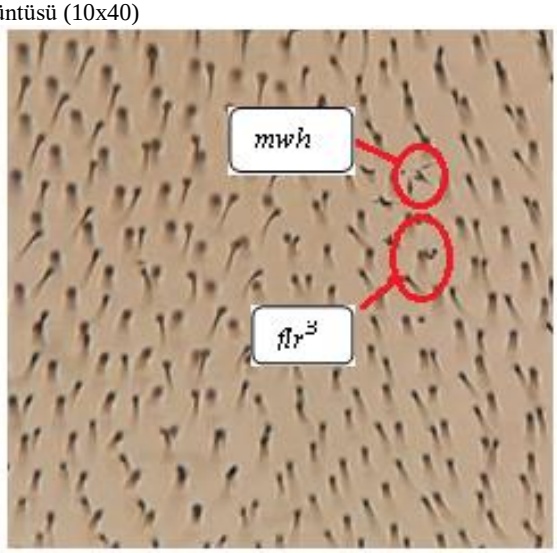

Şekil 5. İkiz mutant klonların mikroskobik görüntüsü (10x40)

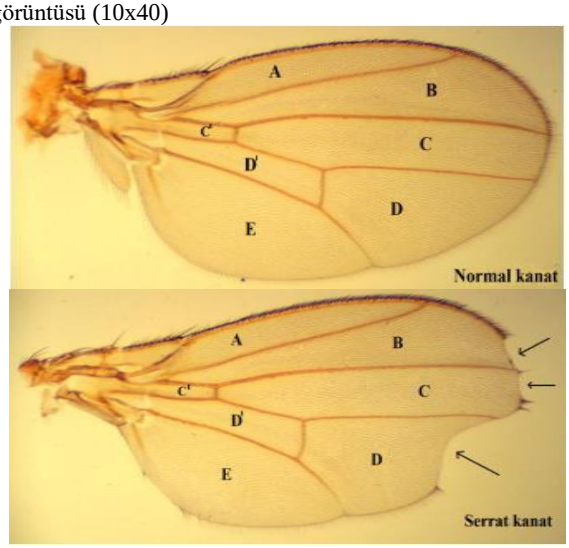

Şekil 6. Normal ve serrat kanatlara ait sektörler (10X40)

Yapılan incelemelerde, distile su negatif kontrol grubunda normal kanat fenotipi (*mwh/flr*^{3}) için yalnızca 8 KTT gözlenirken BTT ve ikiz klon gözlenmemiştir. EMS pozitif kontrol grubunda ise tüm mutant klonlar;27 KTT, 11 BTT ve 8 ikiz klon kaydedilmiştir.Serrat kanat fenotipi (*mwh/TM3*) için de distile su negatif kontrol grubunda yalnızca 6 KTT gözlenirken EMS pozitif kontrol grubunda 20 KTT ve 6 BTT gözlenmiştir. Negatif ve pozitif kontrol gruplarına ait sonuçlar istatistiki olarak birbiri ile karşılaştırıldığında EMS pozitif kontrol grubundamutant klonlarda gözlenen artış her iki kanat fenotipi için p<0,05 düzeyinde önemli olarak değerlendirilmiştir.

Çalışma kapsamında genotoksik etkisi araştırılan SBNNX tekstil boyasına ait normal kanat fenotipi için en düşük doz olan 150 ppm uygulama grubunda 17 KTT, 7 BTT ve 2 ikiz klon olmak üzere toplam 26 toplam mutant klon; 300 ppm'de 20 KTT, 9 BTT ve 3 ikiz klon ve toplam 32 mutant klon gözlenmiştir. En yüksek uygulama grubu olan 450 ppm'de ise doz artışına bağlı olarak daha fazla mutant klon oluşmuştur ve bunlarda 24 KTT, 10 BTT ve 5 ikiz mutant klon olarak değerlendirilmiştir. 450 ppm uygulama grubunda KTT, BTT ve ikiz olmak üzere toplam 39 klon sayılmıştır. Üç uygulama grubuna ait Σ klon frekansları da sırasıyla 0,32, 0,40, 0,45 olarak hesaplanmıştır(Tablo 1). Tablo 1' de de görüldüğü gibi SBNNX'in için 150 ve 300 ppm'de elde edilen veriler distile su kontrol grubu ile istatistiki olarak karşılaştırıldığındaikiz klon tiplerinin oluşumu p>0,05 düzeyinde önemsiz (i) iken KKT, BTT, Σ *mwh* klon veΣ klon tipleri için elde edilen sonuçlar p<0,05 düzeyinde pozitif önemli (+) bulunmuştur. 450 ppm'de ise ikiz klon oluşumu da dahil olmak üzere tüm klon tiplerindeki artış p<0,05 düzeyinde pozitif önemlidir (+). Uygulama grupları için KİF değerleri 1,22, 1,48 ve 1,74 olarak hesaplanırken distile su kontrol grubunda bu değer 0,40'dır (Tablo 1). Artan SBNNX konsantrasyona bağlı olarak KİF değerlerindeki artış tekstil boyasının genotoksik etkili olduğunun göstergesi olarak kabul edilmiştir.

SBNNX tekstil boyasının uygulama gruplarına ait serrat kanat fenotipi için hazırlanan tüm kanat preparatları, mutant klon oluşup oluşmadığı bakımından incelenmiştir. En düşük uygulama olan 150 ppm'de 11 KTT ve 3 BTT olmak üzere toplam 14 mutant klon; 300 ppm'de 14 KTT ve 5 BTT olmak üzere toplam 19 mutant klon ve 450 ppm'de ise 16 KTT ve 6 BTT olmak üzere toplam 22 mutant klon gözlenmiştir.150 ppm uygulama grubu için elde edilen veriler, distile su kontrol grubu ile karşılaştırıldığı zaman sonuçlar KTT, BTT için istatistiki olarak p>0,05 düzeyinde önemsiz (i), Σ *mwh* klon ve Σ klon tipleri için ise p<0,05 düzeyinde pozitif önemli (+) bulunmuştur. 300 ve 450 ppm uygulama gruplarında ise tüm klon tiplerinde sonuçlar p<0,05 düzeyinde pozitif önemlidir (+). Üç uygulama grubuna ait KİF değerleri de sırasıyla 0,71, 0,97 ve 1,12 olarak hesaplanmıştır. Serrat kanat fenotipinde, distile su kontrol grubuna göre her üç uygulama grubu için gözlenen KİF değerindeki artış, somatik mutasyonların artışı olarak değerlendirilmiştir (Tablo 1).

Tablo 1. SBNNX uygulama gruplarına ait kanat benek testi bulguları ve istatistiki analiz sonuçları

Kontrol ve uygulama grupları (ppm)	**Kanat sayısı**	**KTT klon (*m=2*)**			**BTT klon (*m=5*)**			**İkiz klon (*m=5*)**			**Σ *mwh* klon (*m=2*)**			**Σ klon (*m=2*)**			**Klon indüksiyon frekansı (KİF)**
		No	Fr.	D	No	Fr.	D	No	Fr.	D	No	Fr.	D	No	Fr.	D	
Normal kanat(Trans-heterozigot kanat - *mwh/flr*^{3})																	
Kontrol (distile su)	80	8	(0,10)		0	(0,00)		0	(0,00)		8	(0,10)		8	(0,10)		0,40
Kontrol (EMS)	80	27	(0,33)	+	11	(0,13)	+	8	(0,10)	+	38	(0,47)	+	46	(0,57)	+	1,94
150	80	17	(0,21)	+	7	(0,08)	+	2	(0,02)	i	24	(0,30)	+	26	(0,32)	+	1,22
300	80	20	(0,25)	+	9	(0,11)	+	3	(0,03)	i	29	(0,36)	+	32	(0,40)	+	1,48
450	80	24	(0,30)	+	10	(0,12)	+	5	(0,06)	+	34	(0,42)	+	39	(0,45)	+	1,74
Serrat kanat(Dengeleyici heterozigot - *mwh/TM3*)																	
Kontrol (distile su)	80	6	(0,07)		0	(0,00)		Dengeleyici *TM3* kromozomu varlığında *flr*^{3} mutasyonu meydana gelmediğinden ikiz klon gözlenmez.			6	(0,07)		6	(0,07)		0,30
Kontrol (EMS)	80	20	(0,25)	+	6	(0,07)	+				26	(0,32)	+	26	(0,32)	+	1,33
150	80	11	(0,13)	i	3	(0,03)	i				14	(0,17)	+	14	(0,17)	+	0,71
300	80	14	(0,17)	+	5	(0,07)	+				19	(0,23)	+	19	(0,23)	+	0,97
450	80	16	(0,20)	+	6	(0,10)	+				22	(0,27)	+	22	(0,27)	+	1,12

No: Klon Sayısı, Fr: Mutasyon Frekansı, D: İstatistiki Tanı, +: Pozitif (Genotoksik Etkili) , -: Negatif (Genotoksik Etkisiz), i: Önemsiz Etkili, m: Tesir Faktörü, Distile su: Negatif Kontrol, EMS: Pozitif Kontrol

Bazik boya özelliği gösteren SBXFDL, çalışmanın ikinci tekstil boyasıdır ve bu boya için de SBNNX tekstil boyası ile aynı konsantrasyonlarda uygulama gruplarıoluşturulmuştur. SBXFDL'nin verileri normal kanat fenotipi (*mwh/flr*^{3}) için incelendiğindeen düşük uygulama grubu olan 150 ppm uygulama grubunda 15 KTT, 5 BTT ve 2 ikiz klon olmak üzere toplam 22 toplam mutant klon; 300 ppm uygulama grubunda 18 KTT, 8 BTT ve 4 ikiz klon ve toplam 30 mutant klon; en yüksek uygulama grubu olan 450 ppm'de ise 20 KTT, 9 BTT ve 5 ikiz mutant klon olmak üzere 34 toplam klon gözlenmiştir. Üç uygulama grubuna ait KİF değerleri de sırasıyla 1,02, 1,33 ve 1,48 olarak hesaplanmıştır (Tablo 2).

Tablo 2'de de görüldüğü gibiözellikle 150 ppm uygulama grubundatüm klon tipleri için (KTT, BTT ve ikiz klon) gözlenen artış, distile su kontrol grubu ile istatistiki olarak karşılaştırıldığında aradaki fark $p>0,05$ düzeyinde önemsiz (i) iken Σ *mwh* klon ve Σ klon tiplerinde pozitif etkili (+) ve önemli ($p<0,05$) bulunmuştur. 300 ppm'de ise yalnızca ikiz klon oluşumu $p>0,05$düzeyinde önemsiz (i), KKT, BTT, Σ *mwh* klon ve Σ klon tiplerinin oluşumu $p<0,05$ düzeyinde önemli ve pozitif etkilidir (+). 450 ppm uygulama grubunda da istatistiki sonuçlar tüm klon tiplerinde pozitif önemli (+) bulunmuştur ($p<0,05$). Distile su kontrol grubunda KİF değeri 0,40 iken uygulama gruplarına (150, 300 ve 450 ppm) ait KİF değerleri de sırasıyla 1,02, 1,33 ve 1,48 olarak hesaplanmıştır.

SBXFDL uygulama grupları için serrat fenotipine (*mwh/TM3*) ait veriler de Tablo 2'de verilmiştir. Tablo 2'de de görüldüğü gibi 150 ppm'de 10 KTT, 1 BTT ve toplam 11 mutant klon; 300 ppm'de 11 KTT ve 4 BTT olmak üzere toplam 15 mutant klon; 450 ppm'de ise 15 KTT ve 6 BTT olmak üzere toplam 21 mutant klon gözlenmiştir. Distile su kontrol grubu ile 150 ppm uygulama grubuna ait veriler karşılaştırıldığı zaman tüm klon tipleri için istatistiki sonuçlar $p>0,05$ düzeyinde önemsiz (i) bulunmuştur. 300 ppm'de KTT, BTT için sonuçlar $p>0,05$ düzeyinde önemsiz (i) iken Σ *mwh* klon ve Σ klon tiplerinde $p<0,05$ düzeyinde pozitif etkili (+) ve önemli bulunmuştur. 450 ppm'de ise tüm klon tiplerine ait sonuçlar pozitif etkili (+) ve önemlidir ($p<0,05$). Üç uygulama grubuna ait KİF değerleri de sırasıyla 0,56, 0,76 ve 1,07 olarak hesaplanmıştır (Tablo 2).

Tablo 2. SBXFDL uygulama gruplarına ait kanat benek testi bulguları ve istatistiki analiz sonuçları

Kontrol ve uygulama grupları (ppm)	**Kanat sayısı**	**KTT klon (*m=2*)**			**BTT klon (*m=5*)**			**İkiz klon (*m=5*)**			**Σ *mwh* klon (*m=2*)**			**Σ klon (*m=2*)**			**Klon indüksiyon frekansı (KİF)**
		No	Fr.	D	No	Fr.	D	No	Fr.	D	No	Fr.	D	No	Fr.	D	
Normal kanat (Trans-heterozigot kanat - *mwh/flr*^{3})																	
Kontrol (distile su)	80	8	(0,10)		0	(0,00)		0	(0,00)		8	(0,10)		8	(0,10)		0,40
Kontrol (EMS)	80	27	(0,33)	+	11	(0,13)	+	8	(0,10)	+	38	(0,47)	+	46	(0,57)	+	1,94
150	80	15	(0,18)	i	5	(0,06)	i	2	(0,02)	i	20	(0,25)	+	22	(0,27)	+	1,02
300	80	18	(0,22)	+	8	(0,10)	+	4	(0,05)	i	26	(0,32)	+	30	(0,37)	+	1,33
450	80	20	(0,25)	+	9	(0,11)	+	5	(0,06)	+	29	(0,36)	+	34	(0,42)	+	1,48
Serrat kanat (Dengeleyici heterozigot - *mwh/TM3*)																	
Kontrol (distile su)	80	6	(0,07)		0	(0,00)		Dengeleyici *TM3* kromozomu			6	(0,07)		6	(0,07)		0,30
Kontrol (EMS)	80	20	(0,25)	+	6	(0,07)	+	varlığında *flr*^{3} mutasyonu			26	(0,32)	+	26	(0,32)	+	1,33
150	80	10	(0,12)	i	1	(0,01)	i	meydana			11	(0,13)	i	11	(0,13)	i	0,56
300	80	11	(0,13)	i	4	(0,05)	i	gelmediğinden			15	(0,18)	+	15	(0,18)	+	0,76
450	80	15	(0,18)	+	6	(0,08)	+	ikiz klon gözlenmez.			21	(0,26)	+	21	(0,26)	+	1,07

No: Klon Sayısı, Fr: Mutasyon Frekansı, D: İstatistiki Tanı, +: Pozitif (Genotoksik Etkili), -: Negatif (Genotoksik Etkisiz), i:Önemsiz Etkili, m: Tesir Faktörü, Distile su: Negatif Kontrol, EMS: Pozitif Kontrol

Çalışmada kullanılan diğer tekstil boyası RB19 için de aynı dozlarda uygulama yapılmıştır (150, 300 ve 450 ppm). Normal kanat fenotipi için 150 ppm uygulama grubunda 12 KTT, 6 BTT ve 3 ikiz olmak üzere toplam 21 toplam mutant klon; 300 ppm'de 14 KTT, 7 BTT ve 4 ikiz ve toplam 25 mutant klon; en yüksek uygulama grubu olan 450 ppm'de ise 19 KTT, 8 BTT ve 6 ikiz ve toplam 33 klon gözlenmiştir. Üç uygulama grubuna ait KİF değerleri sırasıyla 0,92, 1,07 ve 1,38 olarak hesaplanmıştır (Tablo 3). Tablo 3'de görüldüğü gibi RB19'un için özellikle 150 ppm'de elde edilen veriler, distile su kontrol grubu ile karşılaştırıldığında sonuçlar $p>0,05$ düzeyinde KTT ve ikiz klon tipleri için önemsiz (i) iken, BTT, Σ mwh klon ve Σ klon tiplerinde sonuçlar $p<0,05$ düzeyinde pozitif önemli (+) olarak bulunmuştur. 300 ppm'de KTT ve ikiz klon tipleri ,$p>0,05$ düzeyinde önemsiz (i) iken BTT, Σ *mwh* klon veΣ klon tiplerinde sonuçlar $p<0,05$ düzeyinde pozitif önemlidir (+). 450 ppm'de ise tüm klon tiplerindeki artış, yine $p<0,05$ düzeyinde pozitif önemlidir (+). Distile su kontrol grubunda KİF değeri 0,40 iken RB19 uygulama

gruplarına (150, 300 ve 450 ppm) ait KİF değerleri de sırasıyla 0,92, 1,07 ve 1,48 olarak hesaplanmıştır. Artan RB19 konsantrasyona bağlı olarak KİF değerlerindeki artış mutant klon uyarımını göstermektedir.

Uygulama gruplarının serrat kanat fenotipinin verileri incelendiğinde ise 150 ppm uygulama grubunda 6 KTT ve 2 BTT toplam 8 mutant klon; 300 ppm'de 10 KTT ve 3 BTT olmak üzere toplam 13 mutant klon; 450 ppm' de ise 14 KTT ve 5 BTT olmak üzere toplam 19 mutant klon gözlenmiştir. 150 ppm uygulama grubunda elde edilen veriler, distile kontrol grubu ile karşılaştırıldığı zaman tüm klon tiplerinde sonuçlar $p>0,05$ düzeyinde önemsiz (i) bulunmuştur. 300 ppm'de KTT, BTT için istatistiki olarak önemsiz (i) olan sonuçlar, Σ *mwh* klon ve Σ klon tiplerinde pozitif önemlidir (+). 450 ppm'de ise tüm klon tiplerinde sonuçlar $p<0,05$ düzeyinde pozitif önemlidir (+). Üç uygulama grubuna ait KİF değerleri de sırasıyla 0,40, 0,66 ve 0,97 olarak hesaplanmıştır (Tablo3).

Tablo 3. RB19 uygulama gruplarına ait kanat benek testi bulguları ve istatistiki analiz sonuçları

Kontrol ve Uygulama grupları (ppm)	**Kanat sayısı**	**KTT klon (*m=2*)**			**BTT klon (*m=5*)**			**İkiz klon (*m=5*)**			**Σ *mwh* klon (*m=2*)**			**Σ klon (*m=2*)**			**Klon indüksiyon frekansı (KİF)**
		No	Fr.	D	No	Fr.	D	No	Fr.	D	No	Fr.	D	No	Fr.	D	
Normal kanat (Trans-heterozigot kanat - *mwh/flr³*)																	
Kontrol (distile su)	80	8	(0,10)		0	(0,00)		0	(0,00)		8	(0,10)		8	(0,10)		0,40
Kontrol (EMS)	80	27	(0,33)	+	11	(0,13)	+	8	(0,10)	+	38	(0,47)	+	46	(0,57)	+	1,94
150	80	12	(0,15)	i	6	(0,07)	+	3	(0,03)	i	18	(0,22)	+	21	(0,26)	+	0,92
300	80	14	(0,17)	i	7	(0,08)	+	4	(0,05)	i	21	(0,26)	+	25	(0,31)	+	1,07
450	80	19	(0,23)	+	8	(0,10)	+	6	(0,07)	+	27	(0,33)	+	33	(0,41)	+	1,38
Serrat kanat (Dengeleyici heterozigot - *mwh/TM3*)																	
Kontrol (distile su)	80	6	(0,07)		0	(0,00)		Dengeleyici *TM3* kromozomu varlığında *flr³* mutasyonu meydana gelmediğinden ikiz klon gözlenmez.			6	(0,07)		6	(0,07)		0,30
Kontrol (EMS)	80	20	(0,25)	+	6	(0,07)	+				26	(0,32)	+	26	(0,32)	+	1,33
150	80	6	(0,07)	i	2	(0,02)	i				8	(0,10)	i	8	(0,10)	i	0,40
300	80	10	(0,12)	i	3	(0,03)	i				13	(0,16)	+	13	(0,16)	+	0,66
450	80	14	(0,17)	+	5	(0,06)	+				19	(0,23)	+	19	(0,23)	+	0,97

No: Klon Sayısı, Fr: Mutasyon Frekansı, D: İstatistiki Tanı, +: Pozitif (Genotoksik Etkili) , -: Negatif (Genotoksik Etkisiz), i: Önemsiz Etkili, m: Tesir Faktörü, Distile su: Negatif Kontrol, EMS: Pozitif Kontrol

4. Tartışma

Boyar maddeler, Dünya genelinde çeşitli endüstriyel alanlardayaygın olarak kullanılmaktadır. Zollinger (1987) tarafından 10.000 çeşit pigment ve boyar maddenin dünya çapında kullanıldığı rapor edilmiştir. Bu maddeler, kullanım sonrası doğrudan ya da dolaylı olarak sektörel alanların dışına doğaya az veya çok olarak salınmakta ve ekosistem üzerinde olumsuz etkilere sebep olmaktadırlar.Dünyada artan nüfusa paralel olarak yaşama dair ihtiyaçların artışı ile birlikte endüstrinin gelişmesi,çok daha fazla miktarda kullanılan/kullanılacak boyar maddelere çeşitli canlıların ve özellikle insanların dolaylı ya da dolaysız olarak maruz kalmasına sebep olmaktadır. Khan ve Jain (1995) yaptıkları araştırmalarda, tekstil atık suları ile sulanan arazide yetiştirilen buğdayda (*Triticum aestivum*) büyümenin inhibe edildiğini gözlemişlerdir. Sharma ve Sobti (2000) tarafından Hindistan'da yaygın olarak kullanılan dört farklı boyanın (Sulphur Red Brown 360, Jade Gren 2G, Reactofix Turquoise Blue 5GFL ve Direct Scarlet 31 4BS) prokaryotik organizmalarda (*Bacillus subtilis*) doz artışına bağlı olarak büyümeyi inhibe ettiği gözlenmiştir. İçeriğinde boyar madde bulunan atık suların genotoksik etkilerinin *Allium* testi (çevresel kirliliğin hızlı bir şekilde belirlenmesi için kullanılan standart bir yöntem) ile araştırıldığı bir başka çalışmada, özellikle kağıt sanayi atık sularının oldukça toksik etkiliolduğu görülmüştür (Nielsen ve Rank 1994).

Marwari ve Khan (2012)'ın yaptığı çalışmaya göre, tekstil atık suyu ile muamele edilen domates bitkisinde toplam klorofil, karbonhidrat, protein ve nitrojen içeriği önemli ölçüde azalmıştır. Tekstil boyası olarak kullanılan DB15'in de *Pseudokirchneriella subcapitata* (bir çeşit mikro alg)'da karotenoid miktarını azalttığı gözlenmiştir (Hernández-Zamora ve Martínez-Jerónimo 2019). Daha önce yapılan bir başka çalışmada da, Direct Black 38 (DB38) ve Reactive Blue 15 (RB15) tekstil boyalarının, hayvansal ve bitkisel organizmalarda akut toksik ve genotoksik etkileri araştırılmıştır. *Cucumissativus* (salatalık), *Lactuca sativa* (marul) ve *Lycopersicon esculentum* (domates)'da, çimlenme ve kök uzamasında bu boyaların sebep olduğu herhangi bir toksik etki gözlenmemiştir (de Olivera ve ark. 2018). Ancak 42 çeşit ticari tekstil boyasının sucul toksisitesi, *Daphnia magna* (su piresi) ve *Raphidocelis subcapitata* (bir çeşit yeşil alg) kullanılarak Croce ve ark. (2017) tarafından araştırılmış

ve tüm boyaların her iki grupta özellikle alglerde toksik etkili olduğu bildirilmiştir.

Tekstil boyası olarak kullanılan San G-GELB-GLE, Red FBL, Blue FGRL ve Black FDL boyalarının genotoksik etkileri,önemli genetik model organizmalardan birisi olan *D.melanogaster*'de Eroğlu Doğan (2002) tarafından da araştırılmış ve bu boyaların mutajenik olduğu bildirilmiştir. Özata (2006) tarafından yapılan başka bir çalışmada da, yine bazı tekstil boyalarının *D.melanogaster* üzerinde hem toksik hem de genotoksik etkileri araştırılmış ve tekstil boyalarının bütün konsantrasyonlarının hayatta kalış oranını azalttığı ve somatik mutasyonları uyardığı tespit edilmiştir. Öztürk ve Uysal (2021, 2022), *D.melanogaster*'in erkek ve dişi popülasyonlarında ergin bireylerin ömür uzunluğunu kronik uygulanan Superfix Navy Blue BF ve Synacryl Black XFDL sentetik boyalarının kısalttığını gözlemişlerdir. Boyar maddelerin doz artışına bağlı olarak larval toksisitenin ve malformasyonların arttığı da yine aynı yazarlar tarafından bildirilmiştir. Benzeri sonuçlar, Şahin ve Türkoğlu (2014) tarafından da gözlenmiştir. Yine Direct Yellow 86, Direct Orange 39, Direct Blue 200, Direct Yellow 142 ve Direct Red 243 gibi sentetik boyar maddelerin farklı dozları da farelerde mutajenik etkili bulunmuştur (Şenel ve ark. 2012).

Sunulan bu çalışmada, *Drosophila* kanat benek testi için değerlendirilen benek tiplerinden tek tip klonlar (KTT ve BTT) transisyonal, transversiyonal, insersiyonal veya delesyon tipi gibi nokta mutasyonlar, ayrılmama, delesyon ve mitotik rekombinasyon sonucu meydana gelirken ikiz klon tipi üçüncü kromozomun sentromeri ve *flr*^{3}geni arasındaki mitotik rekombinasyon ile oluşmaktadır. Rai ve ark. (2005)'a göre, Dispers Blue 291 boyası da DNA'da insersiyon veya delesyona sebep olarak genetik kodda hata oluşturmaktadır.

Uygulama gruplarında kullanmış olduğumuz üç farklı tekstil boyasının (SBNNX, SBXFDL, RB19) somatik hücrelerde meydana getirdiği oksidatif strese dayalı hasarların, DNA yapısında değişikliklere neden olabileceğini ve bunun da mutant klonların oluşumunu indüklediğini düşünmekteyiz. Somatik hücrelerde beklenilmeyen/görülmeyen özellikle mitotik rekombinasyon, hem tek tip klonların hem de ikiz klonların oluşumuna yol açmaktadır. Mutant klonların oluşumu da tekstil boyalarının hem mutajenik hem de rekombinojenik olduğunun göstergesi olarak kabul edilebilir. Ayrıca Graf ve ark. (1998)'a göre, somatik mutasyonlar hücre bölünmelerinin yoğun olduğu erken embriyonal evrelerde gerçekleşirse mutant hücrelerin sayısı da artmaktadır. Uygulamalardan elde ettiğimiz veriler, Graf ve ark. (1998)'ın bu görüşüyle uyumludur ve tekstil boyalarının artan dozları ile benek sayısı arasında pozitif bir korelasyon olduğu Tablo 1-3'de görülmektedir. Kullanılan boyaların genotoksisitesi içinde belirlenen dominansi sırası SBNNX > SBXFDL >RB19 şeklindedir.

5. Sonuç

Bu çalışmada, tekstil endüstrisinde kullanılan SBNNX, SBXFDL ve RB19 sentetik boyar maddelerinin genotoksik etkileri *Drosophila* kanat benek testi ile araştırılmış ve doz artışına bağlı olarak her üç boyanın da mutajenik ve rekombinojenik etkili olduğu belirlenmiştir.

Gelecekten bize ödünç olan Dünya mirasını florası, faunası, havası ile sucul ve karasal ekosistemleriyle koruyup bu mirasa sahip çıkabilmek, Dünya'nın gittikçe artan sessiz çığlıklarını duyabilmek, bizlerin gidebileceği başka bir Dünya'nın olmadığını bilmek insanoğlunun en önemli görevleri arasındadır. Ancak, "çevre için renkli bir tehlike" olarak tanımlayabileceğimiz, bir o kadar da hayatımızın vazgeçilmezleri arasında yer alan tekstil endüstrisine ait tehlikeye de dikkat çekebilmek gerekmektedir. Küresel bir düzen içinde sucul ve karasal ekosistem ile elbette ki teneffüs ettiğimiz havanın ait olduğu atmosfer artık kendine ait olmayan kirleticileri bize geri göndermektedir. Yapılacak tek ve en önemli işlev, gelecek nesillere daha az yıpranmış bir yeryüzü bırakabilmektir.

Teşekkür

Bu çalışmayı FYL-2023-12019 numaralı proje ile destekleyen Atatürk Üniversitesi Bilimsel Araştırma Projeleri birimine teşekkür ederiz.

Kaynaklar

Başer İ, İnanıcı, Y. 1990. Boyarmadde Kimyası, Marmara Üniv. Teknik Eğitim Fak. 482(2): İstanbul.

Carmen Z, Daniela S. 2012. Textile organic dyes-characteristics, polluting effects and separation/elimination procedures from industrial effluents-a critical overview (pp. 55- 86). IntechOpen.

Chen MHC, Hsu LC, Wu JL, Yeh CW, Tsai JN, Hseu YC, Hsu LS. 2014. Exposure to benzidine caused apoptosis and malformation of telencephalon region in zebra fish. Environ Toxicol. 29(12): 1428-1436.

Ching Chen S, Hseu YC, Sung JC, Chen CH, Chen LC, Chung KT. 2011. Induction of DNA damage signaling genes in benzidine treated HepG2 cells. Environ Mol Mutagen. 52(8): 664-672.

Choudhary G. 1996. Human health perspectives on environmental exposure to benzidine: a review. Chemosphere. 32(2): 267-291.

Croce R, Cinà F, Lombardo A, Crispeyn G, Cappelli CI, VianM, Maiorana S, Benfenati E, Baderna D. 2017. Aquatic toxicity of several textile dye formulations: acute and chronic assays with *Daphnia magna* and *Raphidocelis subcapitata*. Ecotoxicol Environ Safe. 144: 79-87.

Das L, Das SK, Hooberman BH, Chu EH, Sinsheimer JE. 1994. Chromosomal aberrations in mouse lymphocytes exposed *in vitro* and *in vivo* to benzidine and 5 related aromatic amines. Mutat Res/Genet Toxicol. 320(1-2): 69-74.

de Oliveira GAR, Leme DM, de Lapuente J, Brito LB, Porredón C, de Brito Rodrigues L, Brull N, Serret, JT, Borras M, Disner GR, Cestari MM, de Oliveira DP. 2018. A test battery for assessing the ecotoxic effects of textile dyes. Chem-Biol Interact. 291: 171-179.

Eroğlu Doğan E. 2002. Bazı Astrazon Grubu Tekstil Boyalarının Genotoksik Etkisinin *Drosophila melanogaster* Somatik Mutasyon ve Rekombinasyon Testi (SMART) ile

Araştırılması. Yüksek Lisans Tezi, İnönü Üniv. Fen Bilimleri Ens. Malatya.

Frei H, Würgler FE. 1988. Statistical methods to decide whether mutagenicity test data from *Drosophila* assays indicate a positive, negative or inconclusive result. Mutat Res. 203: 297- 308.

Graf U, Abraham SK, Guzmán-Rincón J. Würgler FE. 1998. Antigenotoxicity studies in *Drosophila melanogaster*. Mutat Res/ Fund Mol Mech Mutagen. 402(1-2): 203-209.

Gottlieb A, Shaw C, Smith A, Wheatley A, Forsythe S. 2003. The toxicity of textile reactive azo dyes after hydrolysis and decolourisation. J Biotechnol. 101(1): 49-56.

Guo R, Wang R, Yin J, Jiao T, Huang H, Zhao X, Zhang L, Li Q, Zhou J, Peng Q. 2019. Fabrication and highly efficient dye removal characterization of betacyclodextrin-based composite polymer fibers by electrospinning. Nanomaterials. 9(1): 127.

Gürcüm BH, Öneş A. 2018. Bakteri ve mikroalglerin tekstil boyacılığında ve baskıcılığında kullanım olanakları. İdil Sanat ve Dil Derg. (46): 701-709.

Hernández-Zamora M, Martínez-Jerónimo F. 2019. Congo red dye diversely affects organisms of different trophic levels: a comparative study with microalgae, cladocerans, and zebrafish embryos. Environ Sci Pollut Res. 26(12): 11743-11755.

Hunger K. 2003. ''Industrial Dyes'', Wiley-VCH, Verlag, 1-6

Kant R. 2012. Tekstil Boyama Endüstrisi Çevresel Bir Tehlike. Doğa Bilimleri. 4: 22-26.

Keşkek Karabulut Y. 2020. Bazı aromatik aminlerin toksikolojik ve ekolojik özelliklerinin QSAR yöntemi ile incelenmesi. Doktora Tezi, Namık Kemal Üniv. Fen Bilimleri Ens. Kimya Ana Bilim Dalı, Tekirdağ.

Khan IT, Jain V. 1995. Effect of textile industry wastewater on growth and some biochemical parameters of *Triticum aestivum*. J Environ Pollut. 2: 97-102.

Lentz S, Eversole R, McHugh Law J, Means JC. 2010. Cellular proliferation, cell death, and liver histology in *Gambusia affinis* after dietary exposure to benzidine and 2-Aminofluorene. Int'l J Toxicol (IJT). 29(3): 247-258.

Majcen-Le Marechal A, Slokar YM, Taufer T. 1997. Decoloration of Chlorotriazine Reactive Azo Dyes with H2O2/UV. Dyes Pigm. 33: 281-298.

Marwari R, Khan TI. 2012. Effect of textile wastewater on tomato plant, *Lycopersicon esculentum*. J Environ Biol. 33(5): 849.

Mercimek HA. 2007. *Trametes versicolor*' ın tekstil boyalarının gideriminde kullanım olanakları, Yüksek Lisans Tezi, Çukurova Üniv. Biyoteknoloji Anabilim Dalı, Adana.

Nielsen MH, Rank J. 1994. Screening of toxicity and genotoxicity in wastewater by the use of the *Allium* test. Hereditas. 121: 249- 254

Novotný Č, Dias N, Kapanen A, Malachová K, Vándrovcová M, Itävaara M, Lima N. 2006. Comparative use of bacterial, algal and protozoan tests to study toxicity of azo-and anthraquinone dyes. Chemosphere. 63(9): 1436-1442.

Ölmez T. 1999. Tekstil Endüstrisinde Reaktif Boya Banyolarında Ozon ile Renk Giderimi. Yüksek Lisans Tezi, İstanbul Teknik Üniv. Fen Bilimleri Ens. İstanbul.

Önal A. 2000. Doğal boyarmaddeler (Ekstraksiyon-Boyama) ders notları. Gaziosmanpaşa Üniv. Fen-Edebiyat Fak Yay. 7: 1-4.

Özata L. 2006. Bazı Tekstil Boyalarının *Drosophila melanogaster* Üzerine Toksik ve Genotoksik Etkilerinin Araştırılması, Doktora Tezi, İnönü Üniv. Fen Bilimleri Ens. Malatya.

Öztürk E, Uysal H. 2021. Investigation of in vivo Biotoxic Effects of Synacryl Black XFDL Textile Dye on Larval Viability and Longevity in Male and Male Populations in *Drosophila melanogaster* Oregon-R. 3rd International Symposium on Biodiversity Research ISBR 2021 , Erzurum, Turkey pp.1-2.

Öztürk E, Uysal H. 2022. The effects of superfix navy blue bf (snbbf) synthetic textile dye on larval viability and longevity in *Drosophila melanogaster* Oregon-R wild strain. 6th International Conference on Advances in Natural and Applied Sciences 11-13 October 2022, Ağrı/Türkiye International, Interdisciplinary, Online , Ağrı, Turkey, pp.67.

Rai HS, Bhattacharyya MS, Singh J, Bansal TK., Vats P, Banerjee UC. 2005. Removal of dyes from the effluent of textile and dyestuff manufacturing industry: A review of emerging techniques with reference to biological treatment. Crit Rev EnvironSci Technol. 35(3): 219-238.

Şahin N, Türkoğlu Ş. 2014 Bazı Tekstil Boyalarının *Drosophila melanogaster*'de Ömür Uzunluğu, Yaşama Yüzdesi ve Yavru Birey Sayısına Etkileri. Cumhuriyet Üniv. Fen Edebiyat Fak. Fen Bilimleri Derg. 35:73-93.

Sarıoğlu H, Kayadibi P. 2012. Tekstil işletmelerinin profili ve üretime ilişkin uygulamaları üzerine bir araştırma. Tekstil Teknolojileri Elektronik Derg. 6 (1): 1- 12.

Sharma MK, Sobti RC. 2000. Rec effect of certain textile dyes in *Bacillus subtilis*. Mutat Res/Genet Toxicol EnvironMutagen. 465(1-2): 27-38.

Şenel M. 2006. Suggestions for Beautifying the Pronunciation of EFL Learners in Turkey. J Lang Linguist Stud. 2: 111 125.

Şenel U, Sur HI. Demirtas M. 2012. Tekstil endüstrisinde kullanılan bazı sentetik reaktif boyarmaddelerin mutajenik etkisinin umu-test ile araştırılması. Ekoloji. 21(85): 49-56.

Tünay O, Kabdasli I, Eremektar G, Orhon D. 1996. Color removal from textile wastewaters. Water Sci Technol. 34(11): 9-16.

Uysal H, Şişman T, Aşkın H. 2006. *Drosophila* Biology and Crossover Methods (Extended 2nd Edition). Atatürk University Publications, ISBN: 975-442-111-0, Erzurum, Türkiye.

Uysal H, Genç S, Ayar A. 2017. Toxic Effects of Chronic Feeding with Food Azo Dyes on *Drosophila melanogaster* Oregon *R*. Sci Iran. 24(6): 3081-3086. doi: 10.24200/sci.2017.4523

Zollinger H. 1987. Color Chemistry: Syntheses, Properties and Applications of Organic Dyes and Pigments. 1st Edition, Weinheim, New York.

RESEARCH ARTICLE
Eurasian J Bio Chem Sci, 6(2):104-108, 2023
https://doi.org/10.46239/ejbcs.1228402

EJBCS

Eurasian Journal of Biological and Chemical Sciences

Journal homepage: www.dergipark.org.tr/ejbcs

Investigation of *in vitro* antidiabetic and antioxidant activity of hawthorn vinegar obtained from Endemic *Crataegus tanacetifolia* (Poir.) Pers.

Feyza Akgün[1], Nigar Sıla Tuğlu[1], Yasemin Gülbahar Açıl[1], Nuraniye Eruygur[2*]
[1]*Selçuk University, Faculty of Pharmacy, Konya, Türkiye.*
[*2]*Selçuk University, Faculty of Pharmacy, Department of Pharmacognosy, Konya, Türkiye*

*Corresponding author : nuraniye.eruygur@selcuk.edu.tr
Orcid No: https://orcid.org/0000-0002-4674-7009

Received : 03/10/2023
Accepted : 16/11/2023

Abstract: In this study, the *in vitro* antidiabetic, antioxidant activity and total flavonoid content (TFC) and total phenolic content (TPC) of vinegar obtained from endemic *Crataegus tanacetifolia* (Lam.) Pers. (Rosaceae), (hawthorn) were examined. The hawthorn vinegar obtained from Malatya province (MS) and the vinegar (TS) obtained from Konya were used as study material. Their antidiabetic activity was determined by α-amylase and α-glucosidase inhibitory methods. Antioxidant activities were determined using 2,2-diphenyl-1-picrylhydrazyl (DPPH), 2,2′-azino-bis (3-ethylbenzothiazoline-6-sulfonic acid) (ABTS) and ferrous iron chelating (FCA) assays. The absorbance were read in the Elisa reader and evaluated with Excel and GraphPad programs. The MS has been found to have higher α- amylase (95.12± 3.71%) and α-glucosidase inhibitory (81.62 ± 0.33%) effects. The TS demonstrated (94.13 ± 3.85%) α-amylase and (75.35 ± 2.19%) α-glucosidase inhibitory activity, respectively. The TPC was found to be in TS (467.59 ± 6.73) mg GAE/mL MS (328.46 ± 5.50) mg GAE/mL. The TFC was found as (1.94 ± 10.36) mg CE/mL and (1.32 ± 10.96) mg CE/mL in TS and MS vinegar, respectively. The FCA was found to be in TS (33.37 ± 0.53%) MS (31.08 ± 10.87%). The DPPH radical scavenging activity was found as (73.82 ± 2.12%) in TS and (80.12 ± 4.45%) in MS. ABTS radical scavenging activity was found to be the highest in TS with (82.51± 0.78%) and in MS found as (78.65 ± 0.55%). The antidiabetic, antioxidant activity, TPC and TFC determinations of these vinegars were performed for the first time with these methods.

Keywords: Bioactivity, *Crataegus tanacetifolia*, phytochemical, vinegar

1. Introduction

Diabetes is the most common metabolic disease worldwide. Diabetes is a disease in which the glucose level in the blood cannot be controlled due to the insulin hormone. The number of people suffering from diabetes is increasing due to nutritional disorders, hormonal and immune problems in Turkey and in the world (Asgari et al. 2022). Traditional treatment methods and herbal treatment options have become increasingly important in the treatment of many metabolic diseases such as diabetes.

During the onset and development of type 2 diabetes, the cellular balance of carbohydrate and lipid metabolism is affected by inappropriate glucose metabolism, resulting in elevated postprandial blood glucose levels. Prolonged hyperglycemia with diabetes leads to the formation of Advanced Glycation End Products (AGEs), which are involved in the generation of reactive oxygen species (ROS) and cause oxidative damage (Haidara et al. 2009). In the natural aging process, the accumulation of AGEs in the organism and their interaction with their receptors are accepted as one of the most important factors that damage cells and tissues, as in diabetes (Yılmaz and Karabudak 2018). Numerous studies have shown that cancer, aging or neurodegenerative diseases are mostly associated with excessive production of free radicals (Forman and Zhang 2021). Increased free radical production and oxidative stress caused by hyperglycemia are the main causes of cognitive dysfunction in diabetic patients (Kucukatay et al. 2007). It has been reported that diabetes accelerates the mild cognitive deterioration of dementia in the elderly (Xu et al. 2010). Moreover, diabetes independently increases the risk of atherosclerosis as an inflammatory response (Folli et al. 2011; Forbes and Cooper 2013). In this case, high homocysteine concentration has an important role in causing vascular complications of diabetes (Hoogeveen et al. 1998). One therapeutic approach for the treatment of diabetes is to reduce postprandial hyperglycemia by delaying glucose absorption through inhibition of enzymes that hydrolyze carbohydrates such as α-glucosidase and α-amylase in the digestive tract (Cheplick et al. 2010). Antioxidant is any substance that can act directly or indirectly on free radicals to delay, prevent or eliminate oxidative damage in target molecules (Halliwell 2020)

Bioactive components with antioxidant effects reported in recent years are mainly phenolics, polysaccharides and alkaloids (Kołodziej et al. 2019)

Vinegar has been used in the world for thousands of years and has many activities such as antioxidant, anti-hyperglycemic activity thanks to its bioactive components. Bioactive compounds are found in small amounts in foodstuffs and their effects on human health are constantly being researched (Butnariu 2014; Rashed and Butnarių 2014). Since vinegar is produced from many fruits and vegetables rich in amino acids, organic acids, phenolics, vitamins and minerals, and shows antioxidant, anti-obesity, antidiabetic and antimicrobial activities (Budak et al. 2011). Bakir et al. (2017). It also has regulatory effects on blood pressure and lipid metabolism. It is one of the most famous folk remedies used to fight infections (Samad et al. 2016). The consumption of vinegar as a home remedy for managing high blood sugar levels was noted before on the advent of today's antidiabetic drugs (OKeefe et al. 2008)

Crataegus L.(hawthorn) genus, belonging to the Rosaceae family, is widely found in Asia, Europe and America and consists of more than 1000 species (Alirezalu et al. 2020). 21 *Crataegus* species grow naturally in our country (Dönmez 2004). Hawthorn contains numerous bioactive compounds with multiple pharmacological activities and functions. These components have been used to treat inflammatory diseases and enhance human immunity (Li et al. 2022). Hawthorn's use dates back to ancient times, has gained an important place in phytotherapy and has become a popular herbal medicine due to its beneficial effects on the cardiovascular system, antioxidant and antimicrobial activity (Alirezalu et al. 2020). It has become a natural treatment option as an alternative to synthetic drugs with many side effects, and many studies have been conducted on some species such as *C. oxyacantha C. monogyna, C. pinnatifida* (Mecheri et al. 2021; Deveci et al. 2020; Chowdhury et al. 2014). Hawthorn contains aromatic amines, essential oils, phenolic acids, flavonoids (hyperine, quercetin, spirein, rutin, and apigenin), picantosivanidins as bioactive compounds (Bruneton 1999). Hawthorn polyphenols mainly contain quercetin (74.58%) and hyperoside (9.58%), which are important sources of biological activity to inhibit α-glucosidase (Li et al. 2022) Hawthorn berries contain a number of biologically active substances expected to have anti-proliferative effects on human cancer cells (Berghe 2012; Li et al. 2013). From the anti-cancer function of triterpenoids in hawthorn. (Qiao et al. 2015). Considering the rich content of flavonoids and polyphenols with strong antioxidant activity in hawthorn, it is expected to be applied in the development of functional foods by improving memory-related dysfunctions (Miguez et al. 2016, Sammari et al. 2021).

In the study, two different commercial products of vinegar were used as study material.. The DPPH and ABTS free radical scavenging test and Fe^{+2} chelating assay were performed to evaluate *in vitro* antioxidant potential of vinegar samples. Total flavonoid quantification (TFC) and total phenol quantification (TPC) were also conducted. In addition, the samples were also investigated against the digestive enzymes of α-amylase and α-glucosidase using 96-well microplate technique.

2. Materials and Method

Two different commercial products of vinegar were used as study material: one is hawthorn vinegar supplied from Malatya province (MS), another one is vinegar from Konya (TS).

2.1. Total Phenol Content (TPC)

The total phenolic content of the vinegars was measured according to the method described previously with some modifications (Ozdemir et al. 2022). 30 µL of TS and MS samples was taken and placed in a 96-well microplate. 150 µL of tenfold diluted F-C reagent was added to it and left for 5 minutes. After adding of 120 µL 7.5% $NaCO_3$ to stop the reaction, it was kept in the dark for 1 hour. Absorbances were read on an Elisa reader at 760 nm. Calibration curve was created by serial dilution of gallic acid. The TPC was calculated according to the equation and expressed as mg equivalent to gallic acid per mL. The equation obtained by the absorbance versus concentration of the serial dilution solution of gallic acid is $y = 0.0071x+0.1927$, $r^2 = 0.9937$.

2.2. Total Flavonoid Content (TFC)

The total flavonoid content of vinegar was determined by method previously reported with minor modifications (Özdemir et al. 2022). Catechin was used for creating calibration curve. 100 µL of TS and MS samples/catechin serial solutions were placed in a 96-well microplate. 30 µL of $NaNO_2$ was added on to it. After waiting for 5 minutes, 50 µL of $AlCl_3$ was added and the mixture was left in the dark for another 6 minutes. Then, 50 µL of NaOH was added and left for 10 min. Their absorbance was read at 510 nm on an Elisa reader. TFC was calculated according to the equation obtained from catechin serial dilutions and expressed as mg equivalent to catechin per mL. The equation obtained by the absorbance versus concentration of the serial dilution solution of catechin is: $y = 0.0003x – 0.0169$, $r^2 = 0.9918$.

2.3. In Vitro Antioxidant Activity

2.3.1. DPPH Radical Scavenging Activity

The DPPH radical scavenging activity of hawthorn vinegar was examined as described in previously published work (Özdemir et al. 2022). 12.5 µl of TS and MS samples were taken with micropipettes and placed in a 96-well microplate. Then 250 µl of 0.1 mM DPPH prepared in methanol was added on it. The BHA was used as positive control. After incubated for 1 hour in the dark at room temperature, the absorbances were read on an Elisa reader at 517 nm. The % radical scavenging activity value was calculated according to the formula:

$$\% \text{ Inhibition} = \frac{\text{Ablank} - \text{Asample}}{\text{Ablank}} \times 100$$

In the formula, A= Absorbance; A_{blank}: Absorbance of the solution without sample; A_{sample}: Absorbance of TS and MS Samples.

2.3.2. Fe^{+2} Chelating Activity (FCA)

The iron chelating activity of hawthorn vinegar was examined as described in previously published work (Özdemir et al. 2022). 50 µl of TS and MS samples were taken with micropipettes and placed in a 96-well microplate. Then, 160 µl of distilled water, 5 µl of 2mM $FeSO_4$ were added to it. After 1 min of incubation at room temperature, 10 µl of 5mM ferrozine was added. The mixture was kept at room temperature for 30 min. The EDTA used as a positive control. Absorbance was read at 562 nm.

2.3.3. ABTS Radical Scavenging Activity

The ABTS radical scavenging activity of hawthorn vinegar was examined as described in previously published work (Özdemir et al. 2022). Briefly, 50 µL of samples of TS and MS diluted with the dilution technique were taken with micropipettes and placed in a 96-well microplate. Trolox used as a positive control. The final volume was made up to 50 µL with distilled water. 100 µL of $ABTS^{\bullet+}$ working solution was added to the wells and kept in the dark at room temperature for 10 min. Absorbances were read on an Elisa reader at 734 nm. The % ABTS radical scavenging activity value was calculated according to the formula given in DPPH method.

2.4. In Vitro Antidiabetic Activity

2.4.1. α-Amylase Inhibition Activity

The α-amylase inhibition activity of hawthorn vinegar was determined with the Caraway Samogyi Iodine/Potassium Iodine (1_2/KI) method with minor modification (Özek 2018). Briefly, 25 µl of TS and MS samples were taken with micropipettes and placed in a 96-well microplate. 50 µl α-amylase (0.8 U/mL enzyme solution prepared with Phosphate buffer) was placed on it. After incubation at 37°C for 10 minutes, 50 µl of starch solution was added. After another 10 min of incubation, 25 µl of 1M HCl solution and 100 µl of 1_2/KI solution were added to stop the reaction. Acarbose was used as a positive control. Absorbances were read on an Elisa reader at 630 nm. The results were evaluated with the formula given in the DPPH assay.

2.4.2. α-Glucosidase Inhibition Activity

The α-glucosidase inhibition effect of hawthorn vinegar was determined with 96-well plate method as described previously (Palanisamy et al. 2011). In this assay, samples were run in 4 parallel. 50 µL of TS and MS samples, 10 µl of 0.4 U/mL α-glucosidase solution were taken and placed in a 96-well microplate, then incubated at 37°C for 20 min. 125 µl of 0.1M phosphate buffer solution (PBS, pH=6.8) was added and incubated for another 20 min at 37°C. After adding 20 µl of 5mM PNPG on the mixture, it was incubated at 37°C for 30 minutes. 50 µl of 0.1N Na_2CO_3 was added to stop the reaction. Acarbose was used as a positive control. The absorbance was measured at 405 nm on an Elisa reader. The results were evaluated with the formula given in the DPPH assay.

3. Results and Discussion

In our study, the vinegar sample obtained from TS from Konya and MS from Malatya were investigated and compared in terms of total phenolic and flavonoid content, antioxidant and inhibitory activity against digestive enzyme of α-amylase and α-glucosidase. Statistical evaluation and drawing graphs were done with Excel Program and GraphPad prism software (8.0).

3.1. Total Phenol and Flavonoid Content (TPC & TFC)

The total phenol and flavonoid amount of vinegar samples are given in Table 1. As seen in the results, the highest TPC was found to be 467.59 ± 6.73 mg GAE/mL in TS vinegar, it was followed by MS vinegar with TPC content of 328.46 ± 5.50 mg GAE/mL. The TFC was found as 1.94 ± 10.36 mg CE/mL and 1.32 ± 10.96 mg CE/mL in TS and MS vinegar, respectively. In a study on *C. tanacetifolia* (Ozdemir, et al. 2021), the total amount of phenol was found to be 0.51 mg/ml. In our study, this value was found to be higher in both vinegars.

3.2. In vitro Antioxidant Activity

The values of the DPPH, ABTS radical scavenging and ferrous chelating activity results are given in Table 1. According to the results, the highest DPPH radical scavenging activity was showed by MS with 80.12 ± 4.45% inhibition, while TS sample was found as 73.82 ± 2.12%. The ABTS radical scavenging activity was found to be highest in TS with 82.51± 0.78% and in MS found as 78.65 ± 0.55%. The FCA was found to be higher in TS (33.37 ± 0.53%) than in MS (31.08 ± 10.87%).

In a study by Murathan et al. (2016), DPPH radical scavenging activity were found to be 67.76% in *C. monogyna* and 74.76% in *C. sinaica*. The *C. tanacetifolia* and *C. sinaica* exhibited ABTS radical scavenging activity 51.62% and 68.61%, respectively. The TS and MS samples in the current study we used showed higher activity in both radical scavenging assay.

Table 1. The total phenolic and flavonoid content and antioxidant activity of *C. tanacetifolia* vinegar

Type of extract	Total Phenol content (TPC) GAE mg/mL sample	Total flavonoid content (TFC) CE mg/mL$_{sample}$	DPPH radical scavenging activity (%)	Fe^{+2} chelating activity (%)	ABTS radical scavenging activity (%)
TS	467.59 ± 6.73	1.94 ± 10.36	73.82 ± 2.12	33.37 ± 0.53	82.51 ± 0.78
MS	328.46 ± 5.50	1.32 ± 10.96	80.12 ± 4.45	31.08 ± 10.8	78.65 ± 0.55
BHA			90.33 ± 0.25	-	-
EDTA			-	23.86 ± 7.83	-
Trolox			-	-	49.15 ± 4.11

The datas were expressed as Mean ± Standard deviation (Mean ± SS) of three parallel mesarements.

3.3. In vitro enzyme inhibition activity

Enzyme inhibition results of vinegar samples and reference substance acarbose are given in Table 2. As can be seen from the table below, the MS has been found to have higher α- amylase (95.12± 3.71%) and α-glucosidase inhibitory (81.62 ± 0.33%) effects. The TS demonstrated 94.13 ± 3.85% α-amylase and 75.35 ± 2.19% α-glucosidase inhibitory activity, respectively. In a study on α- glucosidase inhibition of hawthorn, the percent inhibition activity value of hawthorn sample was found to be 3.37 ± 0.04 mg hawthorn mL^{-1} (Xiao et al., 2016). In our study, this value was higher in TS and MS vinegars.

Table 2. α-amylase and α-glucosidase inhibitory activity of vinegar samples and acarbose

Type of sample	α-amylase	α-glucosidase
TS	94.13 ± 3.85	75.35 ± 2.19
MS	95.13 ± 3.71	81.35 ± 0.33
Acarbose	71.71 ± 2.94	78.68 ± 0.88

Note: TS: The vinegar sample from Konya, MS: The vinegar from Malatya; Acarbose (1mg/ml);
% Inhibition= mean of three measurements ± standard deviation

4. Conclusion

Türkiye is home to many wild fruits. Hawthorn, which is among them, has an important place in terms of its beneficial effect on the cardiovascular system. In addition, although it is known that hawthorn vinegar, which is prepared from its fruit, has a sugar and cholesterol-lowering effect among the public, scientific studies on this are not enough. Therefore, in this study, the total phenol and total flavonoid content were investigated in the vinegar produced from the fruit of *C. tanacetifolia* obtained from Konya and commercial product hawthorn vinegar. In addition to this, in vitro antioxidant activity and inhibition against digestive enzymes of α-amylase and glucosidase were also Turkiye is home to many wild fruits. Hawthorn, which is among them, has an important place in terms of its beneficial effect on the cardiovascular system. In addition, although it is known that hawthorn vinegar, which is prepared from its fruit, has a sugar and cholesterol-lowering effect among the public, scientific studies on this are not enough. Therefore, in this study, the total phenol and total flavonoid content were investigated in the vinegar produced from the fruit of *C. tanacetifolia* obtained from commercial product hawthorn vinegar. In addition to this, *in vitro* antioxidant activity and inhibition against digestive enzymes of α-amylase and glucosidase were also investigated. When the results obtained were evaluated, it was observed that hawthorn vinegar had a significant antioxidant and enzyme inhibitory effect associated with antidiabetic activity. All these values show that hawthorn vinegar can be used to support health. It is recommended by us to support the production of hawthorn plant, which is produced only in certain regions in our country, in other provinces and to carry out studies to increase its consumption among the people.

Acknowledgements

We would like to thank the TUBITAK 2209/A Undergraduate Student Project for the financial support (NO: 1919B012102103).

Authors' contributions:

Study design (NE, YGA), Methodology (FA, NST, NE), Analysis and interpretation of the data (FA, NST, NE), Drafting of the paper (FA), Final approval of the version to be published (FA, NST, NE)

Conflict of interest disclosure:

There is no conflict of interest.

References

Alirezalu, A. Ahmadi N, Salehi P, Sonboli A, Alirezalu K, Mousavi Khaneghah A, Barba FJ, Münekata P, Lorenzo JM. 2020. Physicochemical characterization, antioxidant activity, and phenolic compounds of hawthorn (*Crataegus spp.*) fruits species for potential use in food applications. Foods. 9(4): 436.

Asgari M, Salehi I, Ranjbar K, Khosravi M, Zarrinkalam E, 2022. Interval training and Crataegus persica ameliorate diabetic nephropathy via miR-126/Nrf-2 mediated inhibition of stress oxidative in rats with diabetes after myocardial ischemia-reperfusion injury. Biomed. Pharmacother. 153: 113411.

Bakir S, Devecioglu D, Kayacan S, Toydemir G, Karbancioglu-Guler F, Capanoglu E. 2017. Investigating the antioxidant and antimicrobial activities of different vinegars. Eur Food Res Technol. 243(12): 2083-2094.

Berghe WV. 2012. Epigenetic impact of dietary polyphenols in cancer chemoprevention: lifelong remodeling of our epigenomes. Pharmacol. Res. 65(6): 565-576.

Bruneton J. 1999. Pharmacognosy, Phytochemistry, Medicinal Plants (2rd edition). Lavoisier, Paris. Budak NH. Kumbul Doguc D. Savas CM. Seydim AC. Kok Tas T. Ciris, MI. Guzel Seydim ZB. 2011. Effects of apple cider vinegars produced with different techniques on blood lipids in high-cholesterol-fed rats. J Agric Food Chem. 59(12): 6638-6644.

Butnariu M. 2014. Detection of the polyphenolic components in *Ribes nigrum* L. Ann Agric Environ Med. 21(1).

Cheplick S, Kwon YI, Bhowmik P, Shetty K. 2010. Phenolic-linked variation in strawberry cultivars for potential dietary management of hyperglycemia and related complications of hypertension. Bioresour Technol. 101(1): 404-413.

Chowdhury SS, Islam MN, Jung HA, Choi JS. 2014. *In vitro* antidiabetic potential of the fruits of Crataegus pinnatifida. Res Pharm Sci. 9(1): 11-22.

Deveci E. Tel Çayan G, Karakurt S, Duru ME. 2020. Antioxidant, Cytotoxic, and Enzyme Inhibitory Activities of *Agropyron repens* and *Crataegus monogyna* Species. Eur J Biol. 79(2): 98-105.

Dönmez AA. 2004. The genus *Crataegus* L.(Rosaceae) with special reference to hybridisation and biodiversity in Turkey. Turk J Botany. 28(1): 29-37.

Folli F, Corradi D, Fanti P, Davalli A, Paez A, Giaccari A, Muscogiur G. 2011. The role of oxidative stress in the pathogenesis of type 2 diabetes mellitus micro- and macrovascular complications: avenues for a mechanistic-based therapeutic approach. Curr Diabetes Rev. 7(5): 313-324.

Forbes JM, Cooper ME. 2013. Mechanisms of diabetic complications. Physiol Rev. 93(1): 137-188.

Forman HJ, Zhang H. 2021. Targeting oxidative stress in disease: Promise and limitations of antioxidant therapy. Nat Rev Drug Discov. 20(9): 689-709.

Haidara MA, Mikhailidis DP, Rateb MA, Ahmed ZA, Yassin HZ, Ibrahim IM, Rashed LA. 2009. Evaluation of the effect of oxidative stress and vitamin E supplementation on renal function in rats with streptozotocin-induced Type 1 diabetes. J Diabetes Complications. 23(2): 130-136.

Halliwell B. 2020. Reflections of an aging free radical. Free Radic Biol Med. 161: 234-245.

Hoogeveen EK, Kostense PJ, Beks PJ, Mackaay AJ, Jakobs C. Bouter LM, Stehouwer CD. 1998. Hyperhomocysteinemia is associated with an increased risk of cardiovascular disease, especially in non–insulin-dependent diabetes mellitus: a population-based study. Arterioscler Thromb Vasc Biol. 18(1): 133-138.

Kołodziej B, Sęczyk Ł, Sugier D, Kędzia B, Chernetskyy M, Gevrenova R, Henry M. 2019. Determination of the yield, saponin content and profile, antimicrobial and antioxidant activities of three *Gypsophila* species. Ind Crops Prod. 138: 111422.

Kucukatay V, Agar A, Gumuslu S, Yargicoglu P. 2007. Effect of sulfur dioxide on active and passive avoidance in experimental diabetes mellitus: relation to oxidant stress and antioxidant enzymes. Int J Neurosci. 117(8): 1091-1107.

Li T, Fu S, Huang X, Zhang X, Cui Y, Zhang Z, Li S. 2022. Biological properties and potential application of hawthorn and its major functional components: A review. J Funct Foods. 90: 104988.

Li T, Zhu J, Guo L, Shi X, Liu Y, Yang X. 2013. Differential effects of polyphenols-enriched extracts from hawthorn fruit peels and fleshes on cell cycle and apoptosis in human MCF-7 breast carcinoma cells. Food Chem. 141(2): 1008-1018.

Mecheri A, Amrani A, Benabderrahmane W, Bensouici C, Boubekri N, Benaissa O, Zama D, Benayache F, Benayache S. 2021. *In Vitro* pharmacological screening of antioxidant, photoprotective, cholinesterase, and α-glucosidase inhibitory activities of Algerian *Crataegus oxyacantha* Fruits and leaves extracts. Pharm Chem J. 54 (11): 1150-1156.

Miguez B, Gómez B, Gullón P, Gullón B, Alonso JL. 2016. Pectic oligosaccharides and other emerging prebiotics. Probiotics and prebiotics in human nutrition and health. 301-330.

Murathan ZT, Erbil N, Arslan M. 2016. Elazığ'da yetişen farklı *Crataegus* türlerinin biyoaktif bileşen, antioksidan, antibakteriyel ve mutajenik özelliklerinin karşılaştırılması. Bitlis Eren Univ Fen Bilim Derg. 11(1): 218-226.

OKeefe JH, Gheewala NM, O'Keef JO. 2008. Dietary strategies for improving post-prandial glucose, lipids, inflammation, and cardiovascular health. J Am Coll Cardiol. 51(3): 249-255.

Özdemir N, Pashazadeh H, Zannou O, Koca I. 2022. Phytochemical content, and antioxidant activity, and volatile compounds associated with the aromatic property, of the vinegar produced from rosehip fruit (*Rosa canina* L.). Lwt Food Sci Technol. 154: 112716.

Özek G, 2018. Chemical diversity and biological potential of *Tanacetum praeteritum* subsp. *praeteritum* essential oils. J. Turk Chem Soc. A: Chem. 5(2): 493-510.

Palanisamy UD, Ling LT, Manaharan T, Appleton D. 2011. Rapid isolation of geraniin from *Nephelium lappaceum* rind waste and its anti-hyperglycemic activity. Food Chem. 127(1): 21-27.

Qiao A, Wang Y, Xiang L, Zhang Z, He X. 2015. Novel triterpenoids isolated from hawthorn berries functioned as antioxidant and antiproliferative activities. J Funct Foods. 13: 308-313.

Rashed K, Butnariu M. 2014. Antimicrobial and antioxidant activities of *Bauhinia racemosa* Lam. and chemical content. Iran J Pharm Res. 13(3): 1073.

Samad A, Azlan A, Ismail A. 2016. Therapeutic effects of vinegar: a review. Curr Opin Food Sci. 8: 56-61.

Sammari H, Jedidi S, Selmi H, Rtibi K. Jabri MA, Jridi M, Sebai H. 2021. Protective effects of *Crataegus azarolus* L. berries aqueous extract against castor oil induced diarrhea, oxidative stress, and inflammation in rat. Neurogastroenterol Motil. 33(6): e14065.

Xu W, Caracciolo B, Wang HX, Winblad Bäckman L, Qiu C, Fratiglioni L. 2010. Accelerated progression from mild cognitive impairment to dementia in people with diabetes. Diabetes. 59(11): 2928-2935.

Yılmaz B, Karabudak E. 2018. Diyet Kaynaklı İleri Glikasyon Son Ürünleri ve Sağlık Üzerine Etkileri. Acıbadem Univ Sağlık Bilim Derg. (4): 349-356.

REVIEW ARTICLE
Eurasian J Bio Chem Sci, 6(2):109-113, 2023
https://doi.org/10.46239/ejbcs.1365464

Eurasian Journal of Biological and Chemical Sciences

Journal homepage: www.dergipark.org.tr/ejbcs

Obezite patogenezinde mitojenle aktifleşen protein kinaz ve fosfatidilinositol 3-kinaz/akt sinyal yolları

Adem Keskin[1*]

[*1]*Aydın Adnan Menderes Üniversitesi, Sağlık Bilimleri Enstitüsü, Biyokimya (Tıp) Anabilim Dalı, Aydın, Türkiye.*

*Corresponding author : ademkeskin78@gmail.com
Orcid No: https://orcid.org/0000-0003-1921-2583

Received : 24/09/2023
Accepted : 05/12/2023

Özet: Dünya çapında önemli bir sağlık sorunu olan ve vücutta aşırı yağ birikmesiyle karakterize edilen obezite, tip 2 diyabet, kalp-damar hastalıkları ve alkole bağlı olmayan yağlı karaciğer hastalığı gibi bir dizi kronik hastalık riskini keskin bir şekilde artırır. Diyet ve egzersiz gibi yaşam tarzı müdahalelerinin obeziteyle mücadelede önemli etkileri olmasına rağmen, kilo vermede uzun vadeli başarıyı yakalamak son derece zordur ve obezite prevalansı dünya çapında artmaya devam etmektedir. Geçtiğimiz birkaç on yılda, obezitenin patofizyolojisi kapsamlı bir şekilde araştırılmış ve artan sayıda sinyal yolu obezite ile ilişkilendirilmiş, obeziteyle daha etkili ve kesin bir şekilde mücadele etmek için sinyal yollarına odaklanılmıştır. Mitojenle aktifleşen protein kinaz (MAPK) sinyal yolu iştah kontrolüne, glukoz seviyelerinin düzenlenmesine ve yağ hücresi oluşumuna katkıda bulunurken aynı zamanda insülin direncinin gelişmesine de yol açabilir. MAPK'nın rolü özellikle hipotalamus ve yağ dokusunda vurgulanmıştır. Fosfatidilinositol 3-kinaz/AKT sinyal yolu, hücre büyümesinin ve çoğalmasının düzenlenmesinde kritik bir rol oynar. Bu yolun anormal aktivasyonu obezitenin gelişimini teşvik edebilir ve insülin direncine katkıda bulunabilir. Araştırmalar, iştahın düzenlenmesinde sinyal yolları, yağ dokusu metabolizması ve enerji dengesi arasındaki ilişkilerin daha iyi anlaşılması gerektiğini göstermektedir. Sonuç olarak obezite yönetimine yönelik yenilikçi ve güvenli önlemlerin araştırılması gerekmektedir. Sinyal yolakları obezitenin patogenezinde önemli bir rol oynamaktadır ve gelecekteki çalışmaların bu konuya daha fazla odaklanması gerekmektedir.

Anahtar Kelimeler: Obezite, Sinyal yolu, MAPK sinyal yolu, PI3K/AKT sinyal yolu

Mitogen-activated protein kinase and phosphatidylinositol 3-kinase/akt signaling pathways in the pathogenesis of obesity

Abstract: Obesity, a major health problem worldwide and characterized by excess fat accumulation in the body, sharply increases the risk of a number of chronic diseases, such as type 2 diabetes, cardiovascular diseases and non-alcoholic fatty liver disease. Although lifestyle interventions such as diet and exercise have significant effects in combating obesity, long-term success in weight loss is extremely difficult to achieve and the prevalence of obesity continues to increase worldwide. Over the past few decades, the pathophysiology of obesity has been extensively investigated and an increasing number of signaling pathways have been associated with obesity, focusing on signaling pathways to combat obesity more effectively and precisely. While the mitogen-activated protein kinase (MAPK) signaling pathway contributes to appetite control, regulation of glucose levels and fat cell formation, it may also lead to the development of insulin resistance. The role of MAPK has been particularly emphasized in the hypothalamus and adipose tissue. The phosphatidylinositol 3-kinase/AKT signaling pathway plays a critical role in regulating cell growth and proliferation. Abnormal activation of this pathway may promote the development of obesity and contribute to insulin resistance. Research shows that there is a need for a better understanding of the relationships between signaling pathways, adipose tissue metabolism, and energy balance in the regulation of appetite. As a result, innovative and safe measures for obesity management need to be investigated. Signaling pathways play an important role in the pathogenesis of obesity, and future studies need to focus more on this issue.

Keywords: Obesity, Signaling pathway, MAPK signaling pathway, PI3K/AKT signaling pathway

1. Giriş

Yağ dokusundaki aşırı artış, hem anormal yağ hücresi lipit birikiminin (adiposit hipertrofisi) hem de hiperplazi olarak bilinen öncüllerinin katılımıyla yeni adipositlerin gelişmesinin bir sonucudur. Yağ dokusundaki bu artış sonucu ortaya çıkan obezite, tip 2 diyabetus melltus, kardiyovasküler hastalıklar, metabolik sendrom , alkolsüz yağlı karaciğer hastalığı gibi bulaşıcı olmayan hastalıklarla sıklıkla birlikte görülen, gün geçtikçe kötüleşen bir sağlık sorunudur (Gustafson ve ark. 2019; Shen ve ark. 2022). Obeziteye eşlik eden komorbiditeler, hastaların yaşam kalitesini kötüleştirir (Kivimäki ve ark. 2022). Bu da vücut kitle indeksi ile orantılı olarak sağlık bakım maliyetlerinde artışa karşılık gelir (Kent ve ark. 2019). Yakın zamanda obezite ve aşırı kilo prevalansındaki mevcut eğilim değişmezse, yaklaşık ekonomik maliyetlerin küresel gayri safi yurt içi hasılanın %3,29'una yükseleceği rapor edilmiştir (Okunogbe ve ark. 2021). Toplu olarak, obezitenin geç ve geri döndürülemez sonuçlarının tedavisiyle ilişkili olarak dünya nüfusuna gelen bu önemli sosyo-ekonomik yükler, dikkatleri obezitenin yönetiminde yenilikçi ve güvenli önleme ve erken müdahalelerin araştırılmasına çekmiştir (Müller ve ark. 2022).

Tüm canlı sistemler çevreleri hakkında bilgi edinir. Hücresel düzeyde bunu sinyal yolları aracılığıyla yaparlar. Bu tür yollar, hücre dışı bir işaretin veya sinyalin varlığını algılayan ve hücrenin iç kısmına ileten moleküller arasındaki tersine çevrilebilir bağlanma etkileşimlerine dayanır (Azpeitia ve ark. 2020). Bu etkileşimlerin oluşturduğu sinyal yollarının modüle edilmesinde yer alan eylemlerin anlaşılması, hastalıkların önlenmesi ve tedavisi için yararlı bilgiler sağlamaktadır (Keskin, 2023). Sinyal iletimine ilişkin gelişen bilgi, kişiselleştirilmiş tıpta yeni bir çağa girerken obezite araştırmalarının gelecekteki yönüne ışık tutabilmektedir. Sinyal iletim yolları ile obezite arasındaki ilişkiye ilişkin giderek artan sayıda kanıt bulunmaktadır; Obezitenin patofizyolojisi kapsamlı bir şekilde araştırılmıştır ve bu da obeziteyle daha etkili ve kesin bir şekilde mücadele edilmesini mümkün kılmaktadır (Müller ve ark. 2022).

Bilim ve teknolojideki gelişmelerin yanı sıra ilaç sektörünün de hızla büyümesiyle obeziteyle mücadelede büyük başarılar elde edilmiş; kalori kısıtlaması, yaşam tarzı yönetimi, farmakoterapi ve bariatrik cerrahi gibi çeşitli stratejiler obezite karşıtı çareler olarak önerilmiştir (Wolfe ve ark. 2016; Trepanowski ve ark. 2017). Bununla birlikte, bu müdahaleler küresel boyuttaki tıbbi ihtiyaçları karşılama kapasitesine sahip değildir. Son zamanlarda iştahın düzenlenmesi ve periferik enerji emilimi, depolanması ve tüketimi ile ilgili çok sayıda faktör/sinyal ortaya çıkarılmıştır (Huang ve ark. 2019; Xu ve ark. 2021). Bu ilerlemeler obezitenin ortaya çıkışının anlaşılmasına ışık tutmaktadır. Bu sinyal yolllarının modüle edilmesinde polifenollerin rolü, yakın zamanda yapılan birçok çalışmanın konusu olmuştur (Keskin, 2023). Buna ek olarak, bu sinyalleri hedef alan bazı bileşikler klinik kullanıma dönüştürülmüştür. Örneğin, obezite karşıtı araştırmaların sıcak noktası olan iştah düzenlemesi, hem merkezi melanokortin yolu hem de leptin ve bağırsak hormonları gibi periferik sinyaller tarafından düzenlenir. Kan şekeri düzeylerini düşürebilen ve siklik adenosin monofosfat'a (cAMP) bağımlı sinyal yollarıyla insülin salgılanmasını teşvik ederek glukoz toleransını geliştirebilen bağırsaktan türetilen bir hormon olan glukagon benzeri peptid 1 (GLP-1), aynı zamanda anoreksijenik nöronları doğrudan uyararak iştahı da azaltabilir. Öte yandan oreksijenik nöronları γ-aminobütirik asit (GABA) bağımlı sinyal yoluyla baskılayabilir (Huang ve ark. 2019).

Obezitenin patofizyolojisi hala tam olarak anlaşılmamış olmasına rağmen, birçok yolla kontrol edilen heterojen bir sağlık sorunu olduğu yaygın olarak kabul edilmektedir. Obezitenin ortaya çıkması ve gelişmesinde yer alan sinyal yollarının giderek daha iyi anlaşılması, obeziteyle daha kesin bir şekilde mücadele etmemizi sağlar. Bu derlemede, obezitenin patogenezinde, özellikle iştahın düzenlenmesinde, yağ dokusu metabolizmasında ve fonksiyonunda, glukoz hemostazında ve enerji harcamasında yer alan bazı sinyal yollarının incelenmesi amaçlandı.

2. Materyal ve Metot

Obezite sağlık sorununun patogenezinde sinyal yollarının öneminin daha iyi anlaşılmasını sağlamak amacıyla PubMed, Scopus, Web of Science ve Google Scholar veritabanlarını kullanılarak literatür taraması yapıldı. Anahtar kelime olarak, obezite, sinyal yolu, mitojenle aktifleşen protein kinaz (MAPK) sinyal yolu ve fosfatidilinositol 3-kinaz (PI3K)/AKT sinyal yolu, kelimeleri kullanıldı. Alıntılama sayıları ve yayın tarihleri dikkate alınarak 35 makale seçildi. Ayrıca bu seçim, obezite patogenezi esasına dayalı olarak yapıldı.

Literatür taramasında en çok çalışma yapılan iki sinyal yolu, ana başlıklar altında kategorize edildi. Referans olarak değerlendirmeye alınan çalışmalarda ilgili sinyal yolu ile iştahın düzenlenmesi, yağ dokusu metabolizması ve fonksiyonu, glukoz hemostazı ve enerji harcaması arasındaki ilişkiye odaklanıldı.

3. Memeli hücrelerinde sinyal iletiminin kritik aracı: MAPK sinyal yolu

MAPK sinyali, hücre dışı uyarıları hücre içi sinyallere bağlayan bir kinaz kademesi içerir (Pudewell ve ark. 2021). MAPK tarafından gerçekleştirilen fosforilasyon ile, gen ekspresyonuna aracılık etmek ve proliferasyon, inflamasyon, farklılaşma ve apoptoz gibi hücresel olayları başlatmak için aşağı yöndeki transkripsiyon faktörleri aktive edilir (Sun ve ark. 2015). Hücre dışı sinyalle düzenlenen kinaz (ERK) 1/2, c-Jun N-terminal kinaz (JNK) ve p38 MAPK dahil olmak üzere MAPK sinyal yolu üyeleri iştah, adipogenez, glukoz homeostazisi ve termojenezin düzenlenmesinde önemli bir rol oynar (Kassouf ve Sumara, 2020).

MAPK aracılı iştah düzenlemesinin yanı sıra merkezi sinir sistemindeki diğer MAPK fonksiyonları da obezitenin patogenezine katkıda bulunur. ERK1/2, hipotalamik nöronlarda glukozla uyarılan proopiomelanokortin ekspresyonunu arttırır ve anoreksijenik etkiye katılır

(Zhang ve ark. 2015). Buna ek olarak MAPK sinyal yolu merkezi sinir sistemindeki JNK1 nakavtı, hipotalamik-hipofiz-tiroid ekseninin negatif geri bildirimini bloke ederek gıda alımını azaltır ve enerji harcamasını artırır (Sabio ve ark. 2010). p38 MAPK alt birimi nakavt veya inhibisyonu olan embriyonik farelerden alınan primer embriyonik fibroblastlarda ve yetişkin farelerden alınan preadipositlerde, PPARγ ekspresyonu artar, bu da p38 MAPK'nin adipogenezi baskıladığını gösterir (Aouadi ve ark. 2006). Tersine, in vitro insan preadiposit farklılaşması sırasında p38 MAPK aktivitesinde artış gözlenir ve bu hücrelerde p38 MAPK'nin farmakolojik inhibisyonu, trigliseritlerin birikimini ve diğer adipogenez belirteçleriyle birlikte PPARy ekspresyonunu azaltır (Aouadi ve ark. 2007). İnsan beyaz yağ dokusunda, artan hipertrofik adiposit sayısı aynı zamanda yukarı regüle edilmiş p38 MAPK sinyalleriyle de ilişkilidir ve fosforile edilmiş p38 MAPK, açlık trigliserid, insülin ve glukoz düzeyleriyle bağlantılıdır (Bashan ve ark. 2007). Bu bulgular p38 MAPK'nın adiposit farklılaşması ve adipogenez üzerinde iki işlevli etkileri olduğunu göstermektedir.

MAPK sinyal yolu, insülin direncinin gelişiminde yakından rol oynar. MAPK sinyal yolunun birden fazla noktadan defosforilasyonu ve deaktivasyonu, insülin reseptör substrat-1'in tirozin fosforilasyon seviyesini ve insülin sinyal transdüksiyonuna aracılık etme kapasitesini eski haline getirir (Khoubai ve Grosset, 2021). Benzer şekilde, MAPK sinyal yolunun endojen bir aktivatörü olan kaspaz 9'un eksikliği, yüksek yağlı diyetin neden olduğu insülin direncini ve adiposit büyümesini azaltır (Zeng ve ark. 2018). Yüksek yağlı diyet ile beslenen farelerden alınan yağ dokularında, entegre multiomik analiz, makrofajlardaki MAPK sinyal yollarında inflamatuar genlerin zenginleştiğini göstermektedir (Wang ve ark. 2021).

4. Hücre büyümesi ve çoğalmasının önemli bir düzenleyicisi: PI3K/AKT sinyal yolu

Hücre büyümesi ve çoğalmasının önemli bir düzenleyicisi olan PI3K/AKT sinyal yolunun anormal aktivasyonu, obezitenin gelişimini teşvik etmektedir (Sun ve ark. 2019). PI3K ve AKT, bu yoldaki hormonlar ve büyüme faktörleri gibi yukarı yönlü sinyaller tarafından etkinleştirilen iki ana düğümdür. PI3K aktivasyonu, fosfatidilinositol 4,5-bifosfatı fosfatidilinositol 3,4,5-trisfosfata dönüştürür, fosfoinositid bağımlı kinazları ve AKT'yi aktive eder ve ardından glikojen sentaz kinaz3, sırasıyla glikojen sentezini, glukoz alımını ve adipogenezi düzenleyen forkhead box protein (Fox) ailesini aktive eder (Hemmings ve Restuccia, 2015).

PI3K/AKT sinyal yolunda katalitik bir alt birim olarak bulunan rapamisinin memeli hedefi (mTOR) çok çeşitli önemli hücresel süreçleri kontrol etme konusundaki olağanüstü yeteneğinden dolayı hücresel yaşlanmada önemlidir (Keskin ve ark. 2023). mTOR, mTORC1 ve mTORC2 olmak üzere iki farklı kompleks oluşturur. mTORC1 ve mTORC2 PI3K/AKT/mTOR sinyal yolunda farklı hareket eder ve her ikisi de obezitenin patogeneziyle yakından ilişkilidir. mTOR ayrıca merkezi ve periferik sistemlerde iştahın düzenlenmesine de katkıda bulunur. Hipotalamusta mTOR'un uyarılması, proopiomelanokortin nöronlarını aktive ederek gıda alımını azaltır ve hayvan çalışmalarında yaşa bağlı obeziteyi iyileştirir. PI3K/AKT yolu, merkezi sinir sistemi ve periferik dokular yoluyla iştahı düzenler. Leptinin hipotalamusun mediobazal kısmına etki ederek kısmen PI3K-AKT-FoxO1 yoluyla gıda alımını baskılamaktadır (Kwon ve ark. 2016). PI3K'nın seçici inhibisyonunun leptinin etkisini ortadan kaldırdığı rapor edilmiştir (Hill ve ark. 2008).

PI3K/AKT yolu, insülin sinyal yolu için vazgeçilmezdir. Bu sinyalin düzensizliği obezitenin ciddiyeti ve insülin direnciyle ilişkilidir (Li ve ark. 2017). AKT aktivitesi ile vücut yağ yüzdesi arasında negatif korelasyon hem hayvan modellerinde hem de insanlarda bulunmuştur ve obez popülasyondaki insülin direncinden AKT sorumlu olabilir (Friedrichsen ve ark. 2010; Mackenzie ve Elliot,. 2014). PI3K/AKT sinyallemesinin inhibisyonu, glukoz taşıyıcı 4 (GLUT4) depolama keseciklerinin bir elemanı olan Sort1'in bozulmasına yol açar ve insülin duyarlılığını azaltır (Li ve ark. 2017).

5. Obezite ile mücadelede sinyal yollarının önemi

Obezite tedavisinde egzersiz gibi yaşam tarzı değişikliklerle kilo kaybının kontrollü olması gereklidir. Kilo kaybının kontrolsüz olması, oksidatif stres parametrelerinde artışa ve elektrolit dengesi bozukluklarına yol açabilir ve bu durum yaşamı tehdit edebilir (Keskin ve Aci 2022). Buna ek olarak, obezite tedavisi için klinik ortamda farmokoterapi içeren çeşitli yaklaşımlar yaygın olarak kullanılmaktadır. Ancak bu geleneksel seçenekler hâlâ etkisiz ve elverişsizdir ve olumsuz etki riski taşımaktadır (Li ve ark. 2021). Mekanistik kanıtlardan klinik gözlemlere kadar obezite ile morbidite/mortalite arasındaki nedensel bağlantı uzun süredir bilinmektedir. Obezitenin etiyolojisi ve patofizyolojisinin anlaşılmasında önemli ilerlemeler kaydedilmiş olmasına rağmen, obezite patogenezi ve kişiselleştirilmiş tedaviler hakkında gelişen bilgilerimiz henüz tatmin edici değildir. Hücresel sinyal yollarının kodunun çözülmesi, daha hassas ilaçlara yönelmemizi sağlayarak obeziteyle mücadelede cephaneliğimizi zenginleştirmektedir (Wen ve ark. 2022).

Son yıllarda yapılan çalışmalar ile yağ dokusunun kaderinin belirlenmesi ve yağ doku oluşumunun düzenlenmesi sinyal ve sistemik faktörler tarafından belirlendiği rapor edilmiştir. Ayrıca adipojenik nişin doku adipojenik kapasitesini etkileyebilmektedir. Sinyal ve sistemik faktörler tarafından belirlenen yağ dokusu kütlesinin artmasıyla karakterize edilen obezite, metabolik hastalıklara ve kansere karşı güçlü bir yatkınlık ile ilişkilidir (Ghaben ve Scherer, 2019). Farklı obez popülasyonlarda belirli sinyalleri/yolları hedefleyerek hassas terapiye ulaşılabilir. Bu kişiselleştirilmiş tedavi stratejisinin, artan klinik ve biyolojik veri kümelerine dayalı olarak yüksek performanslı bilgi işlem ve yapay zeka yardımıyla büyük ölçüde geliştirilebileceğine dikkat edilmelidir. Bununla birlikte, sinyal iletimlerinin karmaşıklığı nedeniyle, bireysel hastaların moleküler suçlularının belirlenmesi hala zordur ve bu durum, klinik

uygulamaya çeviriyi engelleyebilir (Wen ve ark. 2022). Diğer bir taraftan, obezite, tümör hücresinin hayatta kalmasını, çoğalmasını ve metabolizmasını destekleyen çok sayıda onkogenik sinyal yolunu aktive eder. Bu nedenle kanserli hastanın bakımında obezitenin etkisinin en aza indirilmesi kritik öneme sahiptir (Hopkins ve ark. 2016).

6. Sonuç

Sonuç olarak MAPK sinyal yolu, iştah kontrolü, glukoz seviyelerinin dengelemesi ve vücut ısısının ayarlanması gibi işlevlerin yanı sıra yağ hücrelerinin oluşumu ve gelişimi üzerinde önemli etkilere sahiptir. Aynı zamanda insülin direncinin gelişiminde de rol oynar, bu da obezitenin patogeneziyle yakından ilişkilidir. PI3K/AKT sinyal yolu da, anormal aktivasyonunda obezitenin gelişimini teşvik etmesinin yanı sıra obez popülasyondaki insülin direncinden AKT sorumlu olabilmektedir. Aynı zamanda merkezi sinir sistemi ve periferik dokular yoluyla iştahı düzenlemesine ve leptin salınımına etki ederek gıda alımını baskılamasına katkıda bulunarak obezitenin patogenezinde önemli rolü olan diğer sinyal yoludur. Obezitenin ve neden olduğu birçok sağlık sorununun tedavi maliyetini en düşük düzeylere indirmek ve toplumdaki sağlıklı birey oranlarını en yüksek düzeylere yükseltmek amacıyla obezitenin önlenmesine yönelik çalışmalar artarak devam edecektir. Bu çalışmalarda, sinyal yollarının iştah düzenlemesi, yağ dokusunun metabolizması ve fonksiyonu, glukoz dengelemesi ve enerji harcaması arasındaki ilişkiler öncelikli bir öneme sahip olacaktır.

Çıkar çatışması beyanı:

Bu çalışmada herhangi bir çıkar çatışması bulunmamaktadır.

Kaynaklar

Aouadi M, Laurent K, Prot M, Le Marchand-Brustel Y, Binétruy B, Bost F. 2006. Inhibition of p38MAPK increases adipogenesis from embryonic to adult stages. Diabetes. 55(2): 281-289.

Aouadi M, Jager J, Laurent K, Gonzalez T, Cormont M, Binétruy B, Le Marchand-Brustel Y, Tanti JF, Bost F. 2007. p38MAP Kinase activity is required for human primary adipocyte differentiation. FEBS Lett., 581(29): 5591-5596.

Azpeitia E, Balanzario EP, Wagner A. 2020. Signaling pathways have an inherent need for noise to acquire information. BMC Bioinformatics. 21(1): 462.

Bashan N, Dorfman K, Tarnovscki T, Harman-Boehm I, Liberty IF, Blüher M, Ovadia S, Maymon-Zilberstein T, Potashnik R, Stumvoll M, Avinoach E, Rudich A. 2007. Mitogen-activated protein kinases, inhibitory-kappaB kinase, and insulin signaling in human omental versus subcutaneous adipose tissue in obesity. Endocrinology. 148(6): 2955-2962.

Friedrichsen M, Poulsen P, Richter EA, Hansen BF, Birk JB, Ribel-Madsen R, Stender-Petersen K, Nilsson E, Beck-Nielsen H, Vaag A, Wojtaszewski JF. 2010. Differential aetiology and impact of phosphoinositide 3-kinase (PI3K) and Akt signalling in skeletal muscle on in vivo insulin action. Diabetologia. 53(9): 1998-2007.

Ghaben AL, Scherer PE. 2019. Adipogenesis and metabolic health. Nat Rev Mol Cell Biol. 20(4): 242-258.

Gustafson B, Nerstedt A, Smith U. 2019. Reduced subcutaneous adipogenesis in human hypertrophic obesity is linked to senescent precursor cells. Nature communications, 10(1): 2757.

Hemmings BA, Restuccia DF. 2015. PI3K-PKB/Akt pathway. Cold Spring Harb Perspect Biol. 2012 Sep 1;4(9):a011189. doi: 10.1101/cshperspect.a011189. Erratum in: Cold Spring Harb Perspect Biol. 7(4). pii: a026609.

Hill JW, Williams KW, Ye C, Luo J, Balthasar N, Coppari R, Cowley MA, Cantley LC, Lowell BB, Elmquist JK. 2008. Acute effects of leptin require PI3K signaling in hypothalamic proopiomelanocortin neurons in mice. J Clin Invest., 118(5): 1796-1805.

Hu E, Kim JB, Sarraf P, Spiegelman BM. 1996. Inhibition of adipogenesis through MAP kinase-mediated phosphorylation of PPARgamma. Science. 274(5295): 2100-2103.

Hopkins BD, Goncalves MD, Cantley LC. 2016. Obesity and Cancer Mechanisms: Cancer Metabolism. J Clin Oncol. 34(35): 4277-4283.

Huang R, Ding X, Fu H, Cai Q. 2019. Potential mechanisms of sleeve gastrectomy for reducing weight and improving metabolism in patients with obesity. Surg Obes Relat Dis. 15(10): 1861-1871.

Kassouf T, Sumara G. 2020. Impact of Conventional and Atypical MAPKs on the Development of Metabolic Diseases. Biomolecules., 10(9): 1256.

Kent S, Jebb SA, Gray A, Green J, Reeves G, Beral V, Mihaylova B, Cairns BJ. 2019. Body mass index and use and costs of primary care services among women aged 55–79 years in England: a cohort and linked data study. International Journal of Obesity, 43(9): 1839-1848.

Keskin A. 2023. Impact of Polyphenolic Compounds on the MAPK Signaling Pathway against Carcinogenesis. Journal of Clinical Practice and Research, 45(3): 217-221.

Keskin A. 2023. Hücre yaşamı ile ilgili sinyal yolakların düzenlenmesinde diyet polifenollerin rolü Turk J Health S. 4(1): 32-36.

Keskin A, Aci R, Ari M, Duran U. 2023. Cellular senescence, mTOR signaling pathway and polyphenol. International Journal of Advanced Biochemistry Research, 7(1): 01-04.

Keskin A, Aci R. 2022. Investıgatıon of Lipid Profile, Malondialdehyde, Sodium, Potassium, Chloride Levels in Rats with Weight Loss. Türkiye Diyabet ve Obezite Dergisi, 6(1): 10-15.

Kivimäki M, Strandberg T, Pentti J, Nyberg ST, Frank P, Jokela M, Ervasti J, Suominen SB, Vahtera J, Sipilä PN, Lindbohm JV, Ferrie JE. 2022. Body-mass index and risk of obesity-related complex multimorbidity: an observational multicohort study. Lancet Diabetes Endocrinol, 10 (2022): 253-263.

Khoubai FZ, Grosset CF. 2021. DUSP9, a Dual-Specificity Phosphatase with a Key Role in Cell Biology and Human Diseases. Int J Mol Sci. 22(21):11538.

Kwon O, Kim KW, Kim MS. 2016. Leptin signalling pathways in hypothalamic neurons. Cell Mol Life Sci., 73(7): 1457-1477.

Li J, Chen C, Li Y, Matye DJ, Wang Y, Ding WX, Li T. 2017. Inhibition of insulin/PI3K/AKT signaling decreases adipose Sortilin 1 in mice and 3T3-L1 adipocytes. Biochim Biophys Acta Mol Basis Dis., 1863(11): 2924-2933.

Li T, Zhang Z, Kolwicz SC Jr, Abell L, Roe ND, Kim M, Zhou B, Cao Y, Ritterhoff J, Gu H, Raftery D, Sun H, Tian R. 2017. Defective Branched-Chain Amino Acid Catabolism Disrupts Glucose Metabolism and Sensitizes the Heart to Ischemia-Reperfusion Injury. Cell Metab. 25(2): 374-385.

Li Z, Fang X, Yu D. 2021. Transdermal Drug Delivery Systems and Their Use in Obesity Treatment. Int J Mol Sci. 22(23): 12754.

Mackenzie RW, Elliott BT. 2014. Akt/PKB activation and insulin signaling: a novel insulin signaling pathway in the treatment of type 2 diabetes. Diabetes Metab Syndr Obes., 7:55-64.

Müller TD, Blüher M, Tschöp MH, DiMarchi RD. 2022. Anti-obesity drug discovery: advances and challenges. Nature Reviews Drug Discovery, 21(3): 201-223.

Okunogbe A, Nugent R, Spencer G, Ralston J, Wilding J. 2021. Economic impacts of overweight and obesity: current and future estimates for eight countries. BMJ global health, 6(10): e006351.

Pudewell S, Wittich C, Kazemein Jasemi NS, Bazgir F, Ahmadian MR. 2021. Accessory proteins of the RAS-MAPK pathway: moving from the side line to the front line. Commun Biol., 4(1): 696.

Sabio G, Cavanagh-Kyros J, Barrett T, Jung DY, Ko HJ, Ong H, Morel C, Mora A, Reilly J, Kim JK, Davis RJ. 2010. Role of the hypothalamic-pituitary-thyroid axis in metabolic regulation by JNK1. Genes Dev. 24(3): 256-264.

Shen H, Huang X, Zhao Y, Wu D, Xue, K, Yao J, Wang Y, Tang T, Qiu Y. 2022. The Hippo pathway links adipocyte plasticity to adipose tissue fibrosis. Nature Communications, 13(1): 6030.

Sun F, Wang J, Sun Q, Li F, Gao H, Xu L, Zhang J, Sun X, Tian Y, Zhao Q, Shen H, Zhang K, Liu J. 2019. Interleukin-8 promotes integrin β3 upregulation and cell invasion through PI3K/Akt pathway in hepatocellular carcinoma. J Exp Clin Cancer Res. 38(1): 449.

Sun Y, Liu WZ, Liu T, Feng X, Yang N, Zhou HF. 2015. Signaling pathway of MAPK/ERK in cell proliferation, differentiation, migration, senescence and apoptosis. J Recept Signal Transduct Res., 35(6): 600-604.

Trepanowski JF, Kroeger CM, Barnosky A, Klempel MC, Bhutani S, Hoddy KK, Gabel K, Freels S, Rigdon J, Rood J, Ravussin E, Varady KA. 2017. Effect of Alternate-Day Fasting on Weight Loss, Weight Maintenance, and Cardioprotection Among Metabolically Healthy Obese Adults: A Randomized Clinical Trial. JAMA Intern Med. 177(7): 930-938.

Xu Q, Ding H, Li S, Dong S, Li L, Shi B, Zhong M, Zhang G. 2021. Sleeve Gastrectomy Ameliorates Diabetes-Induced Cardiac Hypertrophy Correlates With the MAPK Signaling Pathway. Front Physiol. 12: 785799.

Wang Z, Zhu M, Wang M, Gao Y, Zhang C, Liu S, Qu S, Liu Z, Zhang C. 2021. Integrated Multiomic Analysis Reveals the High-Fat Diet Induced Activation of the MAPK Signaling and Inflammation Associated Metabolic Cascades via Histone Modification in Adipose Tissues. Front Genet. 12: 650863.

Wen X, Zhang B, Wu B, Xiao H, Li Z, Li R, Xu X, Li T. 2022. Signaling pathways in obesity: mechanisms and therapeutic interventions. Signal Transduct Target Ther. 7(1): 298.

Wolfe BM, Kvach E, Eckel RH. 2016. Treatment of Obesity: Weight Loss and Bariatric Surgery. Circ Res. 118(11): 1844-1855.

Zeng X, Du X, Zhang J, Jiang S, Liu J, Xie Y, Shan W, He G, Sun Q, Zhao J. 2018. The essential function of CARD9 in diet-induced inflammation and metabolic disorders in mice. J Cell Mol Med., 22(6): 2993-3004.

Zhang J, Zhou Y, Chen C, Yu F, Wang Y, Gu J, Ma L, Ho G. 2015. ERK1/2 mediates glucose-regulated POMC gene expression in hypothalamic neurons. J Mol Endocrinol., 54(2): 125-135.

REVIEW ARTICLE
Eurasian J Bio Chem Sci, 6(2):114-126, 2023
https://doi.org/10.46239/ejbcs.1379553

EJBCS

Eurasian Journal of Biological and Chemical Sciences

Journal homepage: www.dergipark.org.tr/ejbcs

Sideritis species in challenging against cancer: Cytotoxic, antiproliferative and apoptotic roles on different cancer cells

Onder Yumrutas[1*], Mustafa Pehlivan[2], Pınar Yumrutas[3]

*[1]*University of Adıyaman, Faculty of Medicine, Department of Medical Biology, 02200, Adıyaman-Türkiye*
[2]University of Gaziantep, Faculty of Science and Art, Department of Biology, 27410, Gaziantep-Türkiye
[3]University of Gaziantep, Faculty of Medicine, Department of Respiratory Disease and Cancer Biology, 27410, Gaziantep-Türkiye

*Corresponding author : yumrutasonder@gmail.com
Orcid No: https://orcid.org/0000-0001-9657-8306

Received : 22/10/2023
Accepted : 05/12/2023

Abstract: *Sideritis* species belonging to Lamiaceae are represented by many species worldwide. They exhibit many bioactivities including antioxidant, anticancer, antimicrobial, anti-inflammatory due to their important phytochemicals. Moreover, they are thought to be important resources in the fight against cancer, especially due to their cytotoxic effects on cancer cells. Many studies on various cancer cells have reported cytotoxic, antiproliferative and apoptotic properties of *Sideritis* species. In this study, the phytochemical contents of *Sideritis* species growing in different geographies and their cytotoxic, antiproliferative and apoptotic effects in the fight against cancer were discussed in detail.

Keywords: *Sideritis*, anticancer, antiproliferation, apoptosis, bioactivity

1. Introduction

Cancer is among the diseases that cause the death of many people today. Factors such as smoking, an unhealthy diet, high alcohol consumption, physical inactivity, and excess body weight are among the main factors in the emergence of cancer (Islami et al. 2018). According to research conducted in recent years, lung cancer ranks first among the most common types of cancer, although the order may vary between men and women. However, cancer types such as breast, prostate, colon, cervix and thyroid are also quite common. (Siegel et al. 2023). Many patients diagnosed with cancer die and it is thought that these deaths will increase in the future.

There are different methods in the treatment of cancer such as chemotherapy, radiotherapy, immunotherapy and surgery (Huang et al. 2017). There are compounds of synthetic and natural origin used in chemotherapy. However, especially synthetic-based chemicals can cause side effects such as anaphylaxis, cytopenias (including leukopenia and neutropenia, thrombocytopenia, and anaemia), hepatotoxicity, ototoxicity, cardiotoxicity, nausea and vomiting, diarrhea, mucositis, stomatitis, pain, alopecia, anorexia, cachexia, and asthenia (Oun et al. 2018). Therefore, many studies have focused on compounds with fewer side effects isolated from natural sources such as plants. Agents such as vincristine, vinblastine, vindesine, vinorelbine (Vinca Alkaloids), paclitaxel and docetaxel (Taxanes) and epothilones are some of plant-derived agents used in the chemotherapy treatment of cancer (Marzo and Naval 2013). Paclitaxel (taxol) is a compound isolated from *Taxus brevifolia* and is used clinically for the treatment of cancer (Karuppusamy and Pullaiah 2022). The number of chemicals isolated from plants such as taxol is increasing but still remains insufficient.

There are reports in studies conducted with members of many plant families showing the interactions of these plants with cancer cells. Plant extracts and compounds have been shown to suppress events such as cell proliferation, invasion and metastasis by activating the cell death pathway and break acquired drug resistance (Ege et al. 2020; Cocelli et al. 2021, Yumrutas and Yumrutas, 2022, Yumrutas and Bozgeyik, 2023). Anticancer studies using plants generally focus on compounds such as alkaloids, terpenoids and phenolics isolated from them (Jiang and Hu, 2009; Rabi and Bishayee 2009; Carocho and Ferreira 2013). One of the most well-known plant families screened for these substances is Lamiaceae. It is represented by many species around the world, and species belonging to this family have been used since ancient times. The sage is among the most well-known in this family and also many species are also consumed as spices and tea. Among these species, *Sideritis*, which has many chemical compounds and has high pharmacological effects due to these compounds, is quite

remarkable. *Sideritis* genus, known as "mountain tea" in Turkey, has important ethnobotanical characteristics. Compounds such as phenolic and terpenoid contained in it play a role in exhibiting important biological activities, especially antioxidant. In this review, the distribution of *Sideritis* species, their genus characteristics, their pharmacologically valuable phytochemicals, their bioactivities and especially their possible effects on cancer cells are discussed in detail.

2. Characteristics of *Sideritis* species

From past to present, people have used plants for nutrition, shelter, warmth, healing their wounds and treating their diseases. It has been determined that there were 250 plants that people used in treatments in 5000 BC. Hittites, Egyptians, Sumerians, Assyrians and Mesopotamians have used plants for treatment for years. Over time, the use of synthetic drugs has led to a decrease in the use of medicinal aromatic plants. After the 1900s, it has discovered the side effects of synthetic drugs, and therefore the demand for natural products has increased (Göktaş and Gıdık 2019). With developing of modern science, it has been shown that the phytotherapeutic effects of plants are related to biologically active compounds formed through secondary metabolites (Kralova and Jampilek 2021). Medicinal plants, which have economic and medicinal value, are gaining increasing importance and providing increasing benefits to people (Chen et al. 2016).

It has been reported that the medical plants have been used in treatment of diseases including cardiovascular diseases, endocrine system disorders such as diabetes and goiter, prostate, kidney and urinary tract inflammations, lung diseases such as bronchitis, asthma and breath-opening, in upper respiratory tract diseases such as flu, cold, sore throat and cough, in stomach problems such as reflux, ulcers and gastritis, in intestinal diseases such as abdominal pain, constipation and diarrhea, in dermatological disorders, joint pains, arthritis, muscle and joint diseases such as rheumatism, Alzheimer's disease (AD), Parkinson's disease (PD) and cancer (Baytop 1999; Karousou and Deirmentzoglou 2011; Arıtuluk and Ezer 2012; Chiarini et al. 2013; Ozturk et al. 2013; Melikoğlu et al. 2015; Gregory et al. 2021; Yin et al. 2021).

Moreover, in recent years, there has been a global trend towards the use of natural substances. Plants as a source of antioxidants and functional ingredients are used by the food industry to adapt to the consumer market (Dziki et al. 2014). According to available statistics, medicinal plants have attracted more and more attention in recent years. While the market share of medicinal plants in developing countries is increasing, it is high in developed western countries such as Europe (He et al. 2018) In traditional and ethnomedicine, medicinal plants have long been recognized as the basis of materials used in therapeutic practices worldwide. The remarkable healing effect of traditional Chinese medicine using herbal mixtures, especially during the Corona Virus Disease 2019 (COVID-19) epidemic, has attracted great attention worldwide (Zhang and Wang 2023). Lamiaceae is one of the most important families containing a wide variety of plants with biological and medicinal applications (Uritu et al. 2018). It consists of approximately 245 genera and 7886 species. They are distributed almost all over the world, except for the cold polar regions (Abdelhalim and Hanrahan, 2021). Some of these plants and their secondary metabolites are highly appreciated in the food, agricultural, cosmetic and pharmacological industries (Trivellini et al. 2016). Some of the largest genuses are *Salvia* (900), *Scutellaria* (360), *Stachys* (300), *Plectranthus* (300), *Hyptis* (280), *Thymus* (220) and *Nepeta* (200). Many of these plants are used as spices and vegetables (Tamokou et al. 2017).

The Lamiaceae species are distributed almost all over the world, especially in tropical and temperate regions. The Lamiaceae is known for its numerous species with medicinal properties and has a high content of essential oils, polyphenolic compounds, and terpenoids with important biological activities. Numerous studies have been reported on different species of the Lamiaceae and their effects on memory, anxiety, depression and sleep disorders (Abdelhalim and Hanrahan 2021).

Although the *Sideritis* genus is distributed throughout the world, especially in the Mediterranean basin, it is represented by more than 150 species in a wide area from the Bahamas to China, from Germany to Morocco (Öke 2006).

The therapeutic use of *Sideritis* species was first mentioned in Dioscorides' book written in the 1st century; Mentioned in "*De Materia Medica*". The genus *Sideritis* L. takes its name from the Greek word "sideros" (iron) and has been used since ancient times to heal wounds caused by weapons such as swords. Folklorically, decoction or infusion prepared with the aerial parts of *Sideritis* species has been used orally or topically for centuries due to its anti-inflammatory, antiulcerogenic, digestive, antispasmodic, anticonvulsant, antimicrobial, analgesic and wound healing properties (Gonzales-Burgos et al. 2011; Yeşilada et al. 1995).

One of the two main gene centers of *Sideritis* genus is Turkey and therefore the endemism rate is 79.5%. Many medicinal properties have been determined in the extracts obtained from *Sideritis* species, and it is known that interest in the plant has increased due to these properties. In particular, its antistress, antibacterial, insecticidal, antiulcer, analgesic and anti-inflammatory effects have been detected. It attracts special attention due to its antioxidant properties (Arabacı et al. 2014).

3. Overview of biological activities of *Sideritis* species

When the biological activities of *Sideritis* species are evaluated, the first thing that stands out is their strong antioxidant activity. It is thought that the strong phenolic compounds found in its structure are responsible for these activities. In the studies conducted, they exhibited significant activities especially in tests such as DDPH, ABTS and power reducing. Erkan et al. (2011) reported that *S. congesta* and *S. arguta* species showed strong DPPH and ABTS free radical scavenging activities due to their important cinnamic acid and flavonoid derivatives. In a different study, *S. raeseri spp. raeseri* has been shown to reduce the arterial pressure and heart rate at doses of 24.31±3.87 mg/kg and 88.14±7.51 mg/kg (EC_{50}). (Kitic et

al. 2012). Additionally, in the same study, *S. raeseri* (0.005-1.5 mg/ml) showed a vasodilator effect in aortic preparations and caused a decrease in chronotropic and inotropic activity in rat atria. Goulas at al. (2014) reported that the extract obtained from *S. syriaca* by the decoction method showed a remarkable antimicrobial activity against Staphylococcus aureus. It was determined that *S. scardica* methanol extract significantly reduced total tau, activation of GSK3, ERK1 and/or ERK2 kinases of tau, as well as tau hyperphosphorylation in the in vitro Alzheimer's test model with SH-SY5Y and PC12 cells (Chalatsa et al. 2018). In another study (Ververis et al. 2023), it was shown that diethylether, ethylacetate and butanol fractions of *S. scardica*, which were determined to be very rich in phenolics, protected the viability of Aβ25–35-treated SH-SY5Y human neuroblastoma cells. In a different study, anti-aging activity of *S. scardica* was demonstrated through collagenase inhibition, prevention of advanced glycation end product (AGE) formation, antioxidative and antiallergic activities, and ultraviolet B (UVB)-induced matrix metalloproteinase-1 (MMP-1) expression inhibition (Sato et al.2022). Hernandez-Perez et al. (2002) showed that *S. lotsyi* var *mascaensis* ethanol and chloroform fractions had a significant topical anti-inflammatory and analgesic effect in carrageenan and 12-o-tetradecanoyl-phorbol-acetate-induced paw and ear oedema and in an acetic acid-induced pain model in mice. In another study, acetone extract of *S. condensanta* exhibited insecticidal/acaricidal activity against *Bemicia tabaci, Lasioderma serricorne* and *Sitophilus granarius*, while linearol isolated from *Sideritis* condensanta exhibited activity against *Bemicia tabaci, Lasioderma serricorne, Tetranychus urticae* (Kilic et al. 2009). Deveci et al. (2019) reported that while the urease and choline esterase (AChE and BChe) inhibitory activities were detected in hexane, acetone and methanol extracts of *S. albiflora*, tysinase inhibitory activity was shown only in acetone and methanol extracts. Küpeli et al (2007) reported that *S. ozturkii* acetone extract and ozturkoside C showed strong antinociceptive activity in the p-Benzoquinone-induced abdominal constriction test and a strong anti-inflammatory effect in the Carrageenan-induced hind paw edema model. Although the biological activities of some *Sideritis* species have been mentioned above, other information for comparison is given in Table

4. Cytotoxic and antiproliferative effects of *Sideritis* species against cancer cells

The first method used to determine the anticancer activities of an extract or compound is usually cytotoxicity tests. In these tests, cells are grown in vitro and then exposed to the agent used. Finally, the cells are stained with chemicals such as MTT (3- (4,5-dimethylthiazol-2-yl)-2,5-diphenyl-2H-tetrazolium bromide), SRB (sulforhodamine B), XTT ((2,3-bis-(2-methoxy-4-nitro-5-sulfophenyl)-2H-tetrazolium-5-carboxanilide), BrdU (Bromodeoxyuridine) and the cells are measured spectrophotometrically to measure cell viability and proliferation. There are many studies showing the cytotoxic activity of extracts and compounds obtained from medicinal plants on cancer cells. Among these plants, *Sideritis* genus has great importance. Previous studies have shown the cytotoxic effects of *Sideritis* species growing in different geographies on different cancer cells. In the light of the data obtained in the studies, it can be said that *Sideritis* species can significantly inhibit the survival and proliferation of cancer cells. Table 2 shows information about the possible cytotoxic effects of *Sideritis* species on cancer cells.

5. Apoptotic effects of *Sideritis* species against cancer cells

It has been reported in the above studies that the viability and proliferation of cancer cells are significantly reduced by extracts and agents obtained from *Sideritis* species. Although an extract or compound has an antiproliferative and cytotoxic effect, it is not sufficient to evaluate anticancer activity by cytotoxic activity alone. Some of the main reasons for this are that cells can also die from factors other than the extract applied under in vitro conditions. Among these, cells may die spontaneously due to stress conditions such as the high number of passages, storage conditions, quality and content of the media used, sensitivity of the researcher, infection of the cells, and errors that may occur in the devices used in cell incubation. Therefore, it is necessary to use some molecular markers in addition to the cytotoxic effects of an extract or compound whose anticancer activity is tested. One of the most used tests for this is AnnexinV and propodium iodide (alternative stains such as 7ADD are used). The basic principles here are to stain phosphotidylserine, which moves from the cell's inner membrane to its outer membrane when a cell undergoes apoptosis, with fluorescent agents and to determine the rate of apoptosis with cell counting devices or fluorescent microscopes (Van Engeland et al. 1998).

Apoptosis is one of many known death pathways and is a programmed death pathway (Savitskaya and Onishchenko, 2015). Under normal conditions, cells divide, differentiate and die throughout their lives. Apoptosis plays an important role in this process. Irregularities in apoptosis may cause important diseases, especially cancer. Cells that enter the cancer pathway continue to survive by suppressing this pathway and escaping the immune system. As a result, during apoptosis, swelling of the cell membrane, condensation of chromosomes, fragmentation of DNA and small vesicles of the cell membrane, cytoplasm and organelles are observed in late apoptosis (Poon et al. 2014). Apoptosis, which can be grouped as intrinsic and extrinsic, is controlled by important enzymes. Both apoptotic and anti-apoptotic proteins play a role in both apoptotic pathways. Depending on the levels of these proteins, the relevant apoptotic pathway is activated in the cells. Apoptotic proteins such as Bax, Noxa, and Puma serve as proteins that initiate apoptosis. Proteins such as Bcl-2, Mcl1, Bcl-xl are found in the mitochondrial membrane and suppress mitochondrial apoptosis.

Table 1. Overview to the biological activities and phytochemicals of *Sideritis* species

No	Species	Activities	Extracts	Compounds	References
1	*Sideritis brevibracteata*	DPPH free radical scavenging activity, reducing power (CUPRAC) assay, β-carotene antioxidant tests, no anticholinesterase activity, weak butyryl-cholinesterase activity	Acetone, methanol, essential oil	Caryophyllene, germacrene-D, and α-cadinene, quercetagetin-3,6-dimethylether and chlorogenic acid, siderol, linearol, eubotriol, 7-acetyl sideroxol	Sagir et al. 2017
2	*Sideritis sipylea*	DPPH free radical scavenging activity, tyrosinase and elastase inhibitory activity	Methanol, ethyl acetate, acetone, dichloromethane, essential oil	α-pinene, β-pinene, sabinene, verbenol, and borneol, β-caryophyllene and caryophyllene oxide, geranyl linalool, Siderol, sideridiol, and 7-epicandicandiol, echinacoside, forsythoside B, verbascoside,samioside,isoverbascoside, allysonoside, and leucoseptosideA,4-O-methylisoscutellarein 7-O-allosyl- (1→2)-[6"-O-acetyl]-glucoside	Axiotis et al. 2020
3	*Sideritis congesta*	DPPH free radical scavenging and ABTS free radical scavenging activities	Acid hydrolysis of methanol, ethyl acetate, acetone extracts	Rosmarinic acid, ferulic acid, caffeic acid, p-coumaric acid, chlorogenic acid, apigenin, myricetin, kaempferol	Erkan et al. 2011
4	*Sideritis arguta*	DPPH free radical scavenging and ABTS free radical scavenging activities	Acid hydrolysis of methanol, ethyl acetate, acetone extracts	Rosmarinic acid, ferulic acid, caffeic acid, p-coumaric acid, chlorogenic acid, quercetin apigenin, myricetin, kaempferol	Erkan et al. 2011
5	*Sideritis raeseri spp. Raeseri*	Hypotensive, vasorelaxant and cardiodepressant activities	Ethanol		Kitic et al. ,2012
6	*Sideritis syriaca*	Antioxidant and antimicrobial activity	Decoction	Hypoelatine, isoscutellarein diglucosides, verbascoside, martinoside, lavandulifolioside ve klorojenik asit	Goulas et al. 2014

7	*Sideritis scardica*	Anti-Alzheimer's activity	Methanol	Verbascoside, martynoside, echinacoside, lavandulofolioside, allysonoside, leucosceptoside, forsythoside, samioside, scutellarein, isoscutellarein, hypolaetin, and apigenin	Chalatsa et al. 2018
8	*Sideritis erytrantha subsp. erytrantha*	Antimicrobial activity	Essential oil	α-pinene, sabinene, B-caryophyllene, 1-caryophyllene, alfa-bisabolol	Altundag et al 2011
9	*Sideritis lotsyi var. mascaensis*	Analgesic and anti-inflammatory and no antimicrobial activity of the fractions against tested microorganisms	Water and chloroform fractions of ethanol extract		Hernandez-perez et al. 2002
10	*Sideritis brevibracteata*	Anti-inflammatory, antinociceptive, antioxidant and aldose reductase inhibitory activities	Methanol crude extract, chloroform, n-butanol and water fractions	Hypolaetin, Isoscutellarein, 30-Hydroxy-40-O-methylisoscutellarein, Verbascoside	Güvenç et al. 2010
11	*Sideritis condensata*	Insecticidal/acaricidal activity	Acetone	Linearol, isolinearol, siderol, sideridiol, sideroxol, 7-acetylsideroxol,and candol B	Kilic et al. 2009
12	*Sideritis albiflora*	Urease, tyrosinase and cholinesterase inhibitory activity	n-hexane, acetone, and methanol	Gallic acid, caffeic acid, p-coumaric acid, ferulic acid, trans 2-hydrocxycinnamic acid, rosmarinic acid, transcinnamic acid	Deveci et al. 2019
13	*Sideritis leptoclada*	Urease, tyrosinase and cholinesterase inhibitory activity	n-hexane, acetone, and methanol	Fumaric acid, caffeic acid, 2,4-Dihydroxy benzoic acid, ferulic acid, trans-2-Hydroxycinnamic acid, rosmarinic acid, transcinnamic acid	Deveci et al. 2019
14	*Sideritis erythrantha* var. *erythrantha* and *Sideritis erythrantha* var. *cedretorum*	Antioxidant and antimicrobial activities	Essential oil	α-pinene, β-Caryophyllene, β-pinene, sabinene, limonene	Köse et al. 2010

15	*Sideritis stritca*	Antioxidant, anticholinesterase, and anti-tyrosinase activities	Methanol and water	Fumaric acid, gallic acid, protocatechuic acid, p-hydroxybenzoic acid, catechin hydrate, 6,7-dihydroxy coumarin, 2,4-dihydroxybenzoic acid, caffeic acid, vanillin, p-coumaric acid, ferulic acid, coumarins, trans-2-hydroxycinnamic acid, ellagic acid, rosmarinic acid, and trans-cinnamic acid	Deveci et al. 2018
16	*Sideritis italica*	Antioxidant and antibacterial activities	Essential oil	Kaur-15-ene, b-Cubebene, Palmitic acid, p-Metoxyacetophenone	Basile et al. 2006
17	*Sideritis libanotica* ssp. *linearis*	Antioxidant activity	Methanol	(3' -O-methylhypolaetin 7-O-[6"- O-acetyl-B-D-allopyranosyl-(1->2)]-6"-O-acetyl-B-D-glucopyranoside, sideridiol	Demirtas et al. 2009
18	*Sideritis germanicopolitana*	In vitro inhibitory effects on lipoxygenase (LOX), acetylcholinesterase (AChE) and butyrylcholinesterase (BChE) enzymes associated with inflammatory and Alzheimer's diseases	Methanol	5-allosyloxy-aucubine, melittoside, ajugol, five phenylethanoid glycosides, verbascoside, martynoside, leucoseptoside A, amalboside, decaffeoyl-verbascoside, four flavonoids, xanthomicrol, isoscutellarein 7-O-[6'''-O-acetyl-b-allopyranosyl-(1->2)]-b- glucopyranoside, 4'-O-methylisoscutellarein 7-O-[6'''-O-acetyl-b-allopyranosyl-(1->2)]- b-glucopyranoside, 3'-hydroxy-4'-O-methylisoscutellarein 7-O- [6'''-O-acetyl-b-allopyranosyl-(1->2)]-b- glucopyranoside, dehydrodiconiferylalcohol 4-O-b-D-glucopyranose, pinoresinol 4'-O-b-glucopyranoside	Kırmızıpekmez et al. 2021
19	*Sideritis ozturkii*	Anti-inflammatory and antinociceptive activities	Acetone	Ozturkoside A, Ozturkoside B, Ozturkoside C	Küpeli et al. 2007
20	*Sideritis perfoliata*	Antiwrinkle, Hyper/Hypo-Pigmentation, Anti-Acne, Antimycobacterial Activity	Ethanol, essential oil	β-Phellandrene, α-pinene, β-pinene, Sabinene	Lall et al. 2019
21	*Sideritis raeseri*	Antioxidant/antiradical, antimicrobial activity	Essential oil	Geranyl-p-cymene, geranyl-γ-terpinene and geranyl-linalool	Mitropoulou et al. 2020

22	*Sideritis scardica*	Neuroprotective Activity against Alzheimer' disease	Petroleum ether, dichloromethane, methanol extracts and their fractions (diethyl ether, ethyl acetate, butanol)	Apigenin, myricetin-3-galactoside, and ellagic acid, Quercetin-3-O-rhamnoside, Myricetin-3-galactoside, vanillic acid, 4-hydroxybenzoic acid, caffeic acid, Luteolin-7-O-glucoside	Ververis et al. 2023
23	*Sideritis scardica*	Anti-skin Aging Activity	Ethanol	Isoscutellarein,4′-O-methylhypolaetin,4′-O-methylisoscutellarein	Sato et al. 2022
24	*Sidertis perfoliara*	Scocidal activity	Methanol	Fumaric acid, syringiic acid, caffeic acid, luteolin	Çelik et al. 2021
25	*Sideritis spylea*	Antioxidant activity	Water, acetone, ethanol, methanol		Nakiboglu et al. 2007
26	*Sideritis libanotica* subsp. *linearis*	Antimicrobial, antioxidant and anticholinesterase activities	Petroleum ether, acetone, methanol, water	Quinic acid, malic acid, chlorogenic acid, rosmarinic acid, coumarin, naringenin, luteolin, apigenin, kaempferol, rhamnetin	Ertas and Yener, 2020
27	*Stachys thirkei*	Antimicrobial, antioxidant and anticholinesterase activities	Petroleum ether, acetone, methanol, water	Quinic acid, malic acid, tannic acid, chlorogenic acid, rosmarinic acid, coumarin, naringenin, luteolin, apigenin	Ertas and Yener, 2020
28	*Sideritis ozturkii, Sideritis caesarea*	Antimicrobial and antioxidant activity	Methanol		Sagdic et al. 2008
29	*Sideritis raeseri* spp. *Raeseri*	Spasmolytic Activity	Ethanol		Brankovic et al. 2011
30	*Sideritis ozturkii*	Antioxidant, enzyme inhibitory (AChE inhibition, BChE inhibition, Tyrosinase inhibition, Amylase inhibition	Methanol, ethyl acetate, water	Chlorogenic acid, quercetin-3-O-glucoside, quinic acid, loganic acid, apigenin, gallic acid, ferulic acid, naringenin-7-O-glucoside, apigenin-7-O-glucoside	Zengin et al. 2019

Table 2. Anticancer activities, extracts and compounds of *Sideritis* species

No	*Sideritis* sp.	Compounds	Ekstract	Cancer cells	Methods	Activity	referances
1	*Sideritis leptoclada*	Quinic acid, malic acid, chlorogenic acid	Ethanol, ethyl acetate	Malignant melanoma cancer (HT-144)	MTT	Cells were significantly inhibited	Aydoğmuş-Öztürk et al. 2018
2	*Sideritis euboea*	2-(p-hydroxyphenyl)ethylstearate, β-sitosterol, stigmasterol, campesterol, ursolic acid, ursolic acid, eubol, eubotriol, 7-epicandicandiol, xanthomicrol, penduletin	Dichloromethane	DLD1, HeLa, A549)	MTT	Siderol exhibited potent cytotoxic activities	Tomou et al. 2020
3	*Sideritis trojana*	10-O-(E)-feruloylmelittoside, melittoside, 10-O-(E)-p-coumaroylmelittoside, stachysosides E. verbascoside, isoacteoside, lamalboside, leonoside A, isolavandulifolioside, isoscutellarein 7-O-[6‴-O-acetyl-β-allopyranosyl-(1→2)]-β-gluco pyranoside, 4′-O-methyisoscutellarein 7-O-[6‴-O-acetyl-β-allopyranosyl-(1→2)]-β-glucopyr anoside, 3′-hydroxy-4′-O-methyisoscutellarein 7-O-[6‴-O-acetyl-β-allopyranosyl-(1→2)]-β glucopyranoside	Methanol	PC3 prostate cancer	MTT	Only verbascoside showed cytotoxic activity	Kirmizibekmez et al. 2012

4	*Sideritis syriaca*	Gallic acid (GA), Protocatechuic acid (PCA), p-hydroxybenzoic acid (p-HA), cafeic acid (CA), chlorogenic acid (CHA), p-coumaric acid (p-Cou), ferulic acid (FA), o-coumaric acid (o-Cou), rosmarinic acid (RA) and trans-cinnamic acid	Methanol	Breast cancer cell line (MCF-7)	MTT	It exhibited strong cytotoxic activity at 100 and 250 µg/mL	Yumrutas et al. 2015
5	*Sideritis perfoliata*	Quercetin, resveratrol, alizarin, vanillic acid, caffeic acid, hydroxycinnamic acid, hydroxybenzoic acid, salicylic acid, acetohyroxamic acid	Methanol	Human cervical cancer cell lines (HeLa)	MTT	It exhibited dose-dependent activity of 25-200 µg/mL	Cocelli et al. 2021
6	*Sideritis montana*	Sideritins A and B. pomiferin E, 9α,13α-epi-dioxyabiet-8(14)-en-18-ol, paulownin, 6-methoxysakuranetin, 3-oxo-α-ionol and 4-allyl-2,6-dimethoxyphenol glucoside	Methanol	Human cervical cancer cell lines (HeLa, SiHa, and C33A)	MTT	While pomiferin e exhibited cytotoxic activity in HeLa cells, 6-methoxysakuranetin showed strong activity in C33A cells.	Tóth et al. 2017
7	*Sideritis libanotica* subsp. *linearis*		Methanol	Vero, HeLa and C6	BrdU	Extract showed cytotoxic activity on all cells tested	Demirtas et al 2009
8	*Sideritis perfoliata*		Ethanol	Human liver carcinoma (HepG2) and human cervical cancer (HeLa), non-cancerous Vero and HaCat cell	XTT	It showed moderate cytotoxic activity against HepG2 cells and antiproliferation activity against HeLa cells at high doses. Moderately toxic to Vero and HaCat cells at very high doses	Lall et al. 2019
9	*Sideritis pullulans*	Sideritone A, Sideritone B, Sideripullol A, Sideripullol B, Sideripullol C, Sideripullol D, *Sideriti*side A, *Sideriti*side B,	n-hexane, methanol	HeLa, PC3	MTT	All compounds tested showed cytotoxic activity at doses higher than 100 µM.	Faiella et al. 2014
10	*Sideritis raeseri*	Geranyl-p-cymene, geranyl-γ-terpinene and geranyl-linalool	Essential oil	Human immortalized keratinocyte (HaCat), human melananoma A375, human colon adenosarcoma Caco2, and human prostate carcinoma cell lines PC3 and DU145	MTT	It exhibited activity against all cells at doses of 0.114-0.216 mg/ml (EC50)	Mitropoulou et al. 2020

11	*Sideritis libanotica* subsp. *linearis*	Quinic acid, malic acid, chlorogenic acid, rosmarinic acid, coumarin, naringenin, luteolin, apigenin, kaempferol, rhamnetin	Petroleum ether, acetone, methanol, water	Human lung cancer cell line (A549)	MTT	Moderately toxic	Ertas and Yener 2020
12	*Stachys thirkei*	Quinic acid, malic acid, tannic acid, chlorogenic acid, rosmarinic acid, coumarin, naringenin, luteolin, apigenin	Petroleum ether, acetone, methanol, water	Human lung cancer cell line (A549)	MTT	Moderately toxic	Ertas and Yener 2020
13	*Sideritis cypria*	Melittoside, Geniposidic acid, Ajugoside, 8-epi-Loganic acid, Linearol, sidol, Apigenin, Acteoside, Leucosceptoside A, Lavandulifolioside, Lamalboside, Leonoside A, Chlorogenic acid,	Methanol and its fractions	Breast cancer cell line (MDA-MB231)	MTT	Methanol extract did not show cytotoxic activity. The isolated apigenin derivatives showed strong cytotoxic activity.	Lytra et al. 2021
14	*Sideritis niveotomentosa*	Propyl gallate, 1-Monolinoleoylglycerol trimethylsilyl ether,	Methanol, acetone	DLD1, HL60 and ARH77 cell lines	MTT	It showed strong cytotoxic effect at low IC50 against ARH77 cells, leaf extracts were cytotoxic in HL60 cells.	Sezer and Uysal 2021
15	*Sideritis perfoliata*	α-Humulene, trans-Caryophyllene, β-Phellandrene, Sabinene, α-pinene, β-pinene	Essential oil	Amelanotic melanoma (C32), renal cell adenocarcinoma (ACHN), hormone-dependent prostate carcinoma (LNCaP), and breast cancer (MCF-7) cell lines	SRB (protein-staining sulforodamine B)	It showed strong cytotoxic activity at doses of 100, 200, 400 µg/mL	Loizzo et al. 2007
16	*Sideritis scardica*		Hydro ethanol	Colon cancer (mouse colon adenocarcinoma cell line Colon 26)	WST-1	It showed strong cytotoxic activity at doses of 400 and 600 µg/mL	Dobrikova et al. 2023
17	*Sideritis ozturkii*	Chlorogenic acid, quercetin-3-O-glucoside, Quinic acid, loganic acid, Apigenin, gallic acid, ferulic acid, Naringenin-7-O-glucoside, Apigenin-7-O-glucoside	Water, ethyl acetate and methanol	Breast cancer cell line (MDA-MB231)	MTT	Methanol and ethyl acetate extracts showed strong cytotoxic activity	Zengin et al. 2019

When intrinsic apoptosis is stimulated, apoptotic proteins overwhelm antiapoptotic proteins, causing pores to open in the mitocondrial membrane and the release of factors such as cytochrome C, apoptosis initiating factor, smac/diablo (apoptosis inhibitor), OMI/HtrA2 (apoptosis inhibitor), endonuclease G from mitocondria to the cytosol. Then, DNA fragmentation occurs with the activation of stocromC-APAF1-caspase9 and finally with the activation of caspase3 (Savitskaya and Onishchenko, 2015 In the extrinsic apoptotic pathway, receptors and ligands on the cell membrane are involved. As a result of the binding of death ligands such as Tnf-alpha, FasL, TRAIL to Fas and TNF receptors, the death domain (DISC) located in the membrane becomes active and caspase 8 is activated. Caspase 8 either activates Bid and thereby initiates mitochondrial apoptosis or directly activates caspase 3. Caspase 3 activates the caspase 3 CAD enzyme, which is activated in both apoptotic pathways, and breaks DNA into short fragments (Savitskaya and Onishchenko 2015; Larsen and Sorensen 2017).

One of the most sought-after features in the fight against cancer is that the agents tested for anticancer activity selectively trigger apoptosis in cancer cells and have no side effects or weak effects on normal cells. Therefore, compounds obtained from plants are very valuable due to both their suppressive effects on cancer cells and their low side effects on normal cells. There are many studies showing that chemicals obtained from different plants induce apoptosis (Yumrutas et al. 2018; Cocelli et al. 2021). However, the number of studies showing the apoptotic effect of *Sideritis* species is limited. Aydoğmuş-Öztürk et al. (2018) showed that *S. leptoclada* ethanol extract caused an increase in the level of a cytokine such as TNF-alpha, which plays a role in immunity, inflammation, cell differentiation, control of cell proliferation and apoptosis. It has also been reported that ROS content increases in HT-144 melanoma cells due to the increase in TNF-alpha level and thus induction of apoptosis. Sezer and Uysal (2018) showed that as a result of exposing DLD-1 human colon cancer cells to *S. ozturkii* methanol and water extracts, the expression of the pro-apoptotic protein BAX and APAF gene increased significantly and the level of the anti-apoptotic gene BCL-2 decreased. In another study, after of the application of *S.* ozturkii ethyl acetate and methanol extracts (IC_{50} at doses of 65.36 µg/mL and 32.15 µg/mL) on breast cancer cell line, it was determined that the proliferation of the cells decreased depending on dose and time. However, only ethyl acetate extract has been shown to increase Bax expression and decrease Bcl-2 expression (Zengin et al. 2019). Moreover, Cocelli et al (2021) showed that *S. perfoliata* methanol extracts induced apoptosis in HeLa cancer cells at a dose of 200 µg/mL. It has been shown that BAX, APAF and Caspase3 mRNA levels increase after application of flower and leaf acetone and methanol extracts of *S. niveotomentosa* to DLD1, HL60 and ARH77 cells (Sezer and Uysal, 2021). Considering the literature examples mentioned above, it can be said that different extract groups of *Sideritis* species can induce apoptosis in different cancer cells. Although some extracts inhibit the survival and proliferation of cancer cells, they cannot induce apoptosis and therefore it should not be ignored that other death pathways may be activated. However, markers of both apoptotic and other death pathways need to be examined molecularly. Almost all of the studies mentioned here are cell-based in vitro studies, and most of the results of these studies have not been supported in vivo. Therefore, considering the phytochemicals of *Sideritis* species, more comprehensive apoptotic studies including animal experiments are needed.

6. Conclusion

In this review, the biological activities of *Sideritis* species and the phytochemicals such as phenolics, terpenoids and alkaloids that may be responsible for these activities are discussed. Many of *Sideritis* species have been shown to significantly reduce the viability of cancer cells and inhibit their proliferation. In addition to these effects, polar, semipolar and non-polar extracts of these species have been proven to induce apoptosis. Moreover, as a recommendation, it is thought that the anticancer activities of *Sideritis* species can be better understood by testing the effects of these species on death pathways such as ferroptosis, autophagy, necroptosis, as well as their metastasis and invasion suppressor properties in vitro and in vivo.

Authors' contributions: All authors contributed equally to the writing of this review

Conflict of interest disclosure: There is no conflict of interest between the authors

References

Abdelhalim A, Hanrahan J. 2021. Chapter 7 - Biologically active compounds from Lamiaceae family: Central nervous system effects. Stud Nat Prod Chem. 8: 255-315.

Altundag S, Aslim BELMA, Ozturk S. 2011. In vitro Antimicrobial Activities of Essential Oils from Origanum minutiflorum and *Sideritis erytrantha* subsp. *erytrantha* on Phytopathogenic Bacteria. J Essent Oil Res. *23:* 4-8.

Arıtuluk ZC, Ezer N. 2012. Halk arasında diyabete karşı kullanılan bitkiler Türkiye-II. HUJPHARM. 2:179- 208.

Axiotis E, Petrakis EA, Halabalaki M, Mitakou S. 2020. Phytochemical profile and biological activity of endemic *Sideritis sipylea* Boiss. in North Aegean Greek islands. Molecules. *25:* 2022.

Aydoğmuş-Öztürk F, Günaydin K, Öztürk M, Jahan H, Duru ME, Choudhary MI. 2018. Effect of *Sideritis leptoclada* against HT-144 human malignant melanoma. Melanoma Res. *28.* 502-509.

Basile A, Senatore F, Gargano R, Sorbo S, Del Pezzo M, Lavitola A, Ritieni A, Bruno M, Spatuzzi D, Rigano D, Vuotto ML. 2006. Antibacterial and antioxidant activities in *Sideritis italica* (Miller) Greuter et Burdet essential oils. J Ethnopharmacol. 107: 240-248.

Baytop T. 1999. *Türkiye'de bitkiler ile tedavi (Geçmişte ve Bugün)*. İstanbul: Nobel Tıp Kitabevi.

Brankovic S, Kitic D, Radenkovic M, Veljkovic S, Jankovic T, Savikin K, Zdunic G. 2011. Spasmolytic activity of the ethanol extract of *Sideritis raeseri* spp. *raeseri* Boiss. & Heldr. on the isolated rat ileum contractions. J Med Food. *14.* 495-498.

Carocho M, CFR Ferreira I. 2013. The role of phenolic compounds in the fight against cancer–a review. Anti-Cancer Agents Med Chem. 13:1236-1258.

Çelik T, Önderci M, Pehlivan M, Yumrutaş Ö, Üçkardeş, F. 2021. In vitro scolicidal effects of *Sideritis perfoliata* extract against Echinococcus granulosus. Int J Clin Prat. 75*:* e14498.

Chalatsa I, Arvanitis DA, Mikropoulou EV, Giagini A, Papadopoulou-Daifoti Z, Aligiannis N, halabalaki M, Tsarbopoulos A, Skaltsounis LA, Sanoudou D. 2018. Beneficial effects of *Sideritis scardica* and Cichorium spinosum against amyloidogenic pathway and tau misprocessing in Alzheimer's disease neuronal cell culture models. J Alzheimer's Dis. 64: 787-800.

Chen SL, Yu H, Luo HM, Wu Q, Li CF, Steinmetz A. 2016. Conservation and sustainable use of medicinal plants: problems, progress, and prospects. Chin Med. 11: 1-10.

Chiarini A, Micucci M, Malaguti M, Budriesi R, Ioan P, Lenzi M, Fimognari C, Gallina Toschi T, Comandini P, Hrelia S. 2013. Sweet chestnut (*Castanea sativa* Mill.) bark extract: ardiovascular activity and myocyte protection against oxidative damage. Oxid Med Cell Longev. 471790.

Cocelli G, Pehlivan M, Yumrutas O. 2021. *Sideritis perfoliata* inhibits cell proliferation, induces apoptosis and exhibits cellular antioxidant activity in cervical cancer cells. BLACPMA. 20:394-405

Davis P. 1988. Flora of Turkey and The East Aegean Islands, Edinburgh University Press, Edinburgh. p. 178-179.

Demirtas I, Sahin A, Ayhan B, Tekin S, Telci I. 2009. Antiproliferative effects of the methanolic extracts of *Sideritis libanotica* Labill. subsp. linearis. Rec Nat Prod. *3:* 10-109.

Deveci E, Tel-Çayan G, Duru ME, Öztürk M. 2019. Phytochemical contents, antioxidant effects, and inhibitory activities of key enzymes associated with Alzheimer's disease, ulcer, and skin disorders of *Sideritis albiflora* and *Sideritis leptoclad*a. J Food Biochem. 43: e13078.

Deveci E, Tel-Çayan G, Duru ME. 2018. Phenolic profile, antioxidant, anticholinesterase, and anti-tyrosinase activities of the various extracts of Ferula elaeochytris and *Sideritis stricta*. Int J Food Prop. 21*:* 771-783.

Dobrikova A, Gospodinova Z, Stefanov M, Apostolova E, Krasteva N. 2023. Phytochemıcal analysıs and assessment of the antioxıdant actıvıty and cytotoxıcıty potentıal of hydroethanolıc extract of bulgarıan *Sideritis scardıca*. J Chem Technol Metall. 58:93-100

Dziki D, Rozy ´ ło R, Gawlik-Dziki U, Swieca M. 2014. Current trends in the enhancement of antioxidant activity of wheat bread by the Addition of plant materials rich in phenolic compounds. Trends Food Sci Technol. 40: 48–61.

Ege B, Yumrutas O, Ege M, Pehlivan M, Bozgeyik I. 2020 Pharmacological properties and therapeutic potential of saffron (*Crocus sativus* L.) in osteosarcoma. J Pharm Pharmacol. 72*:* 56-67.

Erkan N, Cetin H, Ayranci E. 2011. Antioxidant activities of *Sideritis congesta* Davis et Huber-Morath and *Sideritis* arguta Boiss et Heldr: Identification of free flavonoids and cinnamic acid derivatives. Food Res Int. 44: 297-303.

Ertas A, Yener I. 2020. A comprehensive study on chemical and biological profiles of three herbal teas in Anatolia; rosmarinic and chlorogenic acids. S Afr J Bot. 130: 274-281.

Faiella L, Dal Piaz F, Bader A, Braca A. 2014. Diterpenes and phenolic compounds from *Sideritis pullulans*. Phytochem. 106*:* 164-170.

Göktaş Ö, Gıdık B. 2019. Tıbbi ve Aromatik Bitkilerin Kullanım Alanları. Bayburt Üniversitesi Fen Bilimleri Dergisi, 2:145-151

González-Burgos E, Carretero M, Gómez-Serranillos M. 2011. *Sideritis* spp.: uses, chemical composition and pharmacological activities—a review. J Ethnopharmacol. 135: 209-225.

Goulas V, Exarchou V, Kanetis L, Gerothanassis IP. 2014. Evaluation of the phytochemical content, antioxidant activity and antimicrobial properties of mountain tea (*Sideritis syriaca*) decoction. J Funct Food. 6: 248-258.

Gregory J, Vengalasetti YV, Bredesen DE, Rao RV. 2021 Neuroprotective herbs for the management of Alzheimer's Disease. Biomolecules. 11: 543.

Güvenç A, Okada Y, Akkol EK, Duman H, Okuyama T, Çalış İ. 2010. Investigations of anti-inflammatory, antinociceptive, antioxidant and aldose reductase inhibitory activities of phenolic compounds from *Sideritis brevibracteata*. Food Chem. 118: 686-692.

He J, Yang B, Dong M, Wang Y. 2018. Crossing the roof of the world: Trade in medicinal plants from Nepal to China. J Ethnopharmacol. 224*:* 100-110.

Hernández-Pérez M, Rabanal Gallego RM. 2002. Analgesic and antiinflammatory properties of *Sideritis lotsyi* var. *mascaensis*. Phytother Res. 16(3):264-266.

Melikoğlu G, Kurtoğlu S, Kültür Ş. 2015. Türkiye'de astım tedavisinde geleneksel olarak kullanılan bitkiler, Marmara Pharm J19: 1-11.

Mitropoulou G, Sidira M, Skitsa M, Tsochantaridis I, Pappa A, Dimtsoudis C, Proestos C, Kourkoutas Y. 2020. Assessment of the antimicrobial, antioxidant, and antiproliferative potential of *Sideritis raeseri* subps. *raeseri* essential oil. Foods. 9*:* 860.

Öke F. 2006. Türkiye *Sideritis* L. (Labiatae) Türlerinin Tohum Protein Analizleri. Gazi Üniversitesi Fen Bilimleri Enstitüsü (Biyoloji Bölümü) Yüksek Lisans Tezi, 60 s. Ankara.

Oun R, Moussa YE, Wheate NJ. 2018. The side effects of platinum-based chemotherapy drugs: a review for chemists. Dalton Trans. 47*:* 6645-6653.

Öztürk M, Uysal İ, Gücel S, Altundağ E, Doğan Y, Başlar S. 2013 Türkiye'de doğal boya veren bitkilerin tıbbi kullanımları, Tekstil ve Konfeksiyon Araştırma Dergisi. 17: 69-80.

Poon IK, Lucas CD, Rossi AG, Ravichandran KS. 2014. Apoptotic cell clearance: basic biology and therapeutic potential. Nat Rev Immunol. 14(3), 166-180.

Rabi T, Bishayee A. 2009. Terpenoids and breast cancer chemoprevention. Breast Cancer Res Treat. 115: 223-239.

Sagdic O, Aksoy A, Ozkan G, Ekici L, Albayrak S. 2008. Biological activities of the extracts of two endemic *Sideritis* species in Turkey. IFSET. 9: 80-84.

Sagir ZO, Carikci S, Kilic T, Goren AC. 2017. Metabolic profile and biological activity of *Sideritis brevibracteata* PH Davis endemic to Turkey. Int J Food Prop. 20: 2994-3005.

Sato F, Wong CP, Furuya K, Kuzu C, Kimura R, Udo T, Honda H, Yang J. 2022. Anti-skin Aging Activities of *Sideritis scardica* and 3 Flavonoids with an Uncommon 8-Hydroxyl Moiety. Nat Pro Commun.17: 1934578X221094910.

Savitskaya MA, Onishchenko GE. 2015. Mechanisms of apoptosis. Biochem. 2015;80: 1393-1405.

Sezer ENŞ, Uysal T. 2021. Phytochemical analysis, antioxidant and anticancer potential of *Sideritis niveotomentosa*: Endemic Wild Species of Turkey. Molecules. 26: 2420.

Sezer ENŞ, Uysal T. 2019. The Effects of the *Sideritis ozturkii* Extract on the Expression Levels of some Apoptotic Genes. CUPMAP. 1: 8-12..

Siegel RL, Miller KD, Wagle NS, Jemal A. 2023. Cancer statistics, 2023. Ca Cancer J Clin. 73: 17-48.

Tamokou JDD, Mbaveng AT, Kuete V. 2017. Antimicrobial Activities of African Medicinal Spices and Vegetables, Medicinal Spices and Vegetables from Africa, Chapter 8, 207-237.

Tomou EM, Chatziathanasiadou MV, Chatzopoulou P, Tzakos AG, Skaltsa. 2020. NMR-Based Chemical Profiling, Isolation and Evaluation of the Cytotoxic Potential of the Diterpenoid

Siderol from Cultivated *Sideritis euboea* Heldr. Molecules. 25: 2382.

Tóth B, Kúsz N, Forgo P, Bózsity N, Zupkó I, Pinke G, Hohmann J, Vasas A. 2017. Abietane diterpenoids from *Sideritis montana* L. and their antiproliferative activity. Fitoterapia. 122: 90-94.

Trivellini A, Lucchesini M, Maggini R, Mosadegh H, Villamarin TSS, Vernieri P, Mensuali-Sodi A, Pardossi A. 2016. Lamiaceae phenols as multifaceted compounds: Bioactivity, industrial prospects and role of "positive-stress". Ind Crops Prod. 83: 241-254.

Uritu CM, Mihai CT, Stanciu GD, Dodi G, Alexa-Stratulat T, Luca A, Leon Constantin MM, Stefanescu R, Bild V, Melnic S, Tamba BI. 2018. Medicinal plants of the family Lamiaceae in pain therapy: A review, Pain Res Manag. 7801543.

Van Engeland M, Nieland LJ, Ramaekers FC, Schutte B, Reutelingsperger CP. 1998. Annexin V-affinity assay: a review on an apoptosis detection system based on phosphatidylserine exposure. Cytometry: j Int Soc Anal Cytol. 31: 1-9.

Ververis A, Ioannou K, Kyriakou S, Violaki N, Panayiotidis MI, Plioukas M, Christodoulou K. 2023. *Sideritis scardica* Extracts Demonstrate Neuroprotective Activity against Aβ25-35 Toxicity. Plants (Basel).12(8):1716.

Yeşilada E, Honda G, Sezik E, Tabata M, Fujita T, Tanaka T, Takeda Y, Takaishi Y. 1995. Traditional medicine in Turkey. V. Folk medicine in the inner Taurus Mountains. J Ethnopharmacol. 46, 133-152.

Yumrutas O, Bozgeyik I. 2023, Anticancer activity of *Inula graveolens* by induction of ROS-independent apoptosis and suppression of IL6-IL8 in cervical cancer cells. BLACPMA. 22:314-325

Yumrutas O, Oztuzcu S, Pehlivan M, Ozturk N, Poyraz IE, Igci YZ, Cevik MO, Bozgeyik I, Aksoy AF, Bagıs H, Arslan A. 2015. Cell viability, anti-proliferation and antioxidant activities of *Sideritis syriaca*, *Tanacetum argenteum* sub sp. *argenteum* and *Achillea aleppica* subsp. *zederbaueri* on human breast cancer cell line (MCF-7). J Appl Pharm Sci. 5: 001-005.

Yumrutas O, Saygideger SD, Sokmen M. 2012. DNA protection and antioxidant activities of *Ajuga chamaeptys* (L.) schreber essential oil and its volatile compounds. J Essent Oil Bear Plants. 15, 526-530.

Yumrutas O, Saygideger SD. 2012. Determination of antioxidant and antimutagenic activities of *Phlomis armeniaca* and *Mentha pulegium*. JAppl Pharm Sci. 2:36-40

Yumrutaş Ö, Yumrutaş P. 2022. Phenolic compounds that modulate Multi Drug Resistance through inhibiting of P-glycoprotein encoded by gene ABCB1. Eurasian J Biol Chem. Sci. 5: 162-165.

Zengin G, Uğurlu A, Baloglu MC, Diuzheva A, Jekő J, Cziáky Z, Ceylan R, Aktumsek A, Picot-Allain CMN, Mahomoodally MF., 2019. Chemical fingerprints, antioxidant, enzyme inhibitory, and cell assays of three extracts obtained from *Sideritis ozturkii* Aytaç & Aksoy: An endemic plant from Turkey. J Pharm Biomed Anal 171: 118-125.

Zhang Y, Wang, Y. 2023. Recent trends of machine learning applied to multi-source data of medicinal plants. J Pharm Anal. In press.

EJBCS